Al-Farabi Kazakh National University

UDC 66.097:66.081 A manuscript

IMANGALIYEVA AINUR NURALIKYZY

Sorption and catalytic characteristics of composite materials based on natural raw materials

6D072000 – Chemical technology of inorganic substances

Dissertation submitted in fulfillment of the requirenments
for the degree of
Doctor of Philosophy (PhD)

Scientific supervisors:

G.A. Seilkhanova
Doctor of Chemical Sciences,
Professor

Yitzhak Mastai
PhD, Professor
Bar-Ilan University,
Ramat-Gan, Israel

Republic of Kazakhstan
Almaty, 2019

TABLE OF CONTENTS

NORMATIVE REFERENCES

In this dissertation, references are made to the following standarts:

GOST 24104-2001 Laboratory balance. General technical requirements.

GOST 25336-82 Laboratory glassware and equipment. Types, parameters and sizes.

GOST 4517-87 Reagents. Methods for the preparation of auxiliary reagents and solutions used in the analysis.

GOST 7.1-2003 Bibliographic record. Bibliographic description. General requirements and drafting rules.

GOST 2874-82. Drinking water. M.: Statestandart, 1982. - 26 p.

LIST OF ABBREVIATIONS

AP	aminophenol
BET	Brunnauer-Emmet-Taylor method
BT	bentonite
CM	composite material
HM	heavy metals
IRS	infrared spectroscopy
MMT	montmorillonite
MP	mandarin peel
MPC	maximum permissible concentration
Np	nanoparticle
NP	nitrophenol
OP	orange peel
OPC	organophosphorus compounds
PEI	polyethyleneimine
PEG	polyethylene glycol
PVP	polyvinylpyrrolidone
SEC	sorption exchange capacity
SEM	scanning electron microscopy
XRD	X-ray diffraction analysis
ZT	zeolite

INTRODUCTION

Characterization of the work. The thesis is devoted to the synthesis of new composite materials based on natural raw materials with sorption and catalytic properties. Protocols of synthesis are developed, physico-chemical characteristics of obtained materials are studied and the features of the sorption of heavy metal ions and the catalytic processes of nitrophenol reduction and hydroxidation of yellow phosphorus are investigated. All received data is new, the results are presented in the form of 2 articles in journals reviewed by the Web of Science and Scopus, and are protected by 2 utility model patents.

Relevance of the research topic. The relevance of this work is determined by the need for experimental development of new composite materials based on natural raw materials for use in wastewater treatment. Also for use as catalysts in nitrophenol reduction and butoxylation reactions of yellow phosphorus.

Composite material (CM) is a material consisting of two or more components (phases), where one of them, at least, is a solid, with a special property that can not be achieved by any of the components separately or even not just their sum. The properties of the composites are achieved through the interaction of individual phases, which is called the synergistic effect. Composite materials are widely used in medicine, construction, shipbuilding, sorption, catalysis, as well as in many other branches of science and technology. In this regard, the synthesis and study of the properties of composite materials is of theoretical and practical interest.

Currently, more and more countries, including the Republic of Kazakhstan, are faced with a global environmental problem - environmental pollution, in particular, natural, drinking and waste waters with heavy metals. It is well known that they directly affect the human body, changing its functions and properties, that is, they are able to accumulate in the body and affect the natural metabolism processes.

Therefore, one of the current priorities in the field of environmental protection is the search for effective and environmentally friendly composite materials for wastewater treatment.

In addition, CMs are actively used in various catalytic reactions. In this work, as a model reaction, the processes of reduction of nitro groups, butoxilation and hydroxidation of yellow phosphorus are investigated. The process of reducing nitro groups in amines plays an important role in organic, pharmaceutical and synthetic chemistry. Amine hydrogenation products are widely used as dyes, agrochemical and pharmaceutical products, as well as intermediate products for the preparation of diazonium salts, acylated aminophenols, quinones. It is known that for this process there are a number of catalysts based on noble metals, the disadvantage of which is the high cost of raw materials and the complexity of their synthesis. Natural materials of clay, vegetable and sea origin are the most available reagents for the synthesis of CM with various applied properties.

The catalytic properties of the obtained CMs were also investigated in model reactions — production of phosphoric acid from yellow phosphorus. Phosphoric acid H_3PO_4 is the most important intermediate in the production of concentrated

phosphate fertilizers. In addition, phosphoric acid is used in the production of various technical salts, organophosphorus compounds, including insecticides, semiconductors, ion exchange resins, as well as to create protective coatings on metals. Purified or so-called food phosphoric acid is used in the food industry for the preparation of feed concentrates and pharmaceuticals. Currently, the most common method is an acid decomposition of ores containing more than 25 % P_2O_5. Phosphoric acid is formed directly by dissolving the ore, i.e. direct extraction of phosphorus compounds by extraction. Hence the name of the product - extraction phosphoric acid (EPA). Thermal acid is obtained from poorer ores. The process is based on the recovery of phosphorus from natural phosphates by coke at high temperatures and the further production of H_3PO_4 from phosphorus. These methods have such disadvantages as the formation of acidic waste formed during the reaction. At present, the industrial production of trialkyl phosphates includes, in the first stage, the oxidation of yellow phosphorus P_4 with molecular chlorine. As a result of the reaction, all the chlorine, during the whole process, spent on obtaining PCl_3, turns into a very difficult to utilize chlorine-containing waste. Therefore, the relevance of this work is due to the need to search for alternative "chlorine-free" processes for the synthesis of organic phosphorus compounds (OPC) from yellow phosphorus due to the insufficient development of catalytic chemistry P_4, the lack of production of yellow phosphorus into valuable phosphorus-containing products in Kazakhstan and increased environmental requirements.

Aim of the work – is to obtain cost-effective, efficient composite materials based on natural raw materials, which have a high sorption capacity for heavy metal ions from aqueous solutions and catalytically activity in the reactions of reduction of 4-nitrophenol and the butoxylation of yellow phosphorus.

Research tasks. To achieve this it was necessary to solve the following tasks:

- to synthesize and determine the optimal conditions for the production of composite materials based on natural raw materials: clay, plant origin and various polymer modifiers (PEG, PVP);
- to establish the physico-chemical and textural characteristics of the obtained composite materials;
- to determine the optimal conditions for the sorption of Cu^{2+}, Cd^{2+}, Pb^{2+}, Ni^{2+} heavy metal ions by obtained CM;
- to determine the catalytic characteristics of supported copper-polymer catalysts in the reduction reaction of 4-nitrophenol to 4-aminophenol;
- to determine the catalytic properties of supported copper-polymer catalysts in the oxidation of yellow phosphorus in an aqueous solution in an oxygen atmosphere to produce phosphoric acid;
- establish optimal conditions for catalytic oxidation of yellow phosphorus to phosphoric acid in the presence of homogeneous copper-polymer catalysts in an aqueous medium in an oxygen atmosphere.

Objects of the study: composite materials based on bentonite clays, zeolite, orange and mandarine peel, and polymer modifiers (PEG, PVP).

Subject of the study: synthesis of composite materials; sorption extraction of HM ions from aqueous solutions by obtained CM; catalytic reduction reactions of 4-nitrophenol and hydroxylation of yellow phosphorus.

Novelty of the work. The scientific novelty of the research is to develop optimal conditions for the synthesis of new polymer-inorganic composite materials. For the first time, the possibility of using the obtained CM in water purification from heavy metal ions by the sorption method is shown. The first synthesized copper-containing CMs were investigated as catalysts in the reactions of hydrogenation of 4-nitrophenol and oxidation of yellow phosphorus, followed by the production of phosphoric acids.

Scientific and practical significance. Production of CM contributes to sustainable environmental development of the Republic of Kazakhstan. Studies conducted in the course of work allow us to open up prospects for the use of the materials obtained as effective, affordable and cheap sorbents for the purification of industrial wastewater. Also, the studied reduction reactions of 4-nitrophenol in the presence of in situ Cu_2O nanoparticles immobilized on natural bentonite and zeolite, functionalized with polyethylene glycol, are highly efficient and affordable. Kazakhstan has extensive reserves of phosphate ores. In this regard, obtaining phosphorus-containing products is a priority for the country. Phosphoric acid is used in the production of various technical salts, organophosphorus compounds, including insecticides, semiconductors, ion exchange resins, as well as to create protective coatings on metals. The catalytic properties of new polymer-metal catalysts based on copper (II) ions and polyethylene glycol (PEG) in the reactions of phosphoric acid production was showed in this work. In addition, the study investigated the reaction of oxidative butoxylation of yellow phosphorus in the presence of heterogeneous catalysts — supported $CuCl_2$-PVP, which, due to their high catalytic activity and selectivity, can be recommended for the synthesis of valuable phosphoric esters directly from yellow phosphorus under mild conditions. It should be noted that the obtained results have theoretical interest for the development of physical chemistry (thermodynamics and kinetics of heterogeneous processes: sorption, catalysis) and chemistry of coordination compounds.

Investigation methods. The following physico-chemical methods of analysis were used in this work: X-ray phase analysis, IR spectrometry, electron microscopy, BET, atomic absorption spectroscopy, UV spectrophotometry.

Connection of the topic with the research plan and various government programs. The work was performed in the framework of the project “Development of the Scientific Basis for Producing Phosphorus-Containing Compounds Based on Technogenic Mineral Raw Materials" - 2015-2017 (№ 0115РК00515), funded by the MES RK.

The main statements to be defended:

- The results of physico-chemical studies of the composition and structure of the synthesized composite materials;

- Optimal conditions for purification of aqueous solutions from the Cu^{2+}, Cd^{2+}, Pb^{2+}, Ni^{2+} ions by composites based on natural raw materials;

- The results of the study of the catalytic reduction of 4-nitrophenol in the presence of a composite material – in situ Cu_2O/PEG-bentonite (zeolite);

- The results of the study of the catalytic oxidation of yellow phosphorus in the presence of homogeneous catalyst $[Cu(PEG)_2Cl_2]$;

- The results of the study of the catalytic oxidation of yellow phosphorus in the presence of composite materials - $CuCl_2$-PVP-substrate.

Approbation of the work results. The main results of the work were presented and discussed at international conferences and seminars: V All-Russian Scientific Youth School-Conference "Chemistry under the sign of sigma: research, innovation, technology" (Omsk, May 15-20, 2016); International Scientific Conference "Innovative development and relevance of science in modern Kazakhstan" (Almaty, October 20-21, 2016); International scientific conference of students and young scientists "Farabian readings" (Almaty, April 11-14, 2016); International scientific conference of students and young scientists "Farabian readings" (Almaty, April 11-12, 2017); 4th International Russian-Kazakh Scientific and Practical conference “Chemical Technology of Functional Materials” (Almaty, 12-13 April 2018); International scientific conference of students and young scientists "Farabian readings" (Almaty, April 9-10, 2018); XXVIII Russian youth scientific conference "Problems of theoretical and experimental chemistry" (Ekaterinburg, 25-27 April 2018).

Publications. The results of the thesis were published in 24 papers, including:

- 2 articles published in international scientific journals, indexed by Scopus and Web of Science: Studia UBB Chemia with IF = 0.305 and Bulletin of Materials Science with IF = 0.925;

- 2 utility model patents;

- 6 articles published in journals recommended by the Committee on the Control of Education of the Ministry of Education and Science of the Republic of Kazakhstan;

- 14 materials of International, Republican scientific seminars and conferences.

The personal contribution of the author consists in the formulation and conduction of experiments, interpretation of the theoretical and experimental solution of the problems, discussion and generalization of the obtained results.

The structure and scope of the thesis. The thesis work consists of introduction, literature review, experimental part, results and discussion, conclusion, list of references and application. The total amount of the thesis is 92 pages, includes 45 figures and 28 tables. List of references contains of 204 names.

Acknowledgments. The author is sincerely grateful to the scientific consultants: Doctor of Chemistry, Professor Gulziya Amangeldiyvna Seilkhanova and Professor Yitzhak Mastai, for their advice on performing experiments, interpreting results and writing dissertation work. I would like to express special appreciations to Professor Akbayeva Dina Nauryzbayevna, for her help and guidance in carrying out the formulation and execution of experiments on the catalytic oxidation of yellow phosphorus. Also, I expresses gratitude to all the members of the scientific groups of Professor G.A. Seilkhanova and Professor Yitzhak Mastai.

1 LITERATURE REVIEW

1.1 The influence of toxic metal ions on the human body and methods of wastewater treatment

Environmental impurities and their poisonousness cause a major problem global world. Novel impurities keep developing and pose severe health and scientific challenges. Water pollution is one of the biggest environmental issue causing problems to living beings. Dyeing, battery, printing, mining, metallurgical engineering, electroplating, pigment, PVC stabilizers, nuclear power operations, electric appliances manufacturing, semiconductor, cosmetics, and so on belong to industries that generate various types of pollutants in wastewater effluent [1,2]. Therefore, the only solution is to eliminate them from the waste stream before they are discharged into the ecosystem. Heavy metals are a serious environmental problem because of their poisonousness and abundance. Existence of heavy metals in aquatic environment has been known to cause various health problems to human beings and animals [3]. Heavy metals are the main group of inorganic pollutants and contaminate a large zone of land-living due to its presence in sludge, fertilizers, pesticides, municipal waste, mines residues, and smelting industries [4]. Most heavy metals are known to be carcinogenic agents and may represent a serious threat to the living population because of their non-degradable, insistent, and accumulative nature [5-6]. Some heavy metals, however, are important to life and play irreplaceable role in the human metabolic system like the functioning of critical enzyme sites, but it can be harm the organism in excessive level [7]. Table 1 shows the permissible limits [8]. While Table 2 shows the health effects and sources of various heavy metals [9-12].

Table 1 - Permissible limits of various toxic heavy metals in drinking water according to the World Health Organization (WHO) standards

Permissible limit for drinking water (mg L^{-1})	
Metal	WHO [8]
Nickel	0.020
Lead	0.010
Zinc	3.000
Copper	2.000
Cadmium	0.003
Arsenic	0.010
Chromium	0.050
Iron	0.200
Manganese	0.500
Mercury	0.001

Heavy metal ions can be removed in various ways, such as chemical precipitation, biological treatment, ion exchange, and electrochemical extraction.

These methods have such significant disadvantages as partial removal, high energy requirements and the formation of toxic sludge [13].

Table 2 - Sources and health effects of various toxic metals

Metal	Procedures	Health effects
Nickel	Catalyst and battery manufacture, nickel coating, nickel stainless steel, catalyst and pigment [9, 10]	Causes chronic bronchitis, reduced lung function, cancer of the lungs, intestinal cancer [8]
Lead	Car batteries, pigments, lead crystal glass, radiation protection, architecture [8]	Carcinogenic, anaemia, abdominal, muscle and joint pains, kidney problems, and high blood pressure [8]
Zinc	Batteries, coating, compound, crops, diecasting alloys [8]	Stomach cramps, skin irritations, vomiting, nausea, respiratory disorders, anaemia and mental fever [8]
Copper	Electrical wiring, stoves, portable CD players, transmission wires, copper alloys and coins [8]	Stomach ache, irritation of nose, mouth, and eyes, headaches [8]
Cadmium	Electroplating of steel, nickel-cadmium batteries, cellular telephones [8]	Carcinogenic, causes lung fibrosis, dyspnoea, chronic lung disease and testicular degeneration [8]
Arsenic	Rat poisons, bronzing, in forming special glass and preserve wood [11]	Carcinogenic, producing liver tumors, and gastrointerstinal effects, diabetes [8]
Chromium	Electroplating, stainless steel production, leather tanning, textile manufacturing and wood preservation [12]	Nasal and sinus cancers, kidney and liver damage, nasal and skin irritation, ulceration, eye irritation and damage ение [12]

Another method for separating heavy metals from wastewater is an adsorption. The adsorption method is known as a fast and efficient way to remove heavy metals from aqueous systems, especially in the case of low concentrations of heavy metals. The adsorption process includes a solid adsorbent that binds molecules through chemical bonding, ion exchange and physical attraction forces. One of the issues raised in the adsorption method, is the selection of convenient adsorbent [14].

According to Sabino De Gisi et al. [15], sorbents based on natural materials, in turn, are divided into several groups depending on the composition and structure of the matrix: mineral clay materials, agricultural and household byproducts and sea materials.

Mineral clay sorbents are rocks and minerals with high adsorption and (or) ion exchange properties. These include natural zeolite rocks, flasks, palygorskite rocks, bentonite clays, etc. [16].

Agricultural and household residual products are represented by a wide range of materials from vegetable raw materials such as coals, sawdust, leaves, bark of deciduous and coniferous sorts of trees, shells of nuts, husks of sunflower seeds, fruit peel [17].

Adsorbents based on sea materials include chitosan and seafood processing wastes, peat moss and seaweed and algae. Due to its abundance, chitin appears econonomically attractive as well as environmentally friendly. According to Ali et al. [18] more than 1362 10^6 tons/annum of chitin are available from the fisheries of crustaceans.

Thus, there are a large number of sorbents based on natural raw materials. The classification of various types of natural raw materials, their importance for the extraction of toxic metals from aqueous solutions and the details of the synthesis and studies of the sorption properties of materials were shown in the following sections.

1.2 Sorption characteristics of composite materials based on natural materials

1.2.1 Clay minerals. The composition and structure of clay materials and adsorption properties of sorbents based on them

Clay, a fine-grained natural raw material, is a matter of much attention due to its use as an active adsorbent to trace heavy metal ions present in aqueous solution for more than a decade now. Clay has a property to show plasticity through a variable range of water content, which can harden when dried [19]. Clay evenly disperses and forms a slurry upon contacting with water, because water molecules are strongly attracted to clay mineral surfaces. The use of clays as adsorbent have advantages upon many other commercially available adsorbents in terms of low-cost, an abundant availability, high specific surface area, excellent adsorption properties, non-toxic nature, and large potential for ion exchange [20-21]. The most of the clay minerals are negatively charged and very effective and extensively used to adsorb metal cations from the solution; due to their high cation exchange capacity, high surface area, a pore volume [22]. Also, due to the low cost of clay there is no need to regenerate them. Therefore, the use of clay and materials based on it would solve the problem of waste disposal, as well as access to less expensive material for wastewater treatment.

The main chemical elements that make up silicates are Si, O, Al, Fe^{2+}, Fe^{3+}, Mg, Mn, Na, Ca, K, also Li, B, Be, Zr, Ti, F, H, in the form of (OH^-) or H_2O and others. The structure of all silicates is based on a close bond between silicon and oxygen; this connection proceeds from the crystal-chemical principle, namely from the ratio of the ion radii Si (0.39 Å) and O (0.32 Å). Each silicon atom is surrounded by oxygen atoms tetrahedrally located around it. Therefore, the basis of all silicates are oxygen tetrahedra or groups $[SiO_4]_3$ which are differently combined with each other [23].

The pioneering work of Ross, in 1927 [24], Hendricks, in 1929 [25], Hendricks and Fry, in 1930 [26], and Pauling, in 1930 [27] introduced the crystallinity in the structures of clay minerals.

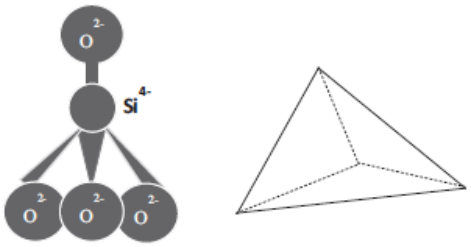

Figure 1 - Silica sheets consist of SiO_4^{2-} tetrahedral connected at three corners forming a hexagonal network in the same direction which is called tetrahedral sheets

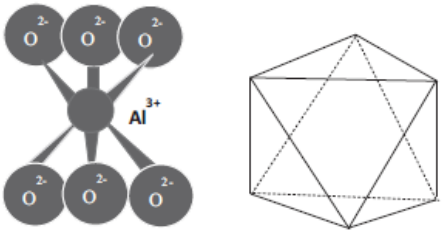

Figure 2 - Octahedron consists central cation (Al^{3+}, Mg^{2+}, Fe^{2+}) surrounded by 6 oxygens (or hydroxyls)

The majority of the clays, mainly composed of layers containing silica and alumina sheets, which belong to the class of layer silicates or phyllosilicates group. These groups can be subdivided according to the type of layer structure. Clays consist of an interconnected silicates sheet combined with a second sheet like grouping of metallic atoms, oxygen, and hydroxyl [28]. The basic structure units are divided into silica sheets and brucite or gibbsite sheets [29, 30]. The 1:1 clay mineral type consists of tetrahedral sheet (Figure 1) and one octahedral sheet (Figure 2) [29].

Octahedron consist two planes of hydroxyl ions between which lies a plane of magnesium or aluminumions, which is typically coordinated by hydroxyl sheets octahedrally.

The 2:1 (three layer) layer lattice silicates consist of two silica tetrahedral sheets between which is an octahedral sheet. The 2:1 clay minerals include the mica and smectite groups, which are the most abundant among the clay minerals. The serpentine and mica group is subdivided on the basis of dioctahedral and trioctahedral type [29].

The structure of some most important clay minerals is briefly summarised as follows:

Montmorillonites (Smectite) have 2:1 layer structure consist of an octahedral alumina sheet sandwiched between two opposing tetrahedral silica sheets [31]. The bonding between two silica sheets is very week, which permits the water and exchangeable ions to enter. This leads to the development of swelling capacity [32].

Illites are also 2:1 type minerals, but the interlayers are bonded together with potassium ion (K^+) to satisfy the charge and lock the structure. The balancing cation is, therefore, potassium (mainy or entirely), while charge deficienly from substitution is at list twice that of smectites and close to the surface of the unit layer [33].

Clinoptilolite is a natural zeolite comprising a microporous arrangement of silica and alumina tetrahedral within which water molecules and exchangeable cations (e.g., calcium, potassium, sodium) migrate freely. It forms as white to reddish tabular monoclinic tectosilicate crystals

Due to such important characteristics of clay minerals as a layered structure, pore size, texture, ion exchange capacity, plasticity, the ability to retain ions, or water on the surface, high adsorption capacity, etc. allow you to remove all types of toxic inorganic and organic pollutants.

Many methods of treatment can modify clay, with an aim to rise the adsorption capacity of the pure clay material. Heavy metal ions can be impassive efficiently by various treatment methods. Many comparative studies have shown that the adsorption capacity of a clay surface is increased with modification or treatment.

Montmorillonite (MMT) is abundantly present in the nature. Montmorillonites are treated and (or) modified to increase surface area and synthesize highly porous composites. Organo-modified montmorillonites (OMMT) have been widely used in polymer/clay nano-composites [34]. Organically modified montmorillonite clay (OMHP-MMT) was used for the removal of Cu^{2+} as a function of solution pH, stirring time, common ion effects, eluent type and concentration [35]. It showed good removal efficiency and selectivity towards Cu^{2+} at a pH range of 3.0-8.0 with a stirring time 10 min. The maximum removal efficiency (99.2 ±0.9 %) was obtained at pH 6.0. In the advancement of organically modified montmorillonite clay and for the removal of copper, recent work was conducted in which organo-montmorillonites (OMts) were modified by a cationic surfactant and a zwitterionic surfactant [36]. The adsorption capacity of the zwitterionic surfactant (Z16) modified montmorillonite toward Cu (II) was comparable with that of raw montmorillonite. The results of this work can provide novel information for developing new effective adsorbents of heavy metals.

Several authors have extensively studied the preparation techniques and adsorption properties of aluminum-pillared clays. Carbon modified aluminum-pillared montmorillonite has shown good uptake of Cd^{2+} from aqueous system [37]. The Cd^{2+} adsorption followed the mechanism based on second-order kinetics. Adsorption of Cd^{2+} was low at pH level <6.0, but sharply increased at the level >6.0. This may be a result of the relatively low H^+ concentration on the clay surface as the surface negatively charged at a high pH; this could allow for strong bonds with Cd^2. Al_{13} pillared montmorillonites (AlPMts) were also prepared with different Al/clay ratios to remove Cd (II) and phosphate from an aqueous solution [38]. In the single adsorption system of this study, Cd (II) was not adsorbed very much, but in a simultaneous system, significantly enhanced Cd (II) adsorption was observed. This result suggested that the formation of surface complexes promoted the uptake of Cd^{2+} for both contaminants (Cd^{2+} and phosphate) the adsorption of one increased with the

other one. However, in simultaneous studies, different results may also be observed. The adsorption and XPS results suggested that the formation of P-bridge ternary surface complexes were the possible adsorption mechanism for promoting uptake of Cd^{2+} and phosphate on AlPMt Aluminum-pillared layered montmorillonites (PILMs) also proved their potential as a sorbent in the removal of copper and cesium from aqueous solutions [39]. The Al/clay ratio appeared to have a significant effect on the sorption of copper on PILMs. With an increasing the Al/clay ratio, the amount of sorbed copper increased. This indicates that the sorption of copper involved a specific group of high-affinity sites on the pillar surfaces. The study concluded that copper sorption should be driven by both a cation exchange mechanism and by complexation reactions with the pillar oxides.

Removal of Pb (II) and Cd (II) from spiked water samples by adsorption onto clays (Kaolinite and Montmorillonite) was studied. Here, Pb (II) adsorbed exothermally, whereas Cd (II) was adsorbed endotermically [40].

Phosphate-modified montmorillonite (PMM) was used for removal of Co^{2+}, Sr^{2+} and Cs^{+} from an aqueous solution. The Freundlich model was the best for indicating the heterogeneous surface property of PMM [41]. Sorption of Co^{2+}, Sr^{2+} was strongly dependent on the initial solution pH and endothermic, but Cs^{+} was not and was exothermic. The strongly pH-dependent sorption of Co^{+} indicated that surface complexation was the main mechanism of Co^{+} sorption onto PMM.

Possible use of montmorillonite modified with polyethyleneimine was investigated for the removal Co (II) and Ni (II) metal ions from aqueous solutions [42]. The increased sorption of cobalt on the modified sorbent being studied (compared with the natural mineral) pointed with binding of cobalt ions with amine groups attached to the sorbent. It was found the employment of such a composite sorbent is promising for the purification of medium and highly mineralized wastewaters with a neutral value of pH.

Humic substances and clay minerals have been studied intensively because of their strong complexation and adsorption capacities. The adsorption and desorption of Ni^{2+} onto Na-montmorillonite was studied using the batch technique under ambitient conditions [43]. The results indicates that the adsorption of Ni^{2+} onto montmorillonite strongly depend on pH and ionic strength. It can be concluded from this study that montmorillonite is a suitable candidate for the pre-concentration and solidification of Ni^{2+} from large volumes of solutions. Humic acid was found to improve the metal adsorption capacity of mineral surfaces. An investigation of the adsorption of lead (II) onto montmorillonite clay modified by humic acid a fixed pH condition was also recently conducted [44]. The adsorption of Pb^{2+} onto humic acid was high; this might be the result of its strong affinity for carboxyl and phenolic groups of humic substances. The adsorption mechanism of Pb (II) might be the result of bridging between the adsorption sites on montmorillonite and HA molecules.

Some other modified forms, such as Chitosan-montmorillonite (KSF-CTS) beads to remove Cu^{2+} [45] and iron-free synthetic montmorillonite to measure the Fe^{2+} uptake from aqueous solutions [46], were also prepared and successfully used as adsorbents. Also, the competitive sorption among Cu (II), Pb (II), and Cr (VI) in a

ternary system on Na-montmorillonite and the effect of varying concentrations of Al (III), Fe (III), Ca (II), and Mg (II) on the sorption of heavy metals were studied [47]. The competitive sorption of Cu (II), Pb (II) and Cr (VI) in a ternary system on montmorillonite followed the sequence of Cr (VI)>Cu (II)>Pb (II). Moreover, the competition was weakened by the increase of pH, whereas it was intensified by the increase in heavy metal concentration. These findings are of fundamental significance for evaluating the mobility of heavy metals in polluted environments.

In another recent work [48], Na-montmorillonite and Ca-montmorillonite were used to remove Pb (II), Cu (II), Co (II), Cd (II), Zn (II), Ag (I), Hg (I), and Cr (VI) from an aqueous solution. The Na-Mt was more effective for heavy metal adsorption than Ca-Mt and proved to be a potentially useful material for Pb (II), Cu (II), Co (II), Cd (II), Zn (II) removal from aqueous solutions. The role of ion exchange was the main mechanism for Ca-Mt, whereas both ion exchange and precipitation were the main mechanism for Na-Mt.

When used as calcium montmorillonite , insights into the control and remediation of a variety of metal pollutants Hg^{2+}, Cr^{3+}, Pb^{2+}, Cu^{2+}, Zn^{2+}, Ba^{2+}, Ni^{2+}, Mn^{2+} and Cd^{2+}, Ag^{+} were studied [49]. It was observed that Cr^{3+}, Pb^{2+} and Cu^{2+} precipitate oxides or hydroxides at a pH level < 5. As the alkalinity increased, the adsorption sites on the clay surface and the amphoteric crystal edges were deprotonated and redied to adsorb metal cations.

Zeolite materials are three-dimensional alumino-silicate frameworks constituted of tetrahedral SiO_4 and AlO_4 arrangements. They have a global anionic surface, which, in turn, is neutralized by an external cationic framework (constituted of Na^{+}, Ca^{2+} or Mg^{2+}). This opens the way to the binding of heavy metal cations by ion-exchange on zeolites [50]. However, the sorption properties are generally relatively weak and it is necessary functionalizing their surface for improving metal recovery. Polymers offer many advantages for the elaboration of sorbents including the possibility to manage (a) the form and porosity of the sorbents, (b) the readily functionalization of the surfaces by grafting new reactive groups having higher affinity or selectivity for target metals. Polymers may improve mechanical properties, textural characteristics, and then mass transfer performance of composite materials, which can be used for metal binding [51, 52]. For example, zeolite Y is an emblematic material having good textural properties [50], and sufficient availability for developing large-scale application. Authors of the article [53] prepared the composite material (PAN-Na-Y-Zeolite) by polymerization of acrylonitrile in the presence of Na-Y zeolite. The composite was also functionalized by amidoximation through the reaction of hydroxylamine on nitrile groups of the composite. It is noteworthy that this effect depends on the type of metal ion; the limiting effect decreases accordingly the sequence: Cu (II) (0.758 mmol/g) > Cd (II) (0.378 mmol/g) > Pb (II) (0.358 mmol/g). In another work the adsorption of Cu (II), Cd (II) and Pb (II) onto methylmathacrylate-Na-Y-Zeolite (MMA-Na-Y-Zeolite) composite were investigated. It was found, that at 298 K and pH 4.5 the maximum recoveries of metal ions are equal: 37.97 mg/g for Cu (II), 79.73 mg/g for Cd (II) and 65.29 mg/g for Pb (II) [54].

Table 3 - The degree of extraction of heavy metal ions by clay materials

Sorbent	Me^{n+}	C_0, mg/L	s (m^2/g)	pH	SEC (mg /g)	t, °C	Amount of sorbent (g/L)	Reference
PAN-Na-Y-Zeolite	Cu^{2+}	10	66.1	4.4	0.552 mmol/g	25	1	[53]
PAN-Na-Y-Zeolite	Cd^{2+}	10	66.1	5.2	0.362 mmol/g	25	1	[53]
PAN-Na-Y-Zeolite	Pb^{2+}	10	66.1	5.7	0.171 mmol/g	25	1	[53]
MMA-Na-Y-Zeolite	Cu^{2+}	100	-	4.5	37.97	25	0.5	[54]
MMA-Na-Y-Zeolite	Cd^{2+}	100	-	4.5	79.73	25	0.5	[54]
MMA-Na-Y-Zeolite	Pb^{2+}	100	-	4.5	65.29	25	0.5	[54]
Ca-MMT	Cu^{2+}	140	-	5	14.87	25	5	[55]
C16- MMT	Cu^{2+}	140	-	5	3.75	25	5	[55]
Z16- MMT	Cu^{2+}	140	-	5	14.12	25	5	[55]
C-Al-MMT	Cd^{2+}	60	107.2	8	26	-	2	[56]
C-Al-PVA-MMT	Cd^{2+}	60	121.7	8	27.5	-	2	[56]
AlPMts-4.0	Cd^{2+}	90	304.94	5	15.0	25	5	[57]
Kaolinite	Pb^{2+}	50	3.8	6	5.6	30	2	[58]
Kaolinite	Cd^{2+}	50	3.8	6	4.0	30	2	[58]
Kaolinite+H_2SO_4	Pb^{2+}	50	15.6	6	6.8	30	2	[58]
Kaolinite+H_2SO_4	Cd^{2+}	50	15.6	6	5.5	30	2	[58]
Montmorillonite	Pb^{2+}	50	19.8	6	22.0	30	2	[58]
Montmorillonite	Cd^{2+}	50	19.8	6	21.8	30	2	[58]
Montmorillonite +H_2SO_4	Cd^{2+}	50	52.3	6	23.2	30	2	[58]
Chitosan- montmorillonite	Cu^{2+}	50	52.3	6	23.3	30	2	[59]
Bentonite	Sb^{3+}	4	99	6	0.50	24.85	25	[60]
Bentonite	Sb^{5+}	4	99	6	0.56	24.85	25	[60]

1.2.2 Investigations of the adsorption properties of various plant materials

This section describes the experience of using sorbents based on agricultural waste to remove heavy metals from aqueous solutions. In a number of studies, due to such characteristics as uniform distribution of pore size, sufficient surface area and the presence of active functional groups, biosorbents are considered as promising materials for wastewater treatment [61-96].

The sorption of dyes and heavy metal ions by various agricultural wastes, such as agave bagasse [61-63], almond shell [64], thistle meal [65-66], barley straw [67], cashew nutshell [68], citric acid [67, 70], corncob [61], glandular shell [69], pomelo peel [71], Egyptian mandarin peel [72], fruit juice residue [73], garden grass [74], garlic peel [75], grapefruit peel [76], hazelnut shell [77], lentil husks [78], mango peel waste [79], musk peel [80], pine sawdust [81], pongam seed shell [82], peanut peel [83], olive seed [84], plum seed [61], pomegranate peel [85], potato peel [86], rice husk [78], rice straw [87], sugarcane bagasse [88], walnut shells [77], yellow passion fruit seeds [89], orange peel [68, 90-93], rice husks [73, 94-99], walnut shell coal [66], white rice husk ash [96] and others.

The basic components of the agricultural waste materials include hemicelluloses, lignin, lipids, proteins, simple sugars, water, hydrocarbons and starch, containing a variety of functional groups with a potential sorption capacity for various pollutants [97].

One is the main purpose of the adsorption of heavy metals is to find an effective modification method of material. Furthermore, the nature of the metal ions to be sorbed also plays a prominent role in the efficiency of the sorption process. Chemical treatment of biosorbents is normally used to enhance their physico-chemical properties and to improve their sorption capacity via the ionization of functional groups. Furthermore, this kind of treatment can improve the properties of sorbents such as wettability and homogeneity and help to address the challenge of treating dilute wastewater, which existing conventional treatment methods are unable to do.

Agave bagasse is a sub-product from alcohol industry that has been very little studied, but that could have the potential to remove a variety of contaminants from aqueous solutions [61-63]. Raw and modified Agave salmiana bagasse was tested to remove metal cations by Velazquez-Jimenez et al. [63]. These materials were tested for the removal of Cd (II), Pb (II) and Zn (II) ions from water at pH 5, and desorption studies were performed at pH 2 and 4 at 25°C The physico-chemical characterization techniques mainly identified carboxyl, hydroxyl, sulfur and nitrogen containing groups in bagasse. Authors showed that mainly the carboxylic groups were responsible for metal uptake. Raw bagasse has an adsorption capacity of about 8, 14 and 36 mg/g for zinc, cadmium and lead, respectively, and this was improved about 27-62 % upon modification with HNO_3 and NaOH. Treatments with citric, oxalic and tartaric acid did not have a significant effect in adsorption capacities. Furthermore, raw agave bagasse has a very acceptable adsorption capacity of metal cations and it can approximately be regenerated in a 45 %, since the biosorption mechanism involves ion exchange and complexation.

Ash gourd (Benincasa hispida) is a commonly consumed vegetable in the Asian subcontinent, known to possess a good medicinal value. Sreenivas et al. [98] investigated the utilization of ash gourd (defatted) peel in biosorption of chromium (Cr), also considered column operations. Peel powder was studied for particle size (446 μm), specific surface area (0.4854 m^2/g) and other characteristics. The sorption capacity of peel for Cr (VI) in batch studies was 18.7 mg/g.

Feng et al. [90] chemically modified orange peel by means of hydrolysis of the grafted copolymer, which was synthesized by interaction of methyl acrylate with cross-linking orange peel. The modified biomass was found to present high adsorption capacity and fast adsorption rate for Cu (II). The adsorption capacity was 289.0 mg/g which is about 6.5 times higher than that of the unmodified biomass. Furthermore, authors showed that the adsorbent was used to remove Cu (II) from electroplating wastewater and it was suitable for repeated use for more than four cycles. In their study, orange peel modified with different chemical reagents as biosorbents were used to remove cadmium ion from aqueous solution.

Lentil husk was found to be a promising low cost adsorbent for removal of lead [99]. The functional groups of lentil husk were modified by treating with different chemicals to investigate their role in adsorption (Formaldehyde-formic acid treatment, Triethyl phosphitenitromethane treatment, Methanol-hydrochloric acid treatment and acetic anhydride treatment). After modification the biomass was dried and used for adsorption tests. Different physiochemical parameters were found to influence the adsorption process. Lead uptake capacity of lentil husk was 81.43 mg/g at optimized pH (5.0) and temperature (30 °C) with an initial metal ion concentration of 250 mg/L. Furthermore, chemical modification of functional groups revealed both hydroxyl and carboxyl groups played crucial role in binding process.

Sawdust, a by-product of the timber industry, is mainly composed of cellulose and lignin, which contain functional groups such as phenols, carboxyls and hydroxyls in their structure. These groups provide sawdust with its metal binding capacity. Acidic modification for treatment of peat (hydrochloric acid) and sawdust (citric acid) was selected based on a literature search. Regarding sawdust modification using citric acid, Pehlivan et al. [67] stated that citric acid forms ester linkages with cellulosic materials due to its crosslinking properties. At high temperature (120 °C), citric acid is converted to citric acid anhydride, which is capable of readily reacting with the O-H groups present in the cellulosic structure, thus creating ester linkages and introducing carboxylic groups into the biomass structure that act as ion exchange sites [70].

Peat is formed from the degradation of a wide range of plant and tree species in marshy, waterlogged lands. This biomass is composed of several organic acids (like humic and fulvic acids), salts of organic acids, minerals as well as polymeric compounds such as protein, cellulose and lignin which contain active functional groups (carboxyl, hydroxyl, sulphonic and phenolic). The polar characteristics imparted by the presence of these functional groups are responsible for binding metal to the peat surface [100]. Peat was modified using HCl and the treatment was selected with the aim of decreasing peat's natural hydrophobicity and improving its poor

settling properties [101]. Furthermore, modification with HCl can lead to desorption of metals ions originally present in natural peat, thus increasing its metal uptake capacity.

It was done modification of straw, which is characteristic waste in the agriculture, to improve its biosorption properties with respect to removal of selected metals from aquatic solutions. Two type of modifications of straw were analyzed: esterification with methanol and modification using the citric acid at elevated temperature. The results showed that citric acid modification increases the recovery of zinc ions from 70 % to 90 %. A modification of straw with methanol showed a decrease in the degree of extraction of zinc ions from 60 % to 30 %. The authors explain the sorption process by the fact that the extraction process occurs due to the ion-exchange mechanism by releasing calcium and magnesium from the surface of the straw into the solution [67].

Mangifera (Mango), Ficus (Fig) and Syzygium (Jamun) are economically important trees for countries in Indonesia, Australia, East Africa and the Philippines. The fruits of Ficus contain glauanol, sitosterol, aldohexose and alternative phytosterols [102]. The phytochemical studies of Mangifera seeds have reported the presence of alkaloids, steroids, tannins, phenol, resins, organic compound and essential oil [103]. Similarly, composition of S. cumini seed contain organic compound jambosine and glycoside jambolin or antimellin. The comparative sorption competencies increased in the following order Mangifera < Ficus < Syzygium seeds (11, 13 and 23 mg/g) for chromium (VI) at neutral pH scale. The highest sorption occurred at high sorbent doses, low hydrogen ion activity, increase in temperature and low Cr (VI) concentration within two hour duration and the process also confirmed the isopleths applications [104].

Quercus crassipes Hump. & Bonpl. is an oak tree species that belongs to the family Fagaceae, which is widely distributed in Mexico. Analyses of the biosorption kinetics, equilibrium and thermodynamics showed that QCS biosorbs Ni (II) ions from aqueous solutions by chemical sorption (chemosorption) reaction. The FTIR analysis revealed that hydroxyl, carbonyl and carboxyl functional groups might act as potential biosorption sites for Ni (II) ions

Table 4 synthesize the main characteristics of sorbents as well as their adsorption capacities with reference to agriculture and household waste applied for the removal of heavy metals. Table 4 shows that specific surface areas are much lower.

Table 4 - The degree of extraction of heavy metal ions by biosorbents

Sorbent	Me^{n+}	C_0, mg/L	s (m^2/g)	pH	SEC (mg/g)	t, °C	Amount of sorbent (g/L)	Reference
Agave bagasse (HCl)	Cd^{2+}	60	-	5	12.50	25	1	[63]
Agave bagasse (HCl)	Pb^{2+}	60	-	5	42.31	25	1	[63]
Agave bagasse (HCl)	Zn^{2+}	60	-	5	12.40	25	1	[63]
Ash gourd peel powder	Cr^{6+}	125	0.485	1	18.7	28	6	[98]
Banana peel	Cd^{2+}	80	-	3	5.71	25	30	[105]
Banana peel	Pb^{2+}	80	-	3	2.18	25	40	[105]
Citric acid barley straw	Cu^{2+}	0.001 mol/l	-	6-7	31.71	25	1	[67]
Straw + Methanol	Zn^{2+}	80	-	5	30%	25	-	[67]
Straw + Citric Acid	Zn^{2+}	80	-	5	90%	25	-	[67]
Cellulose xanthate (CX)	Pb^{2+}	200	5.42	5	134,41	30	4 г/л	[106]
Pine sawdust + Citric acid	Ni^{2+}	60	-	3.4-5.8	10	23	1 г/л	[80]
Peat+HCl	Ni^{2+}	40	-	4.3-5.9	21	23	1 г/л	[101]
Ficus seeds	Cr^{6+}	50	-	7	11	40	0.1/0.1 l	[104]
Syzygium seeds	Cr^{6+}	50	-	7	13	40	0.1/	[104]
Mangifera seeds	Cr^{6+}	50	-	7	23	40	0.1g/l	[104]
Acorn Shell of Quercus crassipes	Ni^{2+}	358	-	8	104.17	60	1 г/л	[107]
Citric acid modified orange peel	Cd^{2+}	0.005 mol/l	-	6	0.90 mol/kg	-	4.3	[69]
Egyptian mandarin peel (carbonized)	Hg^{2+}	200	-	6.02	34.84	19.85	5	[72]
Egyptian mandarin peel (NaOH)	Hg^{2+}	200	-	6.02	23.26	19.85	5	[72]
Egyptian mandarin peel (raw)	Hg^{2+}	200	-	6.02	19.01	19.85	5	[72]

1.2.3 Investigations of the adsorption properties of various sea materials

Adsorbents based on sea materials include chitosan and seafood processing wastes, peat moss and seaweed and algae. Due to its abundance, chitin appears econonomically attractive as well as environmentally friendly. According to Ali et al. [18] more than 1362 10^6 tons/annum of chitin are available from the fisheries of crustaceans.

Some seaweed such as brown algae have significant ion exchange properties associated with their polysaccharide content. Although seaweed has demonstrated extremely high sorption capacities, Holan et al. [108] observed that the biomass had a tendency to disintegrate and swell, which could be effectively used for column operations. Modifications of seaweeds by cross linking increases the stability and mechanical properties as reported in Ali et al. [18].

Chitosan is a natural polysaccharide widely used in fundamental studies as well as practical applications, including in treatment of wastewater, heterogeneous catalysts, delivery vaccines materials, agricultural stimulators, antibacterial agent and medical entersorbents [109-113]. It consists of β-(1→4)-linked D-glucosamine and *N*-acetyl-D-glucosamine units, is a deacetylated derivative of chitin and can be prepared from chitin. Chitosan is a well-known adsorbent for toxic and heavy metal ions. Due to the lone pair of electrons on nitrogen in acetoamido group and hydroxyl group can posse high chelating ability. Furthermore, the ability of chitosan depending on the acidity of the medium to form flaky precipitation can be used in sorption. For instant, in the recent years biosorbents based on chitosan has been synthesized and their sorption characteristics were studied for use in separation of heavy metal ions. Intoxication by heavy metal ions can lead to serious diseases of organism. These metal ions non-degradable and are persistent in the medium. Therefore chitosan has been applied in the synthesis various functional composites, by using clays, inorganic substances, natural and synthetic polymers [111].

In this way, a system which consists of chitosan and polyvinyl alcohol was studied. It was found that the adsorption efficiency of this sorbent has the maximum recovery of cadmium ions at pH = 6 and t = 40 °C [112].

Also, in the work [113] the adsorption of composite material composed from chitosan and polyvinyl chloride was demonstrated. One of the advantages of this polymer is physical and chemical stability in organic solutions as well as in concentrated acidic and alkaline media. The study showed that the adsorption capacity of the chitosan and polyvinyl chloride system were 90% for Cu (II) and Ni (II).

Peng et al. [115] prepared novel nanoporous magnetic cellulose-chitosan composite microspheres (NMCMs) by sol-gel transition method using ionic liquids as solvent for the sorption of Cu (II). Briefly, Fe_3O_4 nanoparticles were firstly synthesized by chemical coprecipitation method under alkaline conditions. Cellulose and chitosan were dissolved in 1-Butyl-3-methylimidazolium chloride [BMIM]Cl at 100 °C for 30 min to obtain a 7 wt% (composition ratio of cellulose: chitosan was 1:2) solution. Then magnetic fluid was immediately added to the solution by vigorous agitation for 15 min. After several emulsion as reported in Peng et al. [115], by slowly decreasing the temperature, the composite microspheres were obtained. The

final NMCMs were washed three times with deionized water followed by washing thoroughly with ethanol. Finally, the products were then stored and the yield of the microspheres production was above 95%. Results revealed that the composite microspheres exhibited efficient adsorption capacity of Cu (II) from aqueous solution, due to their favorable chelating groups in structure. Moreover, the loaded NMCMs can be easily regenerated with HCl and reused repeatedly for Cu (II) adsorption up to five cycles.

Authors Siahkamari M. et al. [116] synthesized chitin nanofibers (CMFs) and chitosan nanoparticles (CNPs) for removal lead ions from aqueous solution. Preparation of chitin nanofibers is an important subject because of their special optical, mechanical, dimensional and other characteristics. Firstly 10 g raw powder of chitin microfibers was added to deionized water to prepare a suspension with the concentration of 1% wt/wt, and then the suspension was stirred for 12 h at 25 °C. Secondly, suspension was poured into a machine mill (MKCA6-3; Masuko Sangyo Co., Ltd., Japan) and passed through the machine with a flow rate of 10 l/h for 15 cycles. As the microfibers passing between the rocks, because of shear and compressive forces fibrillation process occurs at the nanoscale. Synthesis process of chitosan nanoparticles is presented by Lifeng Qi et al.: chitosan was dissolved at the concentration of 0.5% (w/v) in acetic acid 1% (v/v) and then raised to pH = 4.6-4.8 with 10 N sodium hydroxide. Upon addition of 1 ml of an aqueous sodium tripolyphosphate solution with the concentration of 0.25% (w/v) to 3 ml of chitosan solution under magnetic stirring chitosan nanoparticles shaped spontaneously. It was observed that, lead uptake for chitosan nanoparticles (94.34 mg/g) was greater than chitin nanofibers (60.24 mg/g) at all stages.

The authors of work [117] presented the results on an uncomplicated green synthesis of chitosan-Fe_2O_3 nanocomposite. This composite showed excellent removal of Pb^{2+} and Cd^{2+} from the same system. Sorption capacity for Pb^{2+} - 147 mg/g, Cd^{2+} - 120.8 mg/g.

Table 5 shows the main characteristics and adsorption capacity of sorbents based on sea materials for the removal of heavy metal ions.

Table 5 – Main characteristics and uptake capacities of various sea material sorbents for heavy metal removal

№	Sorbent	Me^{n+}	C_0, mg/L	s (m^2/g)	pH	SEC (mg/g)	t, °C	Amount of sorbent (g/L)	Reference
1	Cellulose-chitosan composite	Cu^{2+}	150	102.3	5	65.8	-	2	[115]
2	Chitosan	Boron	100	-	6.5	2.1 mmol/g	-	100	[118]
3	Chitosan	As^{5+}	2	-	5.6-6.2	0.730	19.85	-	[119]
4	Chitosan	Cr^{6+}	30	-	3	7.94	24.85	13	[120]
5	Chitin nanofibers	Pb^{2+}	80	-	5	60.24	25	3	[116]
6	Chitosan nanoparticles	Pb^{2+}	45	-	5	94.34	25	3	[116]
7	Chitosan- Fe_2O_3	Pb^{2+}	100	92.345	5	147	50	0.01	[117]
8	Chitosan- Fe_2O_3	Cd^{2+}	100	92.345	5	120.8	50	0.01	[117]
9	Cystoseira baccata (Algae)	Hg^{2+}	-		6.0	329.0	25	2.5	[121]
10	Gelidium sesquipedale (Algae)	Cd^{2+}	91.8	-	5.3	18.0	20	2	[122]
11	Oedogonium hatei (Algae)	Cr^{6+}	60	1.32	1.0-4.0	31.0	44.8	1.0	[123]
12	Peat moss	Cd^{2+}	500	200	-	5.8	-	1.0	[124]
13	Peat moss	Cr^{6+}	500	200	-	29.0	-	1.0	[124]
14	Peat moss	Cu^{2+}	500	200	-	23.0	-	1.0	[124]
15	Peat moss	Pb^{2+}	500	200	-	40.0	-	1.0	[124]
16	Pumice	Cr^{6+}	300	2.34	1	87.72	-	6	[125]
17	Pumice modified $MgCl_2$	Cr^{6+}	300	41.63	1	105.26	-	6	[125]
18	Sargassum sp. (Algae)	Pb^{2+}	0.2-1 mM	-	5	303.0	-	1	[126]
19	Sargassum sp. (Algae)	Pb^{2+}	150	-	2-7	266.0	24.85	4	[127]

1.3 Catalytic characteristics of composite materials based on natural materials

1.3.1 Catalysts in nitrophenol reduction reactions

Reduction process of nitro groups into amines plays an essential role in organic, medicinal and synthetic chemistry [128]. Substituted aromatic amines are indeed widely used as dyes [129], agrochemical and pharmaceutical products [130], and as intermediates for the production of diazonium salts, acylated aminophenols, quinones, and many other compounds. For example, aminophenol is a precursor of paracetamol, a well-known analgesic, and antipyretic [127-131].

One of the most effective methods for the transformation of nitro groups into amino groups is hydrogenation catalyzed by precious or transition metals [129]. Hydrogenation processes are effectively performed using reducing agents such as H_2 [132], CO/H_2O [133], ammonium formate [134], oxalic acid [134], t-$BuNH_2$-BH_3 [135], NH_2NH_2 [129], $LiBH_4$ [136] and $NaBH_4$ [137-139].

Various metal oxides and metallic complexes are known as catalysts for the reduction of 4-nitrophenol (4-NP) into 4-aminophenol (4-AP) including Pd [132], Pt [140], Au [139, 141, 142], Co [144], Ag [145-146], Cu [138, 147, 148], CuO [149, 109], Cu_2O [151].

It is known that different substrates as a natural origin, such as carbon surface [152], TiO_2 [153], Al_2O_3 [154], silicon [150], chitosan [109], bentonite[138] and zeolite [155, 156] and synthetic origin used in the synthesis of catalysts. For example, in the study [146] reports on the preparation of polyacrylonitrile fiber paper (PANFP) functionalized with polydopamine (PD) and silver nanoparticles (Ag NPs), named as Ag NPs/PD/PANFP. The composite material was obtained via a simple two-step chemical process. First, a thin polydopamine layer was coated onto the PANFP surface through immersion into an alkaline dopamine (pH 8.5) aqueous solution at room temperature. The reductive properties of polydopamine were further exploited for the deposition of Ag NPs. The Ag NPs/PD/PANFP displayed good catalytic performance with a full reduction of 4-nitrophenol into the corresponding 4-aminophenol within 30 min.

In work [145] silver nanocomposites (AgNCs) were produced by adsorption onto an electron-rich polypyrrole-mercaptoacetic acid (PPy-MAA) composite, known to be a highly efficient adsorbent for the removal of Ag^+ ions from aqueous media in the remediation of metal- contaminated water sources. In situ reduction of Ag^+ cations to Ag^0 nanoparticles (NPs) was achieved in the absence of an additional reducing agent. An investigation into the potential application of these AgNCs, effectively a waste product for further processing, as a catalyst for the reduction of variously substituted nitroarenes in water was undertaken in an effort to beneficiate the materials and determine the reaction's specificity. One composite having 11.14 ± 0.05 wt% Ag content was particularly active in these reductions, with aniline derivatives being prepared in 71–94% yields. The kinetics of the reaction was examined using 4- nitrophenol, a common water-soluble pollutant; pseudo-first-order kinetics was observed with predicted activation energy of 68.3 kJ/mol for this

system. Furthermore, this AgNC displayed superior stability over 10 reaction cycles without loss of catalytic activity.

Among the different catalyst substrates, clay materials as bentonites and zeolites are widely used in practice due to their thermal stability, non-toxicity and low cost [138]. However, they do not have high surface area in their natural state and do not give high adsorptive properties and in order to overcome this limitation, they have to be subjected to modifications. First, acid-base treatment of clay surfaces can destroy agglomerates of individual crystallites and enhance surface area [157]. Secondly, functionalization of clay minerals by polymers or surfactants have been widely used in synthesis of nano-composites due to their complex-formation properties as functional groups of polymers can be attached to the surface of the clay. From this point of view, polar polymers are of interest as effective modifiers of clay materials [157].

So work [137] is devoted to the synthesis of gold nanoparticles (AuNPs) using branched polyethylenimine (PEI) and acylated polyethylenimine (PEI-C_{12}) as a reducing and stabilizing agent and their successful use as catalysts. The procedure for nanoparticle synthesis is as follows: in an aqueous solution of HAuCl4 (1.4 mM, 25 ml) is added to 1% PEI or PEI-C_{12} (1 ml) in a round bottom flask (stage I). The reaction mixture is vigorously stirred at room temperature for about 3-5 hours when PEI is used. On the other hand, the reaction mixture is heated to 80 °C when using EI-C_{12}. The authors noticed that the color of the reaction mixture varies from pale brown to dark red, indicating the formation of colloidal Au NPs (stage II). In fact, the size of Au nanoparticles depends on the amount of polyelectrolyte added to the reaction mixture. After completion of the reaction, the reaction mixture is ultra-centrifuged and filtered, and then the precipitate is washed with copious amounts of distilled water. The surface plasmon resonance band at 520 nm in the ultraviolet absorption spectrum showed the formation of Au NPs without the addition of an additional reducing agent. A detailed scheme for the synthesis of Au NPs stabilized on a PEI matrix is shown in Figure 3.

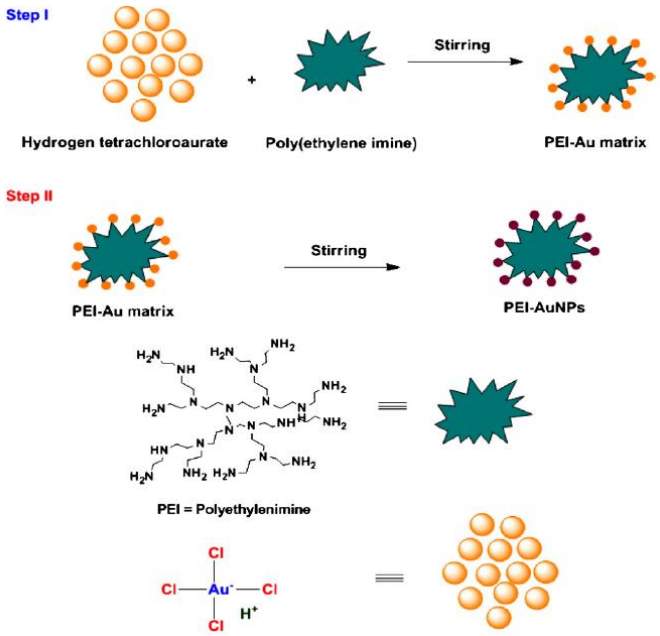

Figure 3 - Scheme for the synthesis of Au NPs using the PEI-C_{12} polymer

Polyethylene glycols (PEG) are polar polymers with low toxicity, low cost, water solubility and biodegradability [159]. Polyethylene glycols are also used as NPs stabilizers and water dispersive agents. In a recent paper, photo catalytic reduction of nitro aromatic compounds employing TiO_2/PEG-H_2O as catalyst was investigated [134]. In this paper, the TiO_2 NPs were stabilized by PEG (400 g/mol) which showed to physically adsorb on the NPs and acted as a dispersive agent, hence increasing the reaction yield.

In another paper, Ag and Au NPs coated with higher molecular weight PEG (2000-5000 g/mol) seemed to be better suited for catalytic and biological applications due to their higher stability and reducing properties [160].

A number of catalysts based on metal and metal oxide supported NPs were investigated for the reduction of 4-NP and showed excellent catalytic activity due to increased surface area and increased stability conferred by the supports [132]. In a recent paper, the performances of Cu_2O, Cu and CuO NPs dispersed on cubic mesoporous carbon were compared for the reduction of 4-NP, showing best catalytic activity for the Cu_2O NPs. The results showed that the best catalytic activity is consistent for Cu_2O NPs [151]. The exceptional catalytic performance of the Cu_2O supported NPs were related to *in-situ* generation of highly active Cu (0) growing NPs during the catalytic process [152]. These catalysts based on copper NPs have the advantages over noble metal NPs that they have low-cost and non-toxicity.

However, the variety of such possible systems has still to be explored, with a lot of possible supports, particle sizes, and additives. In addition, the synthesis of NPs usually requires several steps, which can significantly increase the time for the preparation of the catalyst.

1.3.2 Catalysts in the reactions of oxidation of yellow phosphorus

The authors of work [161] investigated the method of synthesis organophosphorus compounds, namely trialkyl phosphates in the reaction of oxidation of yellow phosphorus. Three alkyl phosphates are valuable chemical products. They have a variable application as a solvents, flotation reagents, pesticides, extractants, as well as feedstock for the production of biologically active substances.

Currently, in the industrial production of a trialkyl phosphate in the first stage the oxidation of yellow phosphorus P_4 by molecular chlorine is carried out. Then the obtained phosphorus trichloride PCl_3 continues to be oxidized to $POCl_3$, which is then subjected to etherification with the formation of $PO(OR)_3$. All chlorine, during the entire process, which was spent to obtain PCl_3, goes into a very difficult recyclable chlorine-containing waste. The most favorable replacement for this toxic oxidizing agent is harmless and affordable oxygen. However, it was found that the rate of formation of the target trialkylphosphates obtaned during oxidation of P_4 with oxygen in alcohols, is significantly lower than the side reaction of ignition of yellow phosphorus with the release of thick white smoke P_4O_6, P_4O_{10}. Therefore, the consumption of catalysts based on Cu (II) and Fe (III) salts allows replacing toxic chlorine with harmless oxygen. It has been established that, without oxygen, the Cu (II) and Fe (III) compounds [162] can serve as stoichiometric oxidizers of P_4 to

phosphorous and phosphoric acids [163]. It has also been established that the composition of the products and the kinetics of the reaction depend on the nature of the catalyst. In particular, in the presence of copper (II) acetylacetate, predominantly dialkylphosphite is formed, and in the presence of Cu (II) and Fe (III) chlorides, trialkylphosphate is made. A series of catalysts' activities for the reaction of oxidation of yellow phosphorus with oxygen in n-butyl solution are presented as follows: $Cu(acac)_2 > CuCl_2 > FeCl_3$.

The mechanism of the redox reaction (1) was studied in detail in the works [164-165]. In the second reaction (2), due to the release of acid HX, trialkylphosphite is dialkallated to dialkylphosphite. Trialkyl phosphate is formed as a result of the action of the MX_n catalyst in reaction (3). In reaction (4), the reaction of acidolysis of dialkylphosphite to monoalkylphosphite is shown. This reaction is adversely affected by high temperature and long duration of the process.

$$P_4 + 6MX_n + 12ROH = 4P(OR)_3 + 6MX_{n-2} + 12HX \quad (1)$$

$$P(OR)_3 + HX = P(O)H(OR)_2 + RX \quad (2)$$

$$P(OR)_3 + MX_n + ROH = P(O)(OR)_3 + MX_{n-2} + HX + RX \quad (3)$$

$$P(O)Y(OR)_2 + HX = P(O)H(OH)(OR) + RX \quad (4)$$

where, M = Cu, Fe; X = Cl, acac; R = nC_4H_9; nFe = 3; nCu = 2.

The catalytic cycle is completed by equation (5), i.e. oxidation of reduced forms of MX_{n-2} with a catalyst to MX_{n-1} (CuX or FeX_2), as well as oxidation of MX_{n-1} with oxygen (6).

$$MX_{n-2} + MX_n = 2MX_{n-1} \quad (5)$$

$$4MX_{n-1} + O_2 + 4HX = 4MX_n + 2H_2O \quad (6)$$

The authors of the article [166] investigated the catalytic oxidation of yellow phosphorus with carbon tetrachloride and elemental sulfur in butanol. It has been established that the addition of CuX_2 catalysts (X = Cl, Br, acac, CH_3CO_2, $C_3H_7CO_2$, $C_{17}H_{35}CO_2$) positively affect the reaction rate of the oxidative alcoholysis of P_4 in a butanol solution [163]. In reaction 7, the main product is dialkyl phosphite (up to 60%).

$$P_4 + 12ROH + 6CCl_4 = 4P(O)H(OR)_2 + 6CHCl_3 + 4RCl + 2HCl \quad (7)$$

In addition, except dialkylphosphite, approximately equal amounts of monoalkylphosphite and trialkylphosphate are also formed. With the extra addition of a P_4 into the catalytic solution $CuX_2/P_4/CCl_4/ROH/Py/PhMe$, except to process (7), in the reaction the double oxidative PO and PS (8) (combination of yellow phosphorus

with alcohol and sulfur, which is not accompanied by side formation toxic hydrogen sulfide) was appeared [168].

$$P_4+12ROH+6CCl_4+ 0,5S_8=4P(S)(OR)_3 + 6CHCl_3 +6\ HCl \quad (8)$$

In the following work, the kinetics of the formation of organophosphorus products by the oxidation of red phosphorus [169] in alcoholic solutions of copper in anaerobic and aerobic media was studied.

$$P_n+0,75nO_2+3nROH +nHCl = nP(O)H(OR)_2 +nRCl +1,5nH_2O \quad (9)$$

$$P_n+1,25nO_2+4nROH +nHCl = nP(O)(OR)_3 +nRCl +1,5nH_2O \quad (10)$$

As a result, the authors concluded that trialkyl phosphates are formed as a result of the oxidation of P_n by copper ions.

$$P_n+2,5nCuX_2+4nROH = nP(O)(OR)_3 +2,5nCu +4nHX+RX \quad (11)$$

$X=Cl^-,Br^-,I^-,C_3H_7CO_2^-$, $acac^-$

The authors of [170] developed effective homogeneous catalytic systems based on copper (II) chloride and polyacrylic acid (PAA) for the reaction of liquid-phase oxidation of P_4 in aqueous-toluene solutions with oxygen under mild conditions (50-70 ^oC, P_{O2} = 1 atm) with the formation of phosphoric acids. The oxidation processes of P_4 with oxygen in water-toluene solutions of the catalytic system Cu(II)-(PAA) proceed through the key reduction reactions of $[Cu(PAA)_2CI_2]$ by yellow phosphorus to form phosphoric acid and oxidation of reduced copper forms $[Cu(PAA)_2]$ by copper (II) chloride $[Cu(PAA)_2CI_2]$. The promoting effect of polyacrylic acid, onto the reaction rate and the yield of phosphorus-containing products. High conversion of P_4 is observed at 50 °C, P_{O2} 1 atm and molar ratio $[Cu(PAA)_2CI_2]:[P_4]=(1:8.8)$.

Thus, the search for new catalysts for the production of phosphorus-containing substances is one of the priority tasks of the chemical and petrochemical industries.

1.3.3 Catalytic systems based on metal-polymer complexes

The presence of deposited systems, in which one of the components is fixed by physical or chemical bonds to a solid carrier, has contributed in many areas of metal complex catalysis. Practically at the same time 2 directions began to develop: 1) consolidation of complexes on inorganic carriers; 2) consolidation of the complexes on organic (polymeric) substrates, which are industrial polymers and copolymers. So in the works [171, 172] the phenomena of fixing of transition metal compounds associated by functional groups with the surface of polymeric or mineral carriers, and their participation in various processes in living and inanimate nature were shown.

The chemistry of fixed catalysts includes two fundamental directions: dynamic aspects, i.e. investigation of the catalytic behavior of immobilized complexes, as well as static aspects - determination of the structure and composition of the complexes. In practice, polymeric carriers of two main groups most often are used. The first is

composed of hard-bonded macroporous resins with a large specific surface. Their ligand groups are localized mainly on the surface, where they come into contact with the substrate and the reagent. The second group consists of linear or weakly crosslinked lattice microporous (gel) polymers or composites. They dissolve or swell in solvents, catalytically active centers are not only on the surface of the polymer, but also in volume.

Recently, metal complexes fixed on organic and inorganic carriers are of great interest as catalysts, since they combine the best properties of homogeneous and heterogeneous catalysts with high activity and selectivity. Homogeneous catalysts play a very important role in organic synthesis. However, they have some disadvantages, such as decomposition during the reaction process, which leads to the loss of metals and contamination of products with catalyst residues. Immobilization of catalytically active metals by covalent bonding to the functional groups of polymers is a promising method to prepare highly active catalysts, and helps to avoid contamination of products with residues of metal cations due to the strong polymer-metal bond [173]. Publications and ways of introducing catalysts immobilized with a polymer-metal bond on the surface of various insoluble carriers began in the 1960s [174]. Their beneficial properties are directly related to the nature and properties of the polymer matrix, as well as the unique microenvironment created by the polymer carrier and the reactant. Their main advantages are physically easy separability of the polymer and its associated component from the reaction mixture, the potential reusability and simplification of work with toxic and volatile substances [175]. Recently, data about catalyst with high stability in the polymer matrix and with improved selectivity in intramolecular reactions and high activity of incorporated chiral catalysts were published [176-178]. One of the requirements for catalyst carriers is a high surface area and a developed porous structure, which favors the formation of maximum dispersion of supported metal particles. For instance, in the article [179], the authors compared two types of activated carbons and concluded that the dispersion of the active component on a highly porous carrier is higher. Furthermore, the material structure itself can have significant impact. The authors [180] investigated the catalytic activity of ruthenium deposited on various carbon materials during the decomposition of ammonia. It was concluded that the degree of graphitization of carbon materials was crucial for the activity of ruthenium catalysts, while the surface area and porosity were less important. Such properties of heteropoly compounds as stability and stability under oxidative conditions make them valuable catalysts for oxidation processes. Polymer-metal complexes of transition metals, especially systems based on Co (II), Cu (II) and Fe (III), are known as effective catalysts for the oxidation of various aliphatic and aromatic hydrocarbons under mild conditions. Usually they are attached to inorganic carriers, such as zeolite, mesoporous molecular lattices, polystyrene resin, as well as by covalent bonding immobilized to polymers insoluble in the reaction medium.

In work [181], a carbon-containing substrate with a highly developed surface obtained by the pyrolysis of rice husk was investigated. The catalysts were prepared by sequential fixing of the polymer and then copper ions on the surface of the

substrate.

Currently, among the catalysts which are promising in oxidation reactions of saturated hydrocarbons with hydrogen peroxide, polymer-metal complexes have an important place [182]. They have many common features with enzymatic catalysis, since they occur at low temperatures and have a high selectivity.

Structures, physicochemical, sensory and catalytic properties of metal-polymer film materials obtained by joint low-temperature deposition of metal and monomer vapors on a substrate followed by low-temperature solid-phase polymerization of co-condensate are presented in works [182-184]. Depending on the nature of the metal and the structure of the monomer, this process allows to obtain metal-containing polymers of various types: metal-organic polymers with atoms or metal clusters in the polymer chain, metal-polymer complexes or metal particles of various sizes physically immobilized in the polymer matrix.

Polymer complexes can be obtained in several ways. The most common of them is the mixing of solutions of ready components in a common solvent by the so-called - complex mixing, also polymer complexes can be obtained by the method of matrix polymerization [182, 183]. The results of many experiments indicate that matrix polymerization produces more highly organized polymer complexes as compared to "mixing complexes," as the matrix controls the rate of formation of the "daughter chain", its length and chemical structure. The polymer complex is formed only when a certain critical degree of polymerization of the "daughter chain" is reached, after which the growing chain is associated with the matrix and the actual matrix polymerization begins [184].

Different methods can be used to synthesize metal-polymer composites: 1) processing polymer films with metal vapors, 2) chemical reactions of metal salts in polymer solutions, followed by separation of the corresponding polymer, 3) polymerization of various metal-containing monomer systems [185]. For example, gel-immobilized palladium nanoparticles showed good stability. The polyacrylamide hydrogel containing palladium-PVP was the most stable catalyst. Its activity during using the same sample (0.03 g of palladium content not less than 0.1 % in it) is preserved by hydrogenation of 1.8 ml of substrate. And which corresponds the TON (turnover number) values for PAAG/PEI-Pd^{o} and PAAG/PVP-Pd^{0} are equal to (4-7)·10^3 catalytic acts per 1 metal atom, respectively [186].

Recently, the polymeric hydrogels as sorbents of metal ions were proposed [187]. A series of metal ions according to their abilities to bind hydrogels were established as follows (weakening of the bond from left to right): Cr (VI) > Fe (III) > Cu (II) > Co (II) > Ni (II) ≈ Mn (II).

In recent decades, researchers have attracted particular attention to polymer-metal complexes of copper ions with poly (4-vinylpyridine) (PVP), due to their high stability and good catalytic activity for a number of chemical transformations.

Polyvinylpyrrolidone (PVP) has unique properties. High tendency to complexation, non-toxicity, good solubility in various solvents, including aqueous media, provides it with wide application in many industries [188]. The relationship between the stability of complexes and their catalytic activity during the oxidation of

thiosols was established in work [189]. At the same time, PVP-Cu^{2+} complexes showed high stability and catalytic activity. Further studies were aimed at the development of complexes of optimal composition, based on a quantitative relationship between catalytic activity and the composition of polymer-metallic complexes PMC. The maximum catalytic activity was shown by the PVP- Cu^{2+} system containing 11–13 % copper.

Catalyst reuse is an important aspect of heterogeneous catalysis. Heterogeneous catalysts can be reused due to their macromolecular nature. The catalytic ability of the mixed ligand complexes Cu (II) [Cu(SC)(SA)], [Cu(SC)(ST)] and [Cu(SC)(VA)] (SC: salicylidenechitosan; SA: salicylicidane aniline; ST: salicylicididen-urea; VA: o-vinylidene ananiline) was investigated in a liquid phase oxidation reaction using hydrogen peroxide as an oxidizing agent. The catalytic efficiency of the complex decreased significantly after the fourth restart. This is due to the low chemical resistance and mechanical strength of the chitosan-biopolymer chain, which ensures the heterogeneity of the complex.

The use of metal complexes, fixed on organic and inorganic carriers, creates prospects for the rejection of expensive materials such as platinum, palladium and others. In this regard, the synthesis of new metal-polyelectrolyte catalysts supported on solid substrates opens up a wide range of their applications, ranging from simple exchange reactions in inorganic chemistry to the most complex transformations of substances in organic synthesis.

2 EXPERIMENTAL PART

2.1 Method of synthesis of sorbents based on natural raw materials

2.1.1 Initial materials

The following reagents are used to prepare composites and to study their sorption characteristics:

1. BT-PEG: Ca - montmorillonite (bentonite) from Dinosaur deposits (95% purity), purchased from the B-clay company (Kazakhstan); water-soluble polyethylene glycol (PEG), produced by AppliChem GmbH (Germany) with molecular weight of 6,000 g/mol; $Pb(NO_3)_2$, $CuCl_2 \cdot 2H_2O$ and $CdCl_2 \cdot 2H_2O$.
2. OP-PVP, MP-PVP: orange peels (OP) and mandarin peels (MP); water-soluble polyvinylpyrrolidone (PVP), produced by Alfa Aesar (Great Britain) with molecular weight of 40,000 g/mol; NaOH, $CuCl_2 \cdot 2H_2O$ и $NiCl_2 \cdot 6H_2O$.

All chemicals were of analytical grade.

2.1.2 Preparation of composite based on clay minerals - BT-PEG

The modification of bentonite clay was conducted with several concentrations of PEG by standard procedure [190, 204]. For this purpose, five samples of sorbent were prepared: 20 g natural bentonite was dispersed in 100 mL of 0.1, 0.5, 1.0, 2.0 and 5.0 % aqueous solutions of PEG, respectively, under continuous stirring. This dispersion was stirred at 25 °C for 1h and left for 24 hours at ambient temperature. The prepared BT-PEG was separated by paper filtration, washed several times with deionized water, and dried at 100 °C for 4 h. Obtained sorbents were ground to a powder of 70 μm in size using a porcelain mortar.

2.1.3 Preparation of composite based on plant materials - OP-PVP, MP-PVP

Activation of citrus peel was carried out according to a two-step procedure: first with sodium hydroxide solution, then polymerization with polyvinylpyrrolidone solution.

Modification of orange peel was carried out according to the following procedure: Orange peel mass of 10 g was placed in a 200 cm^3 beaker, then added aqueous 1 M NaOH (100 cm^3). The obtained solution was stirred for 1 hour. Next, the gel-like solution was left for 24 hours for effective modification. The resulting mixture was washed with distilled water until neutral medium. Then the solution was filtered. The activated peel was dried at 100 °C for 2 hours. In the second stage, the modification with polyvinylpyrrolidone was carried out. To the dried sample was added 100 cm^3 of an aqueous solution of the polymer - PVP, with a concentration of $2.5 \cdot 10^{-2}$ M. The mixture was stirred within 1 hour, and was dried at a temperature of 80-100 ° C for 2 hours. The finished sorbent was machined.

Mandarin peel was modified according to a similar procedure.

2.2 Method of preparation of catalysts

2.2.1 Initial materials

The following reagents are used to prepare composites and to study their catalytic characteristics:

1. Cu^{2+}/PEG-BT and Cu^{2+}/PEG-ZT: Ca - montmorillonite (bentonite) from Dinosaur deposits (95% purity), purchased from the B-clay company (Kazakhstan); zeolite from Chankanay deposits (95% purity) (Kazakhstan); a water-soluble polyethylene glycol (PEG), produced by AppliChem GmbH (Germany) with molecular weight 6,000 g/mol; $CuSO_4 \cdot 5H_2O$; $NaBH_4$;

2. $CuCl_2$-PEG: initial technical white phosphorus (GOST 8986-75), $CuCl_2 \cdot 2H_2O$, toluene ($C_6H_5CH_3$)), produced by AppliChem GmbH (Germany) with molecular weight 6,000 g/mol;

3. Substrate-$CuCl_2$-PVP: initial technical white phosphorus (GOST 8986-75), $CuCl_2 \cdot 2H_2O$, PVP (Alfa Aesar), C_3H_7OH, CCl_4, pyridine (C_5H_5N), toluene ($C_6H_5CH_3$). Butanol was dried by boiling over CaO followed by distillation. Toluene was purified by mixing with concentrated sulfuric acid, decantation and distillation. As a substrates were used SiO_2, Al_2O_3, kieselguhr, zeolite from Chankanay deposits (95% purity) (Kazakhstan), fullerene, cellulose, as well as consumed sorbents based on chitosan, milk thistle meal, walnut coal.

All chemicals were of analytical grade.

2.2.2 Synthesis of composites Cu^{2+}/PEG-BT and Cu^{2+}/PEG-ZT

For the purpose of efficient utilization of the consumed sorbents and further use as catalysts. First, 20 g of substrate (bentonite or zeolite) were put in a 250 mL round-bottomed flask and then 100 mL of PEG (1 wt. %) were added. The resulting mixture was then stirred at 25 ° C for 2 hour. The obtained material was filtered and dried at 100°C for 4 h. Next, this dispersed substrate was mixed with 100 mL 0.2 M $CuSO_4 \cdot 5H_2O$ under continuous stirring for 24 h. The solution was filtered through 2-3 μm filter paper and the filtrate was analyzed by an atomic absorption spectrometer (Shimadzu 6200) to determine the residual concentration of Cu^{2+} in the filtrate. The adsorption capacity q (mg/g) for copper ions adsorption on substrates was obtained as follows:

$$q_e = \frac{(C_0 - C_e) * V}{m} \quad (12)$$

where C_0 and C_e, are the initial and equilibrium concentrations (mg/L) of copper ions in the aqueous solution, respectively; V is the volume of the flask (L); m – is the weight of sorbent (g). After, the prepared composites were dried at 100 °C for 4 h, then ground to a powder.

2.2.3 Protocol of synthesis of homogeneous catalyst $[Cu(PEG)_2Cl_2]$

Copper-polymer catalysts were prepared by mixing ready-made aqueous solutions of copper (II) chloride and polyethylene glycol at room temperature. 20 ml of an aqueous solution of $CuCl_2$ $2H_2O$ (0.1 mol, 0.34 g) were poured into a Petri dish and mixed with 20 ml of an aqueous solution of PEG (0.1 mol, 0.14 g). The mixture was stirred on a magnetic stirrer for 10-20 minutes until complete bonding of the polymer with ions of Cu (II). The synthesized catalyst was dried and stored in air at room temperature. The mass of the obtained catalyst: 0.40 g (83.33 %).

2.2.4 Protocol of synthesis of heterogeneous catalyst: Substrate/$CuCl_2$-PVP

Preparation of the catalyst 10 % Cu (II)-(PVP)/substrate (order of submission - (substrate + PVP + $CuCl_2 \cdot 2H_2O$). In a 250 cm^3 round bottom flask, a carrier with a mass of 1.11 g was placed and an aqueous solution with a volume of 5 cm^3 of polyvinylpyrrolidone with a mass of 0.35 g was added. The resulting mixture was stirred at room temperature for 1 hour. Then a 3 cm^3 aqueous solution of $CuCl_2 \cdot 2H_2O$ with a mass of 0.54 g (0.003 mol) was added. The mixture was stirred for 2 hours. The resulting catalyst was left for a day until complete precipitation, after which the precipitate formed was filtered. The yield of supported catalysts was 36–65 %. The resulting catalysts were dried and stored in air at room temperature.

2.3 Experimental Procedure

2.3.1 Procedure of sorption processes

The sorption process was investigated in static conditions. The adsorption of heavy metals was performed by mixing 1 g of adsorbent with a 100 mL solution of known concentration (Pb^{2+} or Cd^{2+} at 2–250 mg/L, Cu^{2+} at 2-400 mg/L) at constant temperature until equilibrium was reached. The equilibrium time was determined from curves of changes in adsorption capacity with contact time. Samples were taken every 30 minutes from the aqueous solution for determination of metal content; the metal concentration was determined by an atomic absorption spectrometer (Shimadzu 6200).

To study the effect of pH on the sorption, 1 g of sorbent was dispersed in 100 mL solutions containing 100 mg/L of each heavy metal ion at 25 °C. The initial pH values were adjusted from 2 to 6 by adding HCl from a 0.1 N solution, and pH measurements were performed using a pX-150MI pH-meter.

2.3.2 Catalytic reduction of 4-nitrophenol by in situ Cu_2O nanoparticles based on PEG-BT and PEG-ZT

The reaction process was as follows, according to the reported methodology [134], 25 mL of 4-nitrophenol solution (2.5 mM) were mixed with 25 mL of freshly prepared aqueous $NaBH_4$ solution (0.25 M) and were stirred. The color of the solution changed from slightly yellow to bright yellow. Then, 15 mg of the Cu^{2+}/PEG-BT (or Cu^{2+}/PEG-ZT) composite were added to the mixture. To monitor the reaction, 1.0 mL of the solution was removed and diluted to 25 mL for further UV-vis absorption analysis at certain time intervals. The concentration of 4-NP was determined spectrophotometrically at a wavelength of 400 nm. At the end of the reaction, the solution became colorless and precipitates were observed.

2.3.3 Methods of studying the oxidation of yellow phosphorus with oxygen in the presence of homogeneous $CuCl_2$-PEG catalysts in an aqueous medium in an oxygen atmosphere

The experimental process was as follows. A sample of the catalyst was poured into a 150 ml reactor, distilled water was introduced and oxygen was blown. The reactor and the burette were heated to the temperature of the experiment, the initial redox potential of the solution was measured. Then a solution of P_4/C_7H_8 was added

and an electric motor was turned on. During the experiment, the potential in the reaction solution was measured continuously, determined by the ratio of the Cu^{2+}/Cu^{+} (φ, V) pair and measured by the platinum electrode immersed in the solution relative to the calomel half-cell using a pH-340 potentiometer, and then calculated on a hydrogen scale. The temperature was kept with an accuracy of ±0.5 ° C using a U-8 thermostat. After the experiment, the solution from the reactor was decanted and analyzed on a spectrophotometer SPEKOL 1300 (ANALYTIK JENA, Germany).

2.3.4 Methods of studying the oxidative butoxylation of yellow phosphorus in the presence of heterogeneous supported $CuCl_2$-PVP catalysts

The reaction was studied by the volumetric method on a thermostatted installation (Figure 4) with a vigorously shaken reactor and an out-of-glass glass gradient-free thermostatted catalytic duck reactor equipped with a potentiometric device and connected to a gas burette filled with argon.

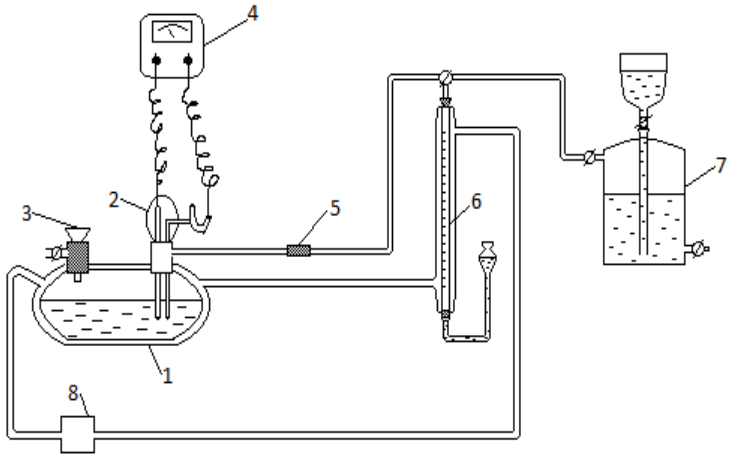

1 - a "duck"-type reactor, 2 — a platinum electrode paired with a saturated calomel half cell, 3 — a device for sampling the reaction solution, 4 — a pH-121 potentiometer, 5 — a calcium chloride tube, 6 — a thermostatted burette, 7 — a gasometer, 8 — a thermostat U-8

Figure 4 – Flowless glass gradient-free thermostatted "duck" reactor

Experiments were performed as follows: the sample of the catalyst was poured into a 150 cm^3 reactor and purged with argon. The reactor and the burette were heated to the temperature of the experiment, the initial redox potential of the solution was measured. Then, butanol, carbon tetrachloride, pyridine, and solution of P_4/C_7H_8 an electric motor was turned on. During the experiment, the potential in the reaction solution was measured continuously, determined by the ratio of the Cu^{2+}/Cu^{+} (φ, V) pair and measured by the platinum electrode immersed in the solution relative to the calomel half-cell using a pH-340 potentiometer, and then calculated on a hydrogen scale. The temperature was kept with an accuracy of ±0.5 ° C using a U-8 thermostat. After the experiment, the solution from the reactor was decanted and analyzed on a gas chromatograph (GC-2010 Plus).

2.4 Physico-chemical methods for the study of composite materials

Scanning electron microscopy. Electron micrographs of composite materials were taken on a high resolution scanning electron microscope (HR-SEM) (FEI, Magellan 400L). SEM experiments and analyzes were carried out at the Institute of Nanotechnology and Advanced Materials at Bar-Ilan University (Israel). For better image quality and charge removal and shielding of the incident beam, some non-conductive samples were sprayed with gold. In addition, the synthesized samples were examined by autoelectron microscope (FE-SEM, FEI QUANTA 3D 200i). Analyzes on this device are made at the National Open-Type Nanotechnology Laboratory at the Al-Farabi Kazakh National University.

IR spectroscopy. The IR spectra of the obtained materials were taken on a Fourier Spectrum 65 IR spectrometer in the range 4000-450 sm^{-1}. Solid tablets with KBr were identified by absorption bands of O-Si groups (for quartz) (1631 sm^{-1}).

X-ray diffraction analysis (XRD). Structural features were investigated by X-ray diffraction (XRD) spectroscopy (AXS D-8 Advance, BRUKER) with Cu Kα (λ=1.5418 Å) operating at 40 kV/40 mA.

Determination of specific surface area (BET method). The textural features were measured by nitrogen sorption (Quantachrome NOVA 3200e) at -196°C. The pore distribution and pore volumes were calculated using the adsorption branch of the N_2 isotherms based on the Barrett-Joyner-Halenda (BJH) model. The specific surface area (S_{BET}) was calculated according to the BET theory up to the nitrogen relative pressure of 0.2.

Methods for studying the composition of polymer-metal complexes include conductometric and potentiometric methods for determining the composition of a complex and for calculating thermodynamic constants.

*Potentiometric titration***.** As is known, potentiometry is one of the methods most widely used to study complexation processes involving both low and high molecular weight ligands. There are several varieties of potentiometric methods for analyzing polymer-metal complexes. In this paper, a modified Bjerrum method is considered, which was used in the work to determine the composition and stability constants of the resulting complex compounds [67].

In order to determine the mechanism of interaction of metal ions with a polymer, potentiometric titration of polyethylene glycol (PEG), a polyligand, was carried out in the absence and in the presence of a complexing agent with acid. From the curve of potentiometric titration of PVP in the absence of a metal, the acid dissociation constant of its functional groups was found.

Conductometric titration. Conductometric studies were performed on an I-4100 ionomer with platinum electrodes under thermostatically controlled conditions. The method of conductometric titration is based on the change in the electrical conductivity of the solution, depending on the addition to it of another solution of a known concentration.

Conductometric and potentiometric titrations were performed simultaneously, controlling in one cell the change in pH and electrical conductivity in the systems under study.

The complexes were obtained by mixing aqueous solutions of the initial components at a certain ratio and pH.

UV-Vis spectroscopy. The conversion of the nitro compound (4-NP) to 4-aminophenol (4-AF) and the reaction kinetics were controlled using a UV-visible spectrophotometer (CARY 100 Bio). The standard quartz cuvettes (10 mm) were used for the experiments.

Atomic Absorption Spectroscopy. The initial and residual concentration of heavy metal ions in aqueous solutions was determined by the AAS method on an atomic absorption spectrophotometer Shimadzu 6200.

Chromatographic analysis. Organophosphorus products were quantitatively analyzed with respect to standard samples on a GC-2010 Plus chromatograph equipped with a flame ionization detector and Supelco SMS capillary columns (30 m×0.25 mm) from «Shimadzu» (Japan). Hydrogen was used as gas carrier. The initial and final temperatures are 120 and 220 ^{o}C, and the initial and final time are 0-7 minutes, respectively. Heating rate is 25 °C/min, detector temperature is 300 ^{o}C. In the studied conditions, the oxidation products of alcohols are not detected, oxygen is consumed only for the oxidation of yellow phosphorus.

3 RESULTS AND DISCUSSION

3.1 Physico-chemical characteristics of composite materials

3.1.1 Synthesis of clay composite material - BT-PEG

The obtained BT-PEG sorbent was thoroughly characterized by EDX, FE-SEM, XRD and BET analysis. Existence of Ca (55.54 % w/w), Si, Al, Mg, Na, Fe and O were observed by elemental analysis. High calcium content in the original and modified BT-PEG sorbent indicates effective sorption capability (Table 6) [157]. After modification, a slight increase in carbon and oxygen content and decrease in calcium content can be seen, which confirm the successful synthesis of BT-PEG.

Table 6 - Elemental composition of BT and BT-PEG

Element	BT		BT-PEG	
	Wt%	At%	Wt%	At%
C	4.87	11.9	6.24	14.48
O	13.85	25.44	14.14	24.66
Na	0.75	0.96	1.52	1.85
Mg	1.76	2.12	3.21	3.68
Al	3.84	4.19	5.01	5.18
Si	10.38	10.86	14.21	14.12
K	0.98	0.74	1.51	1.08
Ca	55.54	40.71	47.44	33.02
Fe	5.08	2.67	2.82	1.41

Physico-chemical and textural characterization of the initial and modified bentonite sorbent are summarized in Table 7. Bentonite in its dry state was shown to have a moisture content of around 8.6 % and ash content of 6.4 %. Moreover, the data shows that modification of the initial bentonite clay leads to a significant reduction in the total pore volume of acetone (from 29.05 to 19.12 %), which indicates a reduction in the number of mesopores. In addition, the increase in iodine adsorption (from 30.60 to 40.00 %) indicates an improvement in the microporous structure. Water sorption measurements indicated that the total pore volume decreased as a result of the polymer modification. Hence, we conclude that the modification of bentonite by PEG leads to a predominance of meso- and micro-pores in the sorbent structure, which significantly enhance the adsorption of heavy metal ions.

Table 7 - Textural characterization of BT and BT-PEG

Characterization	BT	BT-PEG
Moisture , %	8.60	4.90
Ash content , %	6.40	23.30
The total pore volume of acetone, %	29.05	19.12
Adsorption activity on iodine, %	30.60	40.00
The total pore volume of water, cm^3/g	0.010	0.009

Figure 5 shows typical FE-SEM images of non-modified BT and modified BT-PEG after sorption of Pb^{2+} and Cd^{2+} ions. Non-modified BT (Fig. 5 A) had significantly uniform texture provided primarily by micropores with diameter in the range of 1–4 μm. Needle-shaped growths of the polymer can be seen in this image (Fig. 5 B), which indicates the impregnation of PEG. The near absence of crystallinity after loading the sample with Pb^{2+} and Cd^{2+} ions (Fig. 5 C, D) indicates that there was no crystalline phase transformation after sorption.

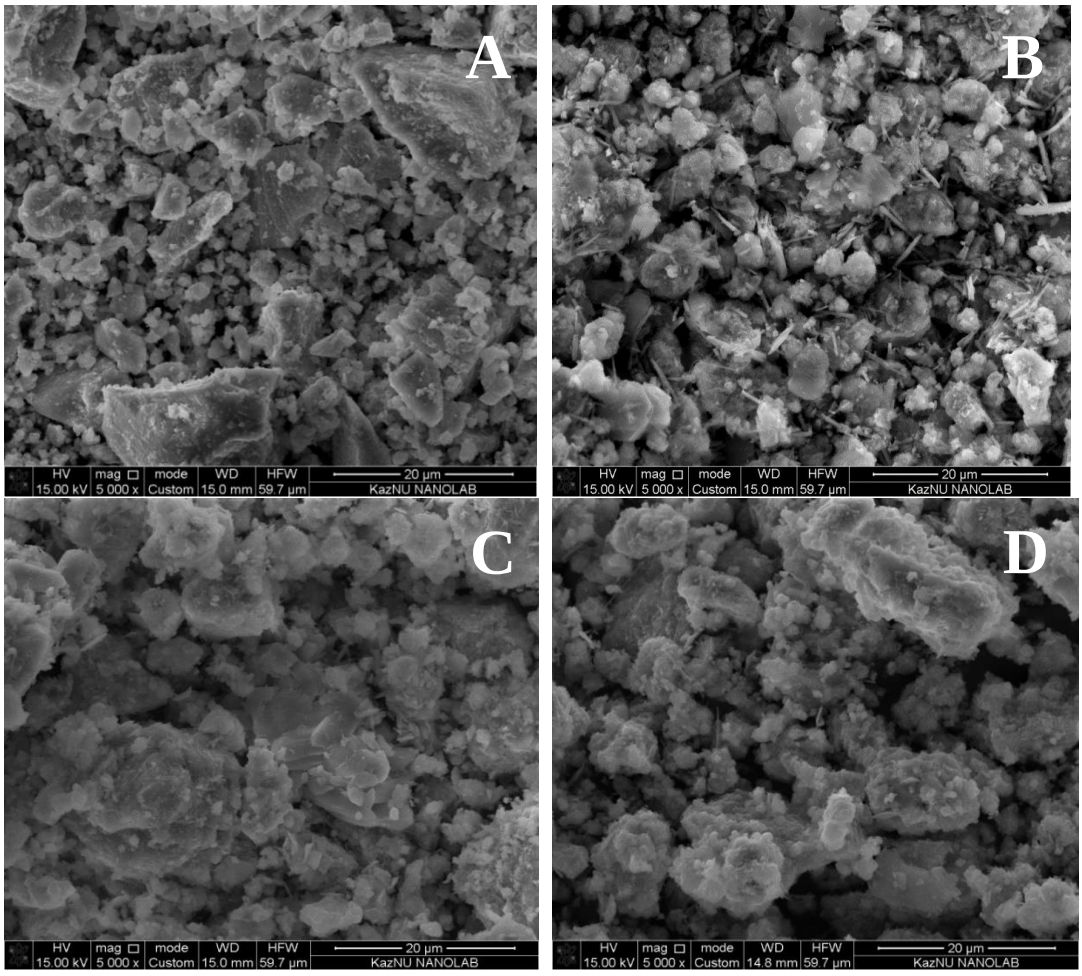

A – BT; B - BT-PEG; C - BT-PEG-Pb and D -BT-PEG-Cd

Figure 5 - SEM images of sorbents

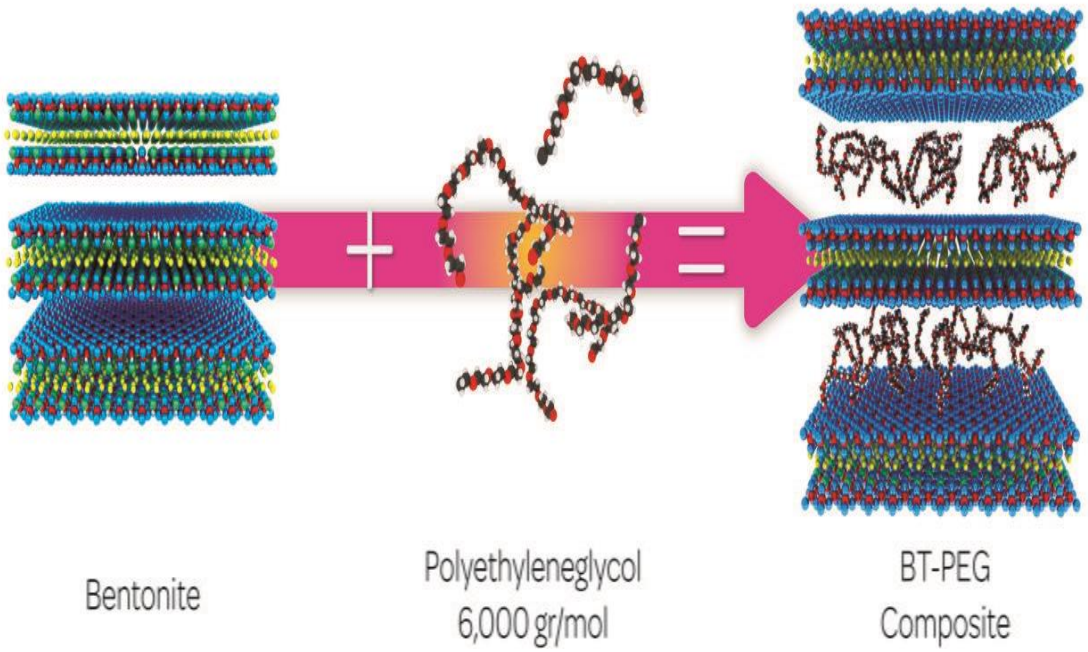

Figure 6 - Schematic illustration of BT modification by PEG

It is known that montmorillonite is the main mineral of bentonite; it has a 2:1 layer structure, consisting of an octahedral alumina sheet sandwiched between opposing tetrahedral silica sheets [34]. The bonding between the two silica sheets is very week, allowing water and exchangeable ions to enter. It was assumed that adsorption of PEG can occur on both external surface and interlayer spaces (Figure 6). Then, the adsorption proceeds according to the ion-exchange mechanism, which is presented for BT (13) and PEG (14) as follows:

$$2 \equiv \mathrm{Si}{-}\,\mathrm{O}{-}\mathrm{H} + \mathrm{Me}^{2+} \rightarrow \equiv \mathrm{Si}{-}\,\mathrm{O}{-}\,\mathrm{Me}^{2+}{-}\,\mathrm{O}{-}\,\mathrm{Si} \equiv + 2H^{+} \quad (13)$$

$$2OH - (CH_2 - CH_2 - O)_n - H + Me^{2+} \rightarrow$$

$$OH - (CH_2 - CH_2 - O)_n - Me^{2+} - O - (CH_2 - CH_2 - O)_n + 2H^{+} \quad (14)$$

The XRD patterns of raw bentonite (A) and modified bentonite (B) are shown in Figure 7. The raw bentonite contains characteristic diffraction peaks of montmorillonite (M), which are located at 2Θ = 20.49, 32.64 and 62.54 and quartz (Q), where the characteristic peaks are located at 2Θ = 37.14, 39.02 and 50.85, respectively. The other peaks are impurities corresponding to crystobalite, field spar and illite [191]. However, as can be seen in the diffraction pattern of BT-PEG shown in Figure 7, while there is a change in the intensity of the peaks, the appearance of new peaks is not detected. This might be due to the low concentration of the modifying agent or to the high dispersion of polymer particles in the bentonite

matrix. EDS data showing polyethylene glycol particles fixed onto the surface of bentonite is given in Table 6.

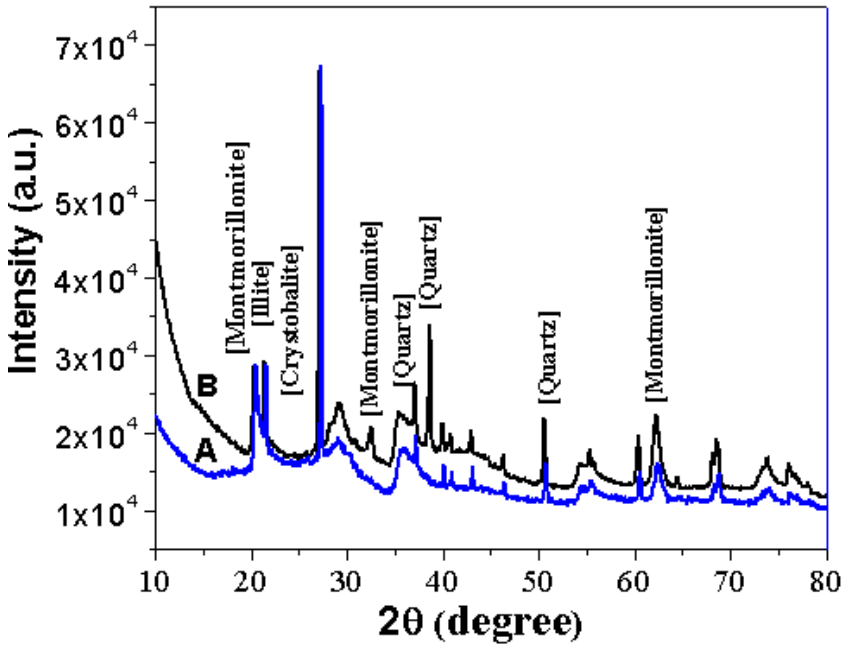

Figure 7 - XRD patterns of (A) natural bentonite and (B) BT-PEG

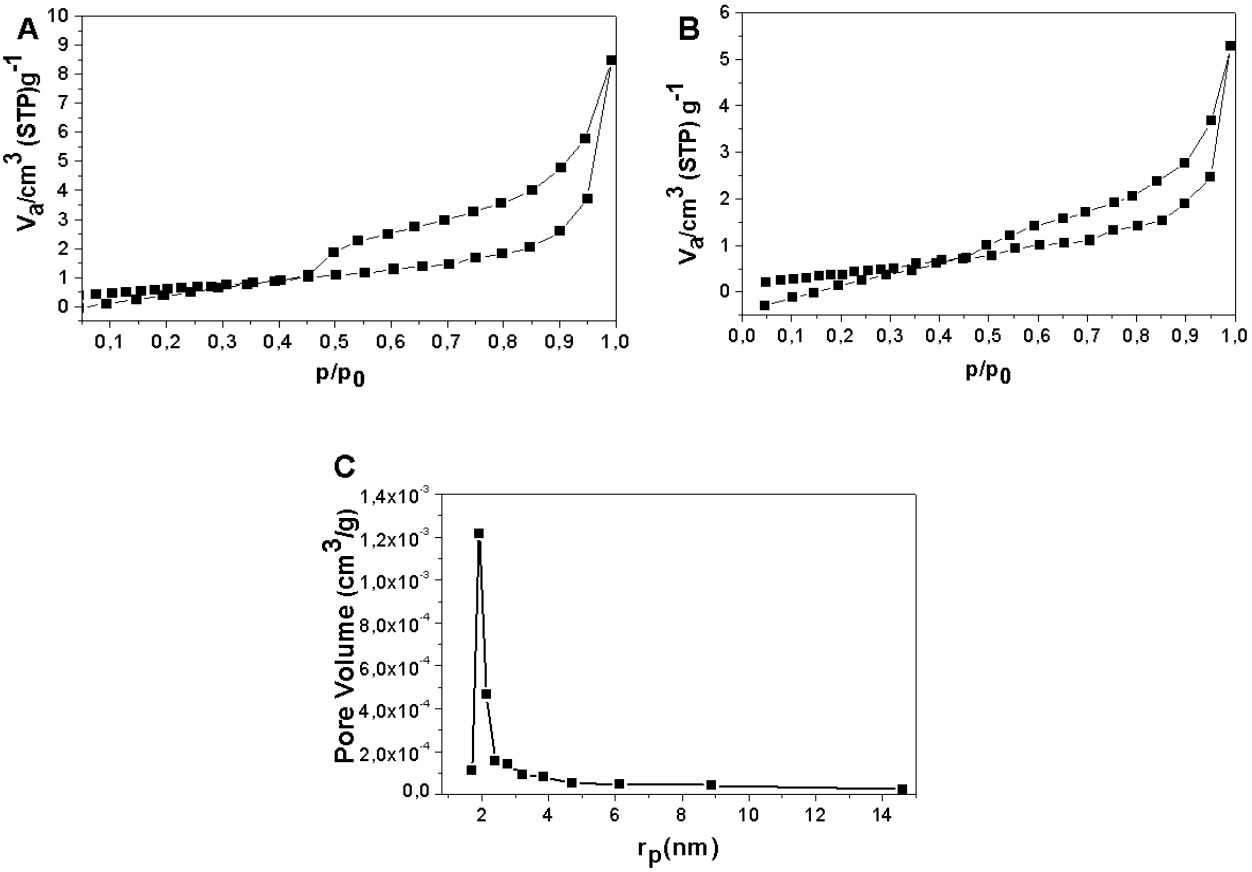

A – BT; B - BT-PEG and C - Barrett-Joyner-Halenda (BJH) pore size distribution plot

Figure 8 - N_2 adsorption-desorption isotherms of the BT-PEG

Adsorption isotherms enable to draw conclusions about the surface area, the porosity of the adsorbent, and the nature of the interaction between the sorbent and the sorbate. Figure 8 shows N_2 adsorption-desorption isotherms indicating that the surface area, total pore volume and average pore diameter decreased significantly by modifying the BT by PEG, from 4.13 to 3.67 m^2/g, 0.0131 to 0.0082 cm^3/g, and 222 to 186 nm, respectively. This reduction in the values of the characteristic attributes of the BET theory was assumed to arise due to the introduction of the polymer in the pores of the initial bentonite. However, from Figure 8C, we can see that the modified bentonite has a narrow pore size distribution of about 2–4 nm.

Hence, the composite material BT-PEG based on bentonite of the Dinozaur deposit were synthesized. The surface area, total pore volume and average pore diameter of BG-PEG were calculated as 3.67 m^2/g, 0.0082 sm^3/g and 186.3 nm. SEM, XRD, and BET analysis indicate intercalation of the PEG polymer into the initial structure of bentonite.

3.1.2 Synthesis of plant composite material – OP-PVP, MP-PVP

It is known from the literature data, that citrus peel shows practical interest as a raw material for the production of effective sorbents with respect to metal ions [72].

In this section the physico-chemical and textural properties of the composite material based on citrus peel are presented. The choice of this material is based on the fact that most of them are thrown away as unnecessary waste and almost never used. However, as a renewable resource, they can be a valuable source of raw materials for environmental and technological developments, including wastewater treatment. The polymer - polyvinylpyrrolidone (PVP) was used as a modifier, due to its good complexing ability, non-toxicity and availability on the market.

The obtained values of the results of physico-chemical analysis of the source objects and the obtained composites are given in the Table 8.

Table 8 - Physico-chemical characteristics of materials based on vegetable raw materials

Sorbent	Moisture, %	Ash content, %	Total Acetone Porosity, %	Total Pore Volume by Water, cm^3/g	Activity by I_2, %
Orange Peel (OP)	7.86	11.55	60.36	7.23	32.59
OP + PVP	7.56	26.51	42.31	8.63	37.20
Mandarin Peel (MP)	8.29	19.85	48.43	5.63	33.52
MP + PVP	6.67	28.57	31.33	6.45	38.24

Based on the data presented in Table 8, it can be noted that the preliminary materials have rather high textural characteristics, such as total acetone porosity and

iodine activity. Especially, the total porosity of acetone - for orange peel reached 60%, which is 12 % higher than the value for mandarin peel. Perhaps this is due to the mesoporous surface structure of the orange peel and the microporous structure of the mandarin surface, as evidenced by the value of iodine activity.

As a result of two-stage modification of citrus peel, such characteristics as total pore volume of water and iodine activity increased. Other values as the total pore volume of acetone and the humidity are reduced. It can be concluded that the functionalization of pristine orange and mandarin peel with PVP polymer increases the amount of meso- and micropores in the sorbent structure.

The surface of the composites was studied by the SEM method (Figure 9). This method allows you to simultaneously explore the size and shape of the grain of the sample, the distribution of grains and phases in size, to determine their composition and distribution of chemical elements on its area and on the area of the material, the chemical heterogeneity on the area of thin section.

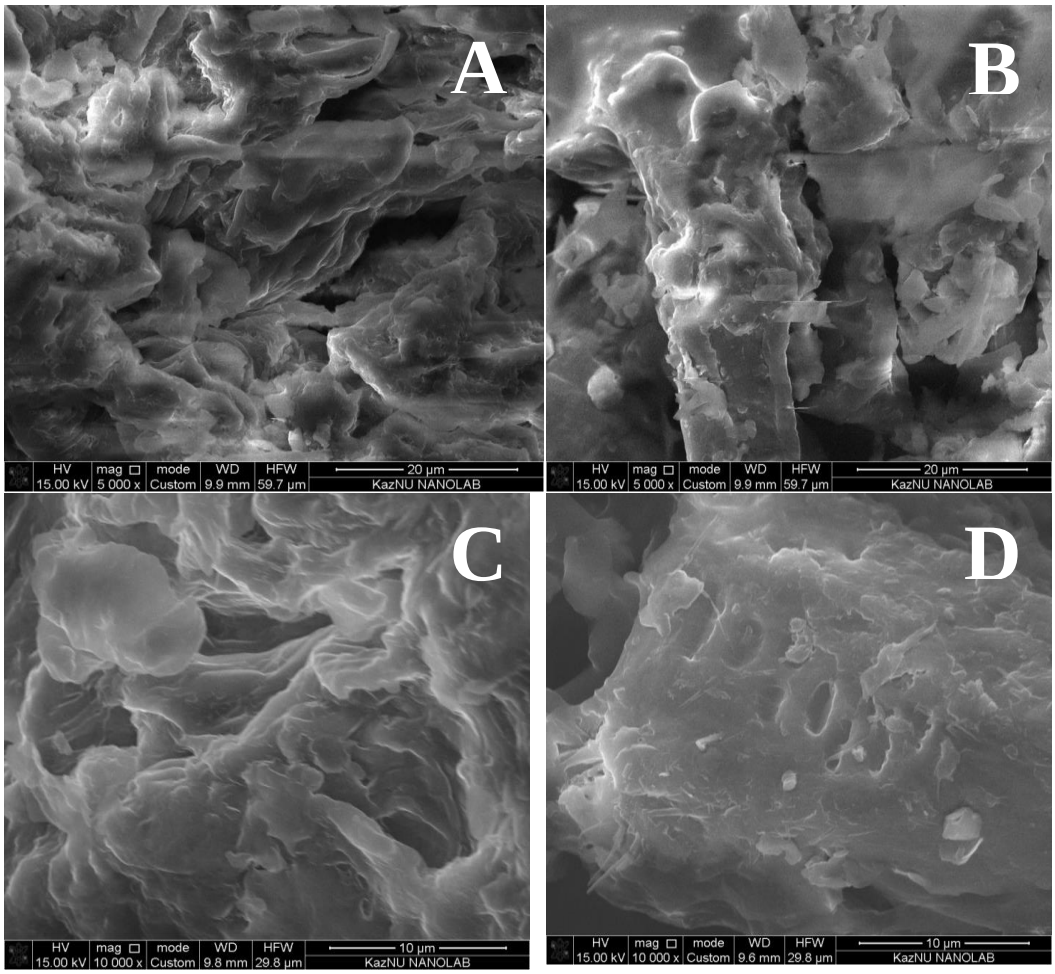

A –OP; B – MP; C - OP-PVP and D - MP-PVP

Figure 9 – SEM images of sorbents

SEM images show that modifying the initial OP leads to the development of amorphous structure, which ensures the effective extraction of HM ions from

aqueous solutions with this material. Similar results were obtained with mandarin peel, where a more porous surface structure is observed after treatment MP with the modifier.

In order to study the structure and structure of composite materials, an IR spectroscopic study of the original and modified samples were carried out. The data are presented in the Table 9.

The assignment of the bands was carried out by comparing the obtained IR spectra with the IR spectra of various types of lignin and cellulose of plant materials, as well as with the correlation diagrams of group frequencies.

Table 9 – IR spectra of CM based on the orange and mandarin peel

OP	OP-PVP	MP	MP-PVP	Description of IR bands
Peak position (frequency, cm^{-1})				
2925	2928	2928	2929	Asymmetric stretching bond vibrations CH_2
1736	1738	1740	1740	Symmetric stretching bond vibrations –O-N=O
1632	1630	1634	1622	Deformation vibrations H-O-H
1517	1517	1516	1517	Bond oscillations Ar-N=O (Ar – arenes)
1441	1441	1441	1441	Symmetric deformation oscillations CH_3
1265	1263	1268	1267	Asymmetric stretching bond vibrations –C-O-C- (esters)
1054	1068	1055	1052	Bond oscillations –C-OH (unsaturated alcohols)

In the IR spectra of the pristine materials: OP and MP, there are a series of bands with peaks at 2956, 1265, 1054 cm^{-1}, which are identified as fluctuations in the functional groups of cellulose, which are the main component of plant tissue. This is known to be a polysaccharide whose molecules are long chains with a spatially correct structure consisting of β-D-glucose units (β-D-glucopyranase) linked by glucoside bonds.

For example, the band with a maximum at 1054 cm^{-1} corresponds to the stretching vibrations of hydroxyl groups included in hydrogen bonds. Bands with peaks at wave numbers of 1517 cm^{-1}, thanks to skeletal vibrations of aromatic rings, indicate the presence of lignin, which is a natural polymer consisting of structural elements (type I and II) C_6C_3 - oxygen derivatives of phenylpropane produced from carbohydrates.

The presence of absorption bands at 1265 cm^{-1} can be explained by the presence of valent asymmetric vibrations of C–O–C bonds in the methoxyl groups of lignin.

As a result, according to IR spectroscopy, it follows that materials based on orange and tangerine peel is a complex complex of organic components. Analysis of the IR spectrum of modified KM indicates the presence of CH_2 - groups (2925 cm^{-1}),

as well as the presence of = C – H, Ar – N = O groups, which can easily be replaced by heavy metal ions [192].

3.1.3 Synthesis and characterization of the catalysts - Cu^{2+}/PEG-BT and Cu^{2+}/PEG-ZT

The catalysts were prepared by a simple, low-cost and rapid method, which consists of two steps. First, the impregnation of copper ions onto bentonite and zeolite using a protective and stabilizing polymer polyethylene glycol. Secondly, Cu_2O NPs were obtained in the presence of $NaBH_4$ during the catalytic reduction of 4-NP to 4-AP. These synthesized composites were investigated by a number of methods as XRD, HR-SEM, EDX and BET analysis.

The XRD patterns of the raw bentonite, composite Cu^{2+}/PEG-BT, and catalyst after reaction Cu_2O/PEG-BT are shown in Figure 10.

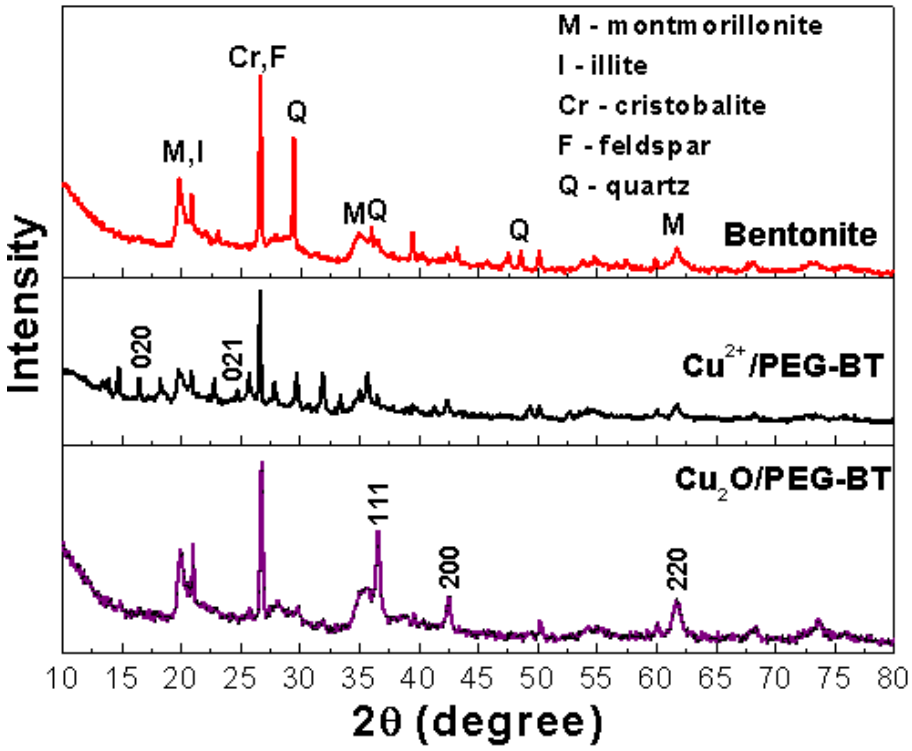

Figure 10 - XRD patterns of bentonite, Cu^{2+}/PEG-BT and catalyst after reaction Cu_2O/PEG-BT

The main minerals contained in the bentonite are montmorillonite and quartz. Montmorillonite is characterized by the peaks at 2θ = 19.72, 34.92 and 61.82 corresponding to the (020), (130) and (060) planes. The other peaks at 2θ = 29.45, 36.04 and 48.59 were indexed to the (101), (110) and (201) planes of quartz. The other peaks are related to cristobalite, feldspar and illite contents.

The XRD pattern of Cu^{2+}/PEG-BT in the black curve of Figure 10 reveals the formation of copper hydroxide $Ca(OH)_2$ compound, with the peaks at 2θ = 16.56, 24.87 corresponding respectively to the (020) and (021) planes of copper hydroxide (JCPDS No. 13-0420). The XRD diffraction pattern of the catalyst after the reaction

as shown in the purple curve of Figure 10 shows the formation of Cu_2O compound. The peaks at 2θ = 36.77, 42.55 and 61.68 correspond respectively to the (111), (200) and (220) planes of the cubic lattice structure of Cu_2O. The average crystallite size, calculated by Scherrer formula from peaks of Cu_2O is about 20 nm.

The XRD pattern of the initial sample of zeolite (red curve of Figure 11) shows sharp peaks that indicates the presence of clinoptilolite-Ca ($(NaKCa)_6(SiAl_{36})O_{72}$) as the major phase, heulandites ($CaAl_2Si_7O_{18}\cdot 6H_2O$) as the secondary phase and muscovite-($KAl_2(AlSi_3O_{10})(OH)_2$) as the minor phase.

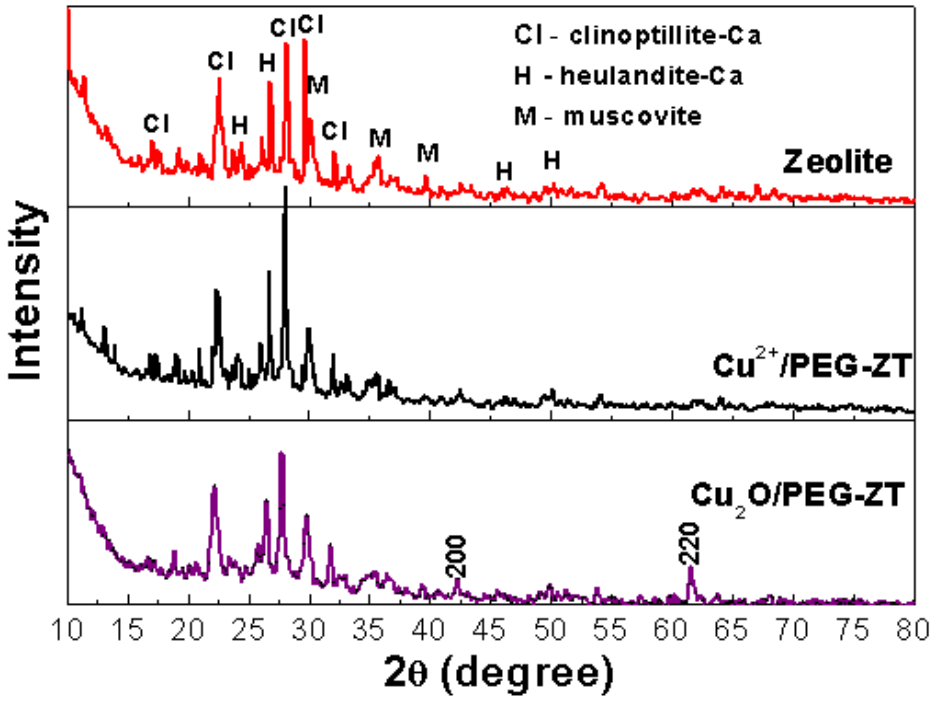

Figure 11 - XRD patterns of zeolite, Cu^{2+}/PEG-ZT and catalyst after reaction Cu_2O/PEG-ZT

As seen from the XRD pattern of Cu^{2+}/PEG-ZT in the black curve of Figure 13, no new peaks were obtained. This can be explained by the absence of crystal structure of the copper-containing compounds. However, the presence of copper element was confirmed by EDS analysis. The diffraction peaks of the catalyst after reaction were assigned to Cu_2O (JCPDS No. 05-0667), with peaks at 2θ = 42.19, 61.50 corresponding to the (200), (220) planes. The average crystallite size calculated by the Scherrer formula is about 20 nm.

The sheet like structures of the precursors Cu^{2+}/PEG-BT and Cu^{2+}/PEG-ZT can be seen in the HR-SEM images of Figure 12 (A-B).

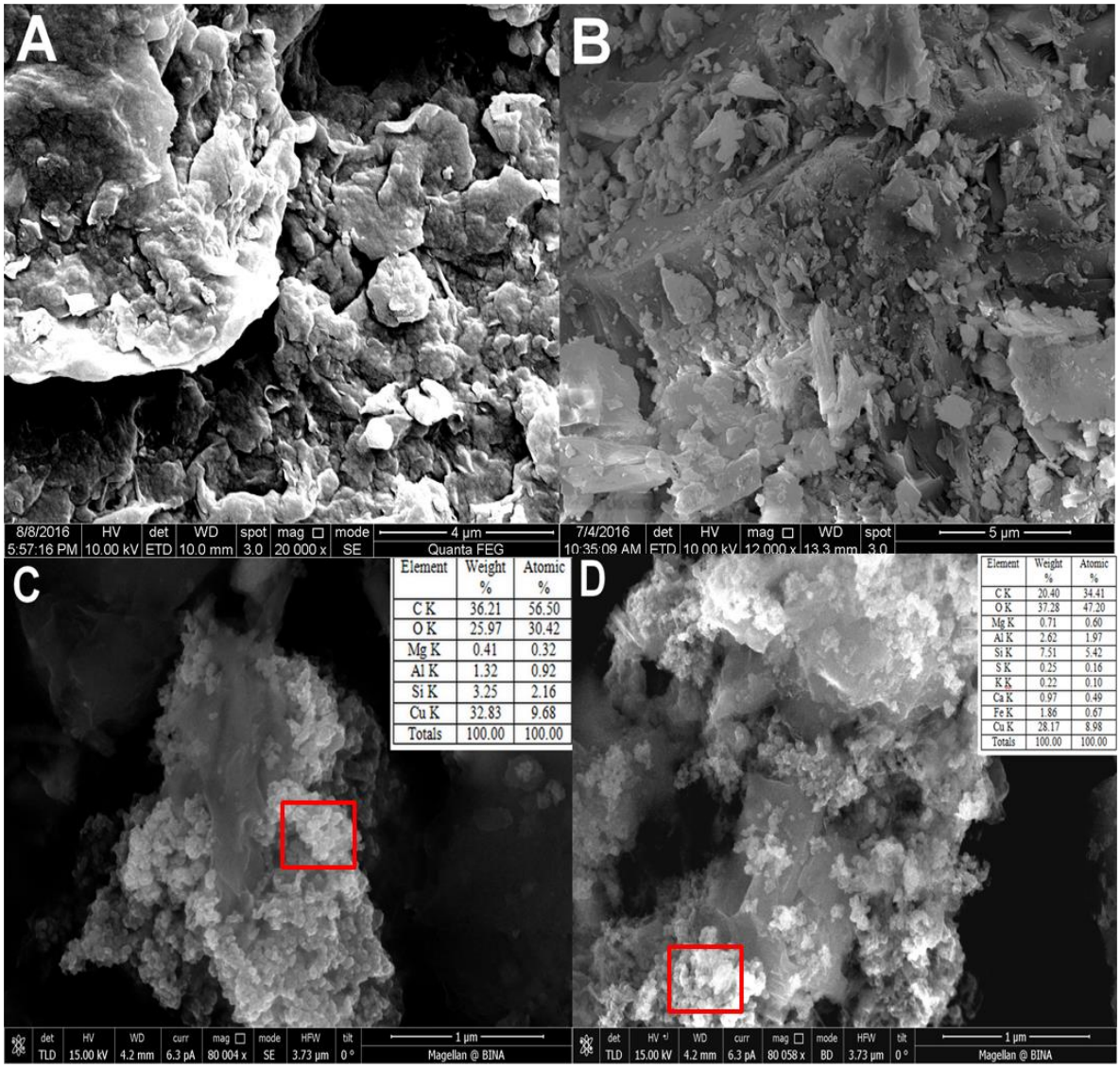

Element	Weight %	Atomic %
C K	36.21	56.50
O K	25.97	30.42
Mg K	0.41	0.32
Al K	1.32	0.92
Si K	3.25	2.16
Cu K	32.83	9.68
Totals	100.00	100.00

Element	Weight %	Atomic %
C K	20.40	34.41
O K	37.28	47.20
Mg K	0.71	0.60
Al K	2.62	1.97
Si K	7.51	5.42
S K	0.25	0.16
K K	0.22	0.10
Ca K	0.97	0.49
Fe K	1.86	0.67
Cu K	28.17	8.98
Totals	100.00	100.00

A - Cu^{2+}/PEG-BT; B - Cu^{2+}/PEG-ZT composites; and catalysts C - Cu_2O/PEG-BT; D - Cu_2O/PEG-ZT after catalytic reaction

Figure 12 - HR-SEM images and EDS analysis of catalysts

The elemental analysis of the precursors obtained with EDS shows the peaks related to Cu at 2.26 % w/w and 1.34 % w/w respectively in the Cu^{2+}/PEG-BT and Cu^{2+}/PEG-ZT, which confirmed the successful impregnation of Cu onto the supporting materials. On the surface of the catalysts after reaction (Figure 12 C-D) the formation of tubular NPs of copper oxides can be seen, which are presumably formed as a result of the reduction by $NaBH_4$. For further confirmation, EDS analysis was performed for the synthesized Cu_2O NPs after reaction. The EDS results given in the insets of figure 14 C-D show the presence of copper and oxygen as elementary components with high mass percentages, which confirm the formation of copper oxide NPs. In addition, the particle size was found to be about 20 nm, in agreement with the results obtained from the Scherrer formula.

The nitrogen adsorption-desorption isotherms and surface area measurements of Cu_2O/PEG-BT and Cu_2O/PEG-ZT are presented on Table 10 and Figure 13.

According to IUPAC classification, the two curves of Figure 15 are well described by a type II isotherm with hysteresis loop of type H_3. The type H_3 loop does not exhibit any limiting adsorption at high p/p^0. This type of isotherm is supposed to occur with aggregates of plate-like particles giving rise to slit-shaped pores.

The surface area characteristics obtained by BET analysis for the initial bentonite and zeolite and the samples after reaction are given in Table 10. The samples after reaction were characterized by reduced surface areas and pore volumes as compared to the initial bentonite and zeolite. For Cu_2O/PEG-BT, the surface area decreased from 4.14 to 0.50 m^2/g and the total pore volume decreased from 0.023 to 0.010 cm^3/g, while its pore size increased from 22.20 to 80.7 nm. For Cu_2O/PEG-ZT, the surface area decreased from 3.51 to 2.24 m^2/g and the total pore volume decreased from 0.016 to 0.014 cm^3/g, while its pore size increased from 17.81 to 25.64 nm. The increase in the average pore diameter for both Cu_2O/PEG-BT and Cu_2O/PEG-ZT is possibly related with the blocking of the smaller micropores of the initial clays by the PEG and the copper oxide (I) particles.

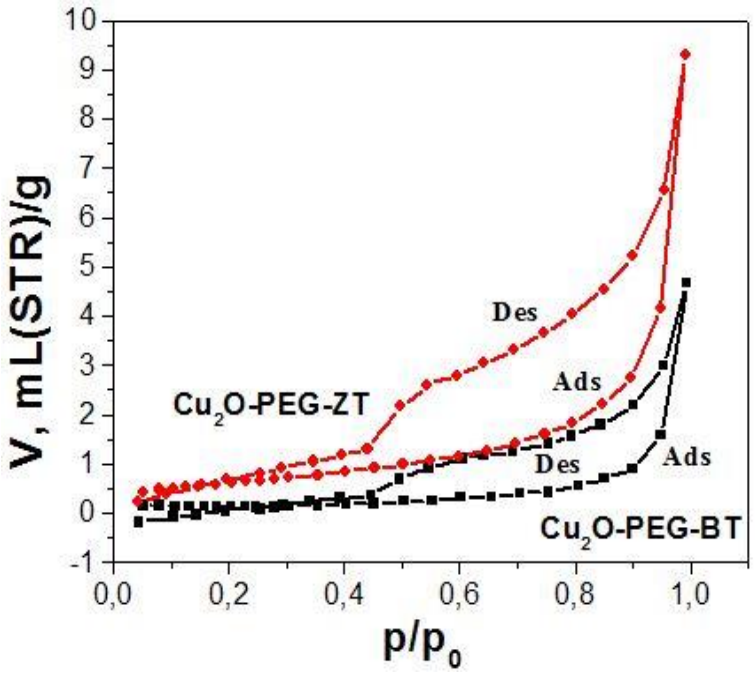

Figure 13 - The N_2 adsorption-desorption isotherms of Cu_2O/PEG-BT and Cu_2O/PEG-ZT

Table 10 – Surface area characteristics obtained by BET analysis

Sample	Surface area, m^2/g	Total pore volume, cm^3/g	Average pore diameter, nm
Initial Bentonite	4.14	0.023	22.20
Cu_2O/PEG-BT	0.50	0.010	80.70
Initial Zeolite	3.51	0.016	17.81
Cu_2O/PEG-ZT	2.24	0.014	25.64

Consequently, new composites Cu_2O/PEG-BT and Cu_2O/PEG-ZT were synthesized. Based on the XRD results, the formation of the cubic phase of Cu_2O was established. The presence of nano-sized copper (I) oxide (20 nm) was confirmed by HR-SEM and EDS.

3.1.4 Physico-chemical study of the complexation process of Cu^{2+} ions with polyethylene glycol

Catalysis by polymers, based on the chemistry of high-molecular compounds, is one of the intensively developing areas of coordination and catalytic chemistry. For instance, complexes which acting on the principle of enzymes, many of which are ionic coordinated with metal ions. It is known that such polymer-metal complexes exhibit high catalytic activity, stability, selectivity of the action [181-184]. Catalytically active metal complexes fixed on polymer substrates have great prospects in chemical technology of inorganic and organic materials to solve problems in the field of petrochemical production. The study of the complexation processes of the latter with the polymer ligand is not only of theoretical interest for expanding the field of coordination chemistry of polymers, but also has a practical direction. Polymeric compounds containing functional groups are suitable carriers of metal ions. In the interaction of polymers with metal ions, new coordination compounds are formed, combining the properties of the initial components, as well as possessing a number of unique properties, in particular, high catalytic activity. In this regard, this section presents the results of a physicochemical study of the complex formation of polymeric ligands with copper (II) ions in order to further establish their catalytic activity.

Table 11 – Characteristic IR spectra of the investigated samples (ν, cm^{-1})

Sample	ν NH	ν CH_3	δ CH_3	ν –C-N-	ν fluct. arom. ring.	ν OH	ν C=O	ν CH_2	δ CH
PVP	3438	2921		1320 1275 1168	-	-	1643	-	-
$[Cu(ПВП)_3Cl_2]$	3427	-	1443	-	1494	-	1618	-	-
10% $CuCl_2$-PVP/cellulose	-	-	-	1348 1335 1304	-	2562	-	2934	1427
10% $CuCl_2$-PVP/coal	3399	-	-	-	1495	-	-	-	1445 1419
10% $CuCl_2$-PVP/thistle	3396	-	1421 1466	1321 1294	1497	2927	-	-	-
10% $CuCl_2$-PVP/chitosan	3432	-	1466 1385	1172	1496	-	-	2957	1445

Polyvinylpyrrolidone (PVP) and polyethylene glycol (PEG) were used as the polymer ligand. High tendency to complexation, non-toxicity, good solubility in

various solvents, including high solubility in aqueous media, provides them wide application in the textile, food, pharmaceutical industry and medicine.

The nature of the modifying effect of PVP on Cu (II) ions and the possible molecular structure of the PVP-$CuCl_2$ complexes was studied using IR spectroscopy, the results are presented in the Table 11.

The carbonyl group in PVP is characterized by a peak at 1643 cm^{-1}, broadened due to the C = N bond in the lactam ring. This band shifts to 1618 cm^{-1} in the complexes of PVP-$CuCl_2$. The difference in the IR spectra of PVP and the PVP-$CuCl_2$ complexes is observed due to the donor-acceptor interaction between the oxygen atom in the polymer ligand PVP and Cu (II) ions [193].

Attaching the copper in the polymer/substrate system can be refereed from the results of IR spectroscopy and scanning electron microscopy (SEM). As can be seen from the IR spectra, the peak characteristic of the C = O bond in PVP becomes asymmetric in the complex, which indicates the interaction between PVP and Cu (II) with the formation of a PVP-$CuCl_2$ complex. The IR spectra of PVP and PVP-$CuCl_2$ complexes contain bands at 3400 cm^{-1}, characteristic of PVP.

Polyvinylpyrrolidone is a polymer, soluble in water and organic solvents, which contains a lactam ring associated with the polymer chain. The resonant mechanism of the lactam ring is formed by nitrogen and oxygen atoms, which act as a dipole. PVP contains imine bond C = N and exhibits a polybasic behavior in aqueous solutions due to the protonation/deprotonation of the oxygen atom.

The study of the complexation of metal ions with a polymer ligand is not only of theoretical interest for expanding the field of coordination chemistry of polymers, but also has a practical direction. To study the surface of polymer-metal complexes of copper, the method of scanning electron microscopy was used, the results are presented in the Figures 14-15.

The formation of polymer films in the shape of various fibrillar small spherolites of various sizes was occurred (Figures 14-15). The obtained supported polymer-metal complexes (PMC) were used as catalysts in the reactions of oxidation of yellow phosphorus. SEM images of catalyst surfaces after the reaction are characterized by a heterogeneous, friable structure.

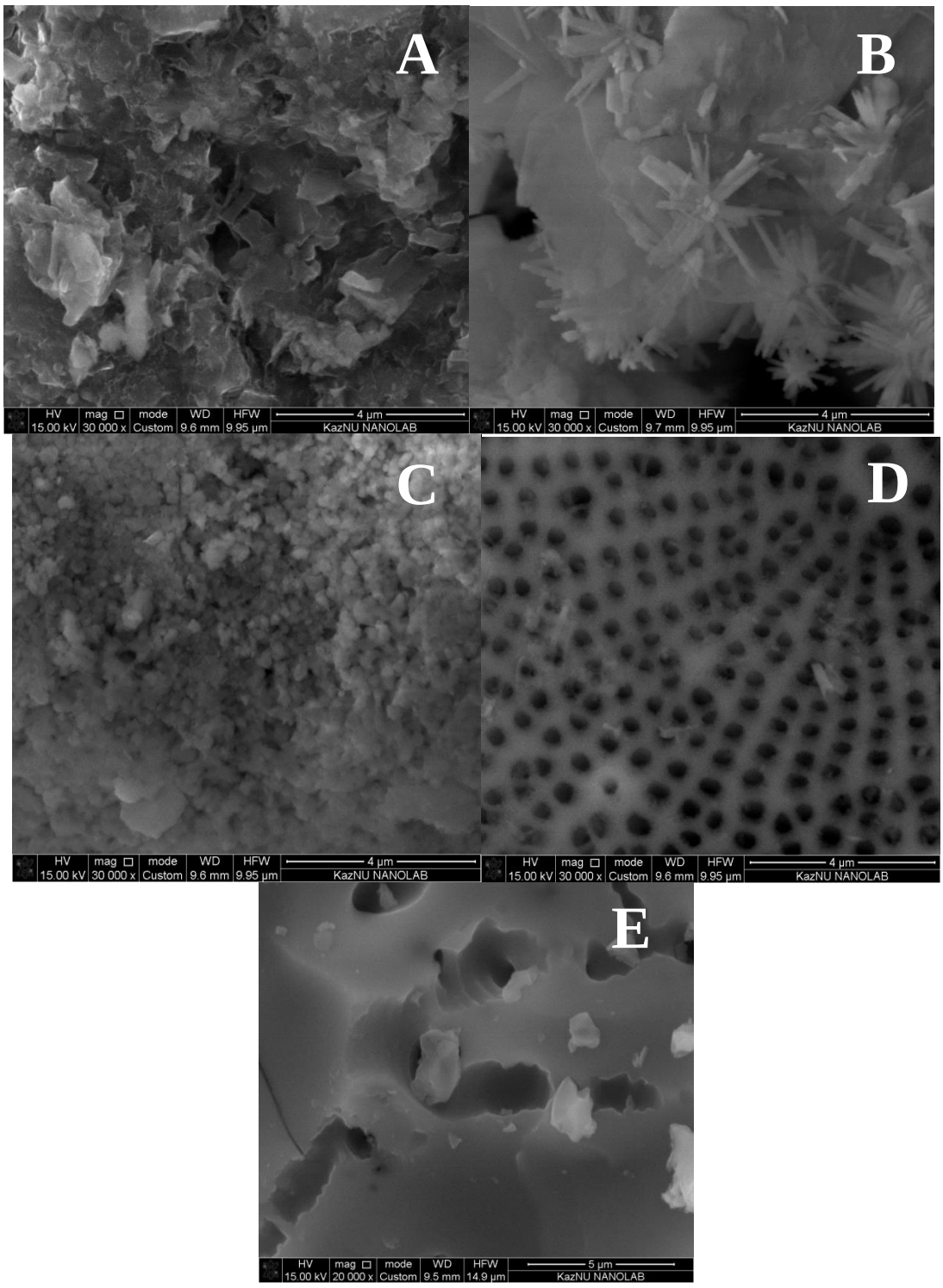

A – 10% $CuCl_2$-PVP/zeolite; B – 10 % $CuCl_2$-PVP/Al_2O_3; C – 10 % $CuCl_2$- PVP /SiO_2; D – 10 % $CuCl_2$-PVP/kieselguhr;
E – 10% $CuCl_2$-PVP/walnut charcoal

Figure 14 – SEM images of heterogeneous catalysts before experiment

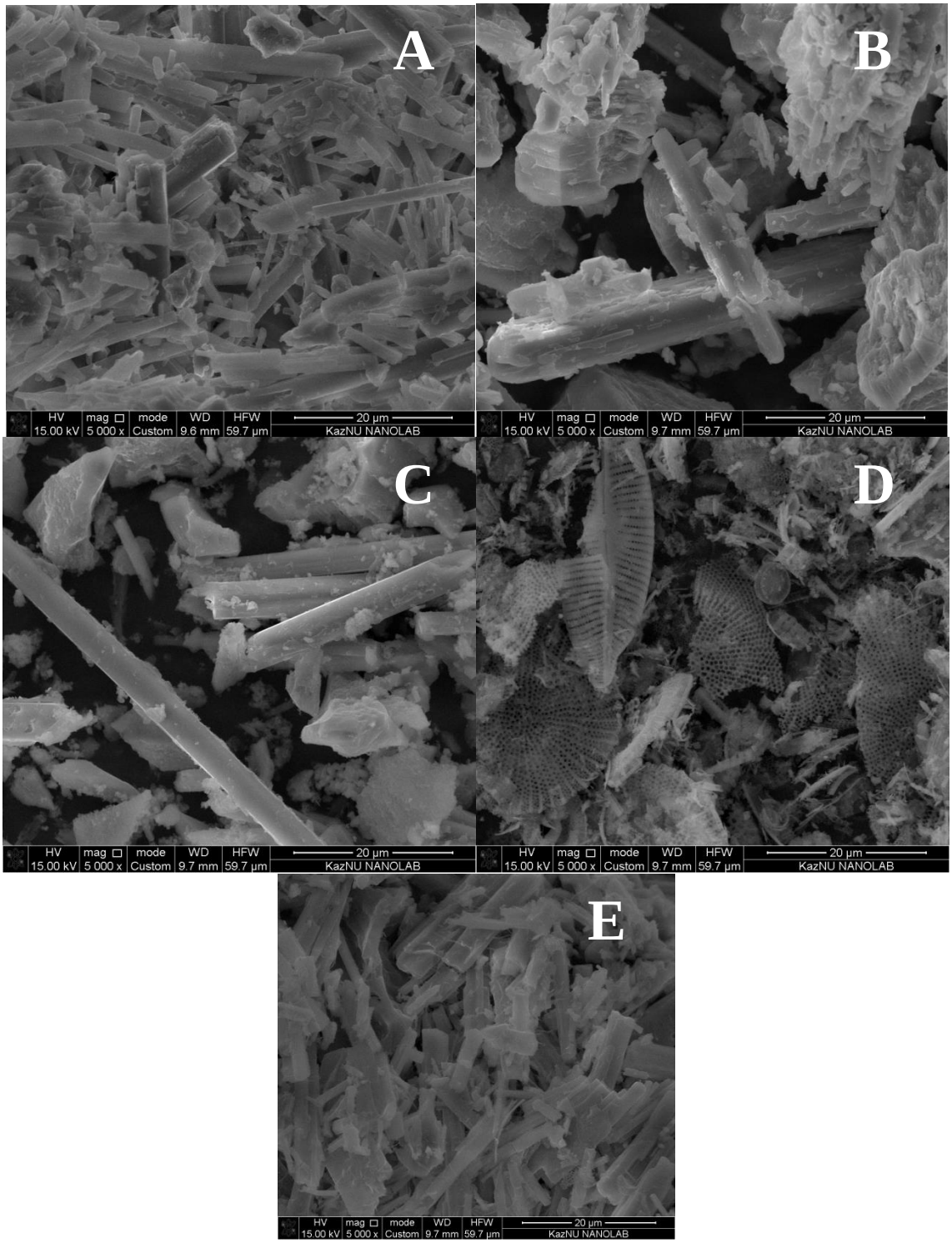

A – 10% $CuCl_2$-PVP/zeolite; B – 10% $CuCl_2$-PVP/Al_2O_3; C – 10% $CuCl_2$-PVP/SiO_2;
D – 10% $CuCl_2$-PVP/kieselguhr;
E – 10% $CuCl_2$-PVP/walnut charcoal

Figure 15 – SEM images of heterogeneous catalysts after experiment

The IR spectra of PEG and the PEG-$CuCl_2$ complex was shown in Figures 16 and 17. Carbonyl groups in PEG are characterized by peaks at 1058 (sym.) and 1282 (asym.) cm^{-1}. These bands shift to 833 and 1247 cm^{-1} in the complex PEG-$CuCl_2$.

The shift of the peaks corresponding to the vibrations of the carbonyl group of the polymer to the lower frequency region is due to the formation of the coordination bond due to the donor-acceptor interaction between the O atom of the PEG polymer ligand and ions Cu (II). It is known that the polymer ligand PEG, due to the presence in its chain of an oxygen atom - an electron donor, is able to form complexes with transition metal ions having vacant orbitals, in particular with Cu (II) ions [34].

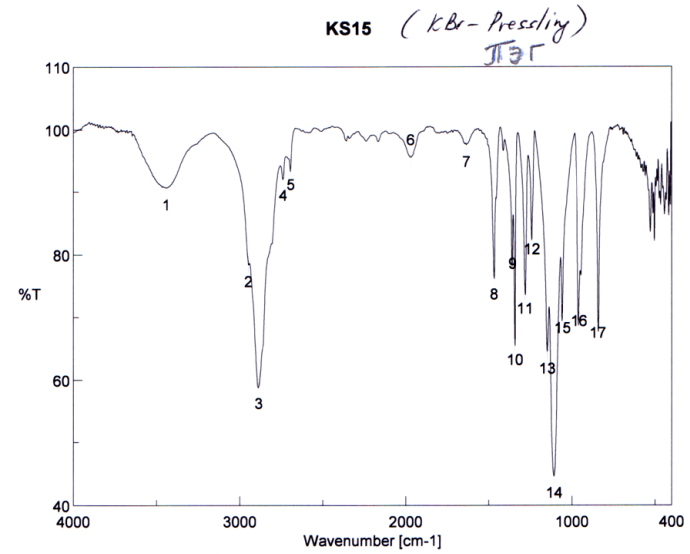

[Result of Peak Picking]

No.	Position	Intensity	No.	Position	Intensity
1	3441.35	90.6046	2	2946.7	78.3825
3	2885.95	58.9166	4	2737.46	92.1387
5	2692.14	93.8417	6	1969.93	95.5559
7	1635.34	97.5106	8	1468.53	76.3882
9	1357.64	81.2858	10	1343.18	65.8936
11	1282.43	74.0877	12	1240	83.5858
13	1149.37	64.5156	14	1106.94	44.7092
15	1057.76	71.0087	16	958.448	72.11
17	844.669	70.2168			

Figure 16 – IR – spectrum of PEG

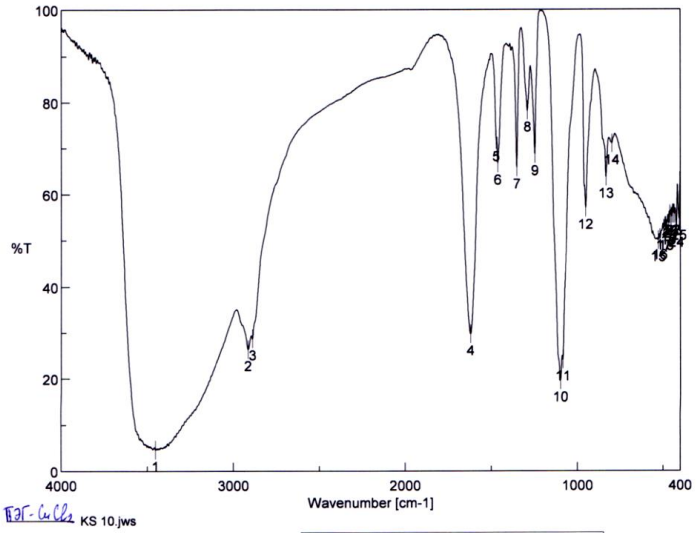

Results of Peak Find

No.	Position	Intensity	No.	Position	Intensity
1	3451.96	4.62743	2	2914.88	26.2834
3	2889.81	28.6208	4	1618.95	29.68
5	1471.42	71.8219	6	1461.78	66.6941
7	1351.86	65.8286	8	1290.14	78.1494
9	1246.75	68.6806	10	1098.26	19.5234
11	1084.76	24.0699	12	950.734	57.113
13	833.098	63.7467	14	799.35	70.9591
15	529.364	50.0428	16	517.793	50.4648
17	497.544	52.5669	18	483.081	52.4355
19	468.617	53.6101	20	460.904	55.6142
21	453.19	55.0987	22	444.512	55.794
23	434.869	55.7228	24	422.334	53.1175
25	406.907	54.65			

[Comments]
Sample name
Comment
User
Division
Company KL

Figure 17 - IR – spectrum of complex $[Cu(PEG)_2Cl_2]$

The physicochemical studies of binary systems containing Cu^{2+} ions and polymer ligands were carried out by potentiometric and conductometric methods.

Earlier, the authors of work [194] established the composition of the complex Cu^{2+}-PVP. It has been found that the optimum molar ratio of the reactants k (k = $[Cu^{2+}]/[PVP]$), is k = 0.35, indicating the formation of complex particles PVP:Cu^{2+} = 3:1, i.e. three monomer unit of the polymeric ligand have one complexing metal ion.

The titration curve of PEG polymers with copper salt $CuCl_2 \cdot 2H_2O$ was shown in Figure 18. As can be seen from the figure, the mixing of aqueous solutions of reagents is accompanied by a decrease in the pH of the medium. Which is probably due to the release of protons of PEG hydroxide groups in the process of interaction with copper ions.

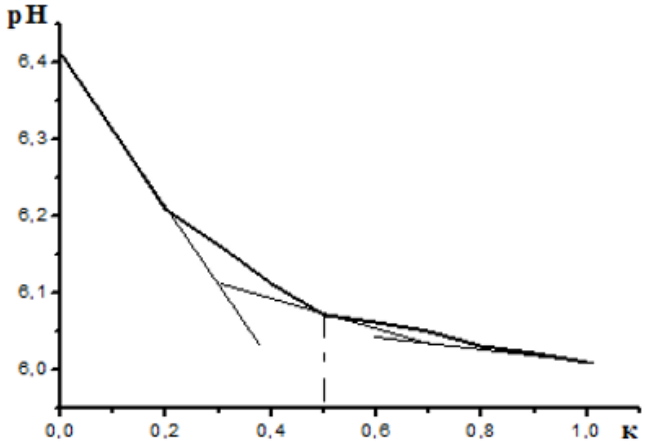

C (PEG)=$1 \cdot 10^{-2}$ mol/L, C($CuCl_2$)=$1 \cdot 10^{-2}$ mol/L

Figure 18 - Curve potentiometric titration of PEG with copper chloride, k = $[Cu^{2+}]/[PEG]$

It was found that the optimal molar ratio of the components k (k = $[Cu^{2+}]/[PEG]$) is k = 0.50, that is, in a complex complex compound one metal ion forms a complex with two monojunctions of the PEG polymer.

To confirm the composition of the formed polymer-metal complex PEG-Cu^{2+}, the dependence of the specific conductivity on the ratio of the initial components (k) was investigated (Figure 19).

The increase in electrical conductivity is probably due to the released H^+ ions during the reactions of PEG with copper ions. Therefore, the dependence of the specific electrical conductivity of the solutions on the relative concentration of copper ions passes through the inflection point when the reactant ratio is k = 0.5, which corresponds to the formation of a complex of the following composition PEG:Cu^{2+}=2:1.

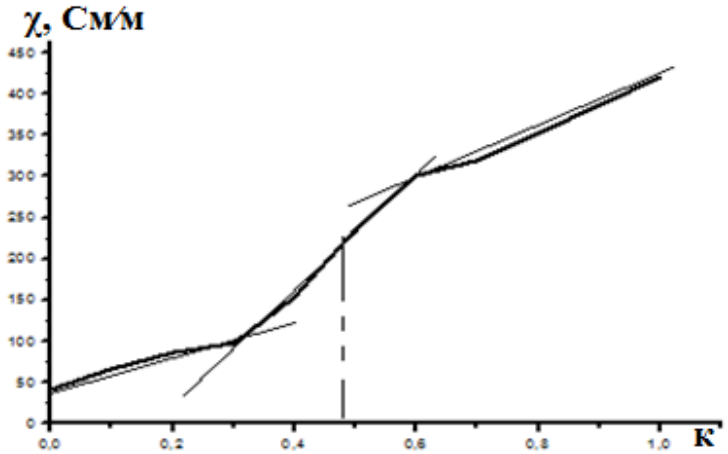

C (PEG)=1·10^{-2} mol/L, C($CuCl_2$)=1·10^{-2} mol/L

Figure 19 - Curve conductometric titration of PEG with copper chloride

Analysis of the literature and these dependencies confirmed the formation and composition of the polymer-metal complexes PVP:Cu^{2+}=3:1 and PEG:Cu^{2+}=2:1 According to the literature [194] and experimental data, it can be assumed that the following systems are formed in the system under study (Figure 20):

A

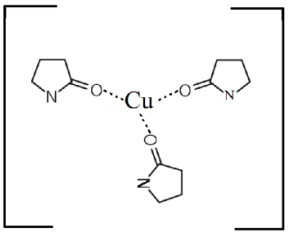

B

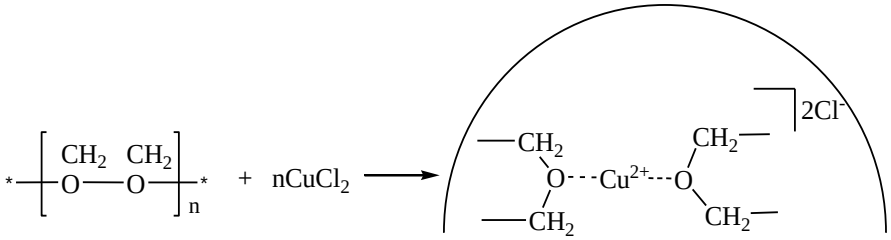

$Cu(ПЭГ)_2Cl_2$

Figure 20 – The structure of the polymer complexes A - PVP:Cu^{2+} = 3:1, B - PEG:Cu^{2+} = 2:1

To clarify the composition and determine the strength of the PEG:Cu^{2+} polymer-metal complex, a modified Bjerrum method was used [67]. In this case, the polymer ligand was titrated with acid in the absence and presence of the metal ion of the complexing agent in this system in the temperature range 298–318 K, with five values of the ionic strength of the solution 0.1; 0.15; 0.20 ($NaNO_3$).

Table 12 shows the values of the Bjerrum formation functions (n) for the complex under study at T=298 K, I=0.1; 0.15; 0.20.

Table 12 - The calculated values of the functions of Bjerrum complex formation PEG–Cu^{2+}, T = 298 K, I=0.1, 0.15, 0.2.

$[LH^+]$, mol/L	$[L_k]$, mol/L	p[L]	n
1	2	3	4
I=0.1			
$1.28 \cdot 10^{-5}$	$3.52 \cdot 10^{-3}$	3.78	2.02
$2.26 \cdot 10^{-4}$	$1.76 \cdot 10^{-3}$	2.87	1.13
$5.37 \cdot 10^{-4}$	$1.17 \cdot 10^{-3}$	2.79	0.75
$8.37 \cdot 10^{-4}$	$1.42 \cdot 10^{-3}$	2.97	0.91
$11.46 \cdot 10^{-4}$	$1.29 \cdot 10^{-3}$	3.05	0.83
$14.56 \cdot 10^{-4}$	$1.15 \cdot 10^{-3}$	3.14	0.74
$17.64 \cdot 10^{-4}$	$0.98 \cdot 10^{-3}$	3.23	0.63
$20.74 \cdot 10^{-4}$	$0.77 \cdot 10^{-3}$	3.31	0.49
$23.95 \cdot 10^{-4}$	$0.46 \cdot 10^{-3}$	3.32	0.29
$27.02 \cdot 10^{-4}$	$0.25 \cdot 10^{-3}$	3.42	0.16
$29.99 \cdot 10^{-4}$	$0.05 \cdot 10^{-3}$	3.56	0.04
I=0.15			
$0.24 \cdot 10^{-4}$	$3.11 \cdot 10^{-3}$	3.71	1.99
$2.07 \cdot 10^{-4}$	$1.92 \cdot 10^{-3}$	2.92	1.23
$4.96 \cdot 10^{-4}$	$1.55 \cdot 10^{-3}$	2.89	0.99
$7.99 \cdot 10^{-4}$	$1.21 \cdot 10^{-3}$	2.88	0.78
$11.08 \cdot 10^{-4}$	$0.90 \cdot 10^{-3}$	2.88	0.58
$14.08 \cdot 10^{-4}$	$0.75 \cdot 10^{-3}$	2.93	0.48
$17.10 \cdot 10^{-4}$	$0.60 \cdot 10^{-3}$	2.99	0.38
$20.07 \cdot 10^{-4}$	$0.43 \cdot 10^{-3}$	3.05	0.28
$23.17 \cdot 10^{-4}$	$0.16 \cdot 10^{-3}$	3.07	0.10
I=0.20			
$0.21 \cdot 10^{-4}$	$2.99 \cdot 10^{-3}$	3.43	1.89
$2.28 \cdot 10^{-4}$	$1.06 \cdot 10^{-3}$	2.69	0.68
$5.18 \cdot 10^{-4}$	$0.95 \cdot 10^{-3}$	2.73	0.61
$8.29 \cdot 10^{-4}$	$0.46 \cdot 10^{-3}$	2.69	0.29
$11.32 \cdot 10^{-4}$	$0.38 \cdot 10^{-3}$	2.74	0.24
$14.31 \cdot 10^{-4}$	$0.35 \cdot 10^{-3}$	2.81	0.22
$17.35 \cdot 10^{-4}$	$0.25 \cdot 10^{-3}$	2.87	0.16
$20.36 \cdot 10^{-4}$	$0.12 \cdot 10^{-3}$	2.93	0.08

For a more detailed understanding of the complexation of high-molecular ligands with metal ions, it is necessary to consider the changes observed in this important thermodynamic parameters: Gibbs energy, enthalpy and entropy. In this case, it can be assumed that systems containing macromolecules obey the same laws of thermodynamics as systems consisting only of low molecular weight molecules.

This approach is used by many researchers in the study of processes involving polymeric compounds [67].

The thermodynamic parameters of the formation of polymer-metal complexes is shown in Table 13. Confirmation of possible complexation reaction in these systems in the forward direction are negative in sign values of the Gibbs energy of the investigated processes.

Table 13 - Thermodynamic characteristics of the complexation of ions Cu^{2+} with PVP and PEG

System	T, K	$lg\beta^0$	- Δr G, kJ/mol	Δr H, kJ/mol	Δr S, kJ/mol·K
*PVP- Cu^{2+}	298	14,5±0,19	82,719±1,09	-277,50±10,96	0,64±1,30
	308	14,4±0,18	84,906±1,11		
	318	11,50±0,25	71,834±1,08		
PEG- Cu^{2+}	298	5,98±0,06	34,11±0,42	117,17±5,15	0,26±1,11
	308	6,10±0,07	35,98±0,41		
	318	7,25±0,09	44,13±0,45		
*- data from [194]					

The enthalpy of reaction between the complex compounds of copper ions and PEG is positive - i.e. endothermic processes. That is, the equilibrium with increasing temperature shifts in the direction of product formation. While the reaction between PVP and copper ions is exothermic, which means that with increasing temperature the reaction equilibrium shifts towards the starting substances. As can be seen from the data presented in Table 14, complex formation processes in binary systems, both PVP-copper ion and PEG-copper ion are characterized by positive entropy values, which is caused by the destruction of the hydration shells of the ligand groups of the polymer, the displacement of water molecules from the first coordination sphere of metal ions.

A comparative analysis of the thermodynamic characteristics of complexation showed that the PVP-Cu^{2+} complex has higher stability constants, compared to PEG-Cu^{2+}. Also, increasing the temperature negatively affects the process of complex formation of PVP-Cu^{2+}, while with increasing temperature the stability constants of PEG-Cu^{2+} increase.

So, the analysis of the literature and the obtained data indicates the formation of the polymer complex PVP–Cu^{2+} with composition 3:1, and PEG–Cu^{2+} with composition 2:1; their stability constants and thermodynamic characteristics of the studied processes were established.

3.2 Sorption characteristics of composite materials based on natural raw materials

3.2.1 Sorption of Pb^{2+}, Cd^{2+} and Cu^{2+} ions from aqueous solutions with BT-PEG composite material

The sorption process is influenced by various factors, such as the concentration of the modifier, the dose of the sorbent, the concentration of the pollutant, the pH of the medium, the temperature, the presence of various metal ions in the solution, etc. First, the effect of the polymer concentration in the BT-PEG material on the adsorption of the metal ions was studied. The effect of the polyethylene glycol concentration was studied at 25°C, and the results are presented in Figure 21.

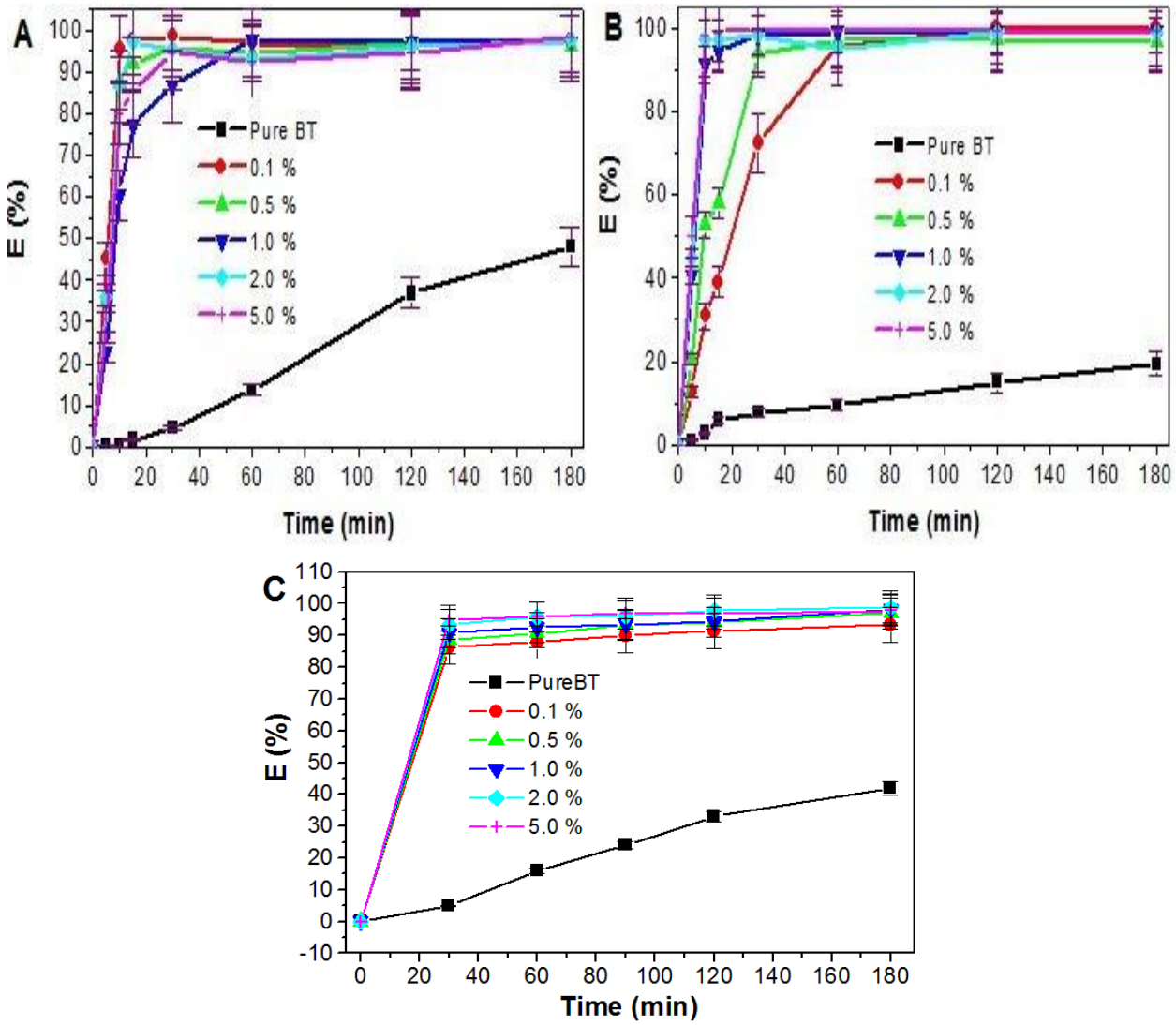

A - Pb^{2+}; B - Cd^{2+} and C - Cu^{2+}

Figure 21 - Effect of PEG concentration on the extent of adsorption of ions onto BT-PEG (adsorbent dose = 10 g/L; pH = 6.0; temperature = 25°C)

It was found that increasing the concentration of polymer in the BT-PEG material increases the amount of adsorbed metal ions. This behavior might be due to the fact that at higher polymer concentrations, metal ions are adsorbed onto the

sorbent surface not only by the mechanism of physical sorption, but also by functional groups of PEG. The saturation period of the sorbent is defined by the nature of both adsorbent and sorbate. The sorption equilibrium of lead cadmium and copper ions occurs within 30 minutes; this short time period required to attain equilibrium suggests an excellent affinity of the metal ions for the BT-PEG composite.

Based on these graphs, regardless of the quantity of the modifying polymer, all sorbents nearly completely adsorbed the lead, cadmium and copper ions. Therefore, for economic efficiency, the sorbent containing the minimum quantity of PEG (0.1 %) was selected for further studies.

Figure 22 reveals the effect of the adsorbent dose on the adsorption characteristics. Comparative analysis shows that the optimal dose of adsorbent for removal of lead and cadmium ions is 10 g/L. This dose is quite high, but due to the low-cost and non-toxic properties of BT-PEG, this composite can be applied.

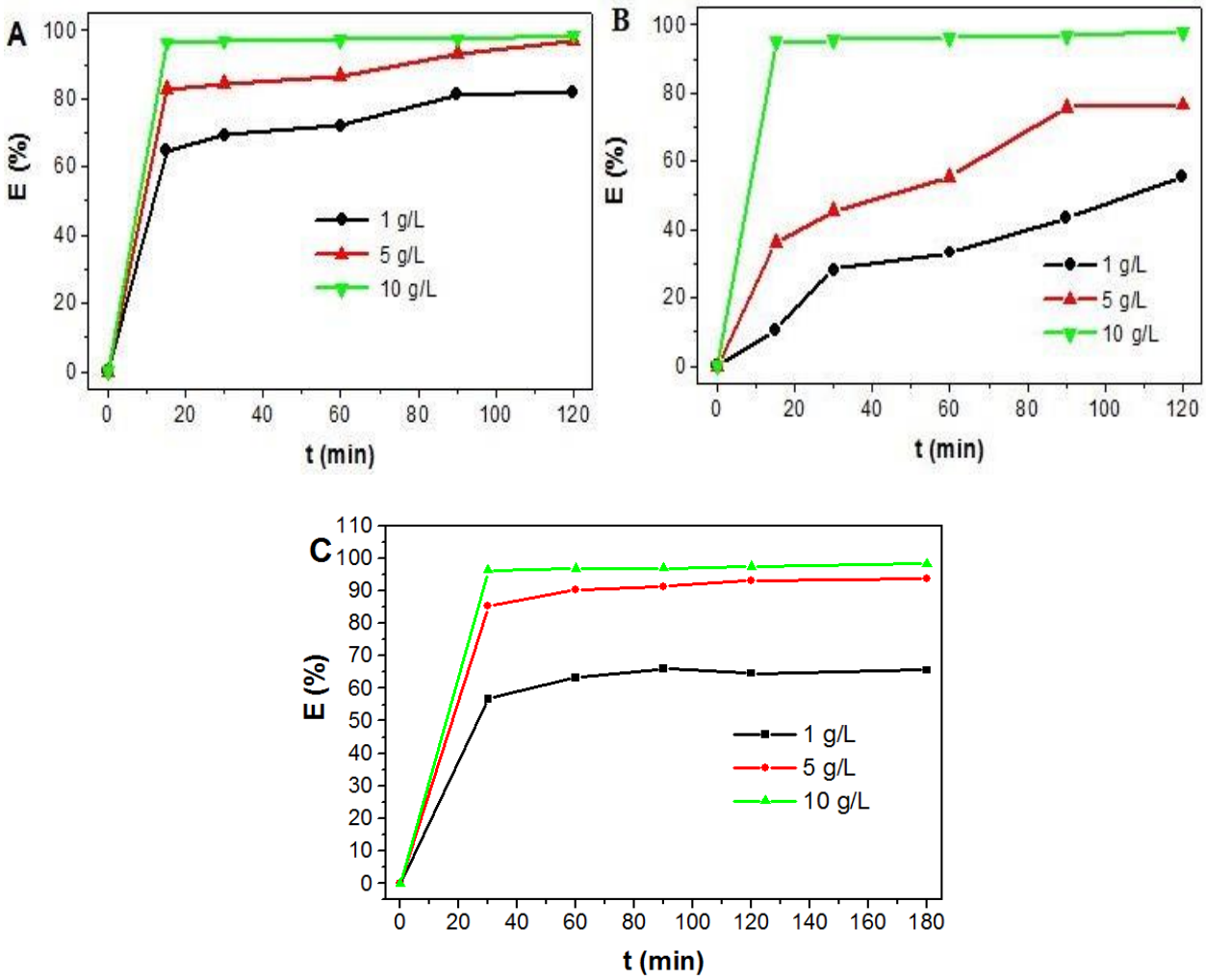

A - Pb^{2+}; B - Cd^{2+} and C- Cu^{2+}

Figure 22 - Effect of dose of BT-PEG on the adsorption degree of ions (initial metal ions concentration = 5 mg/L; pH = 6.0; temperature = 25°C)

It is known that at pH values above 6.0, most of the heavy metals tend to form hydroxides, which can mask the "true" degree of adsorption. Therefore, the dependence of the adsorption on the acidity of the metal ion solutions was studied at pH values ranging from 2 to 6.

The effect of pH on its sorption properties of BT-PEG composite material is shown in Figure 23.

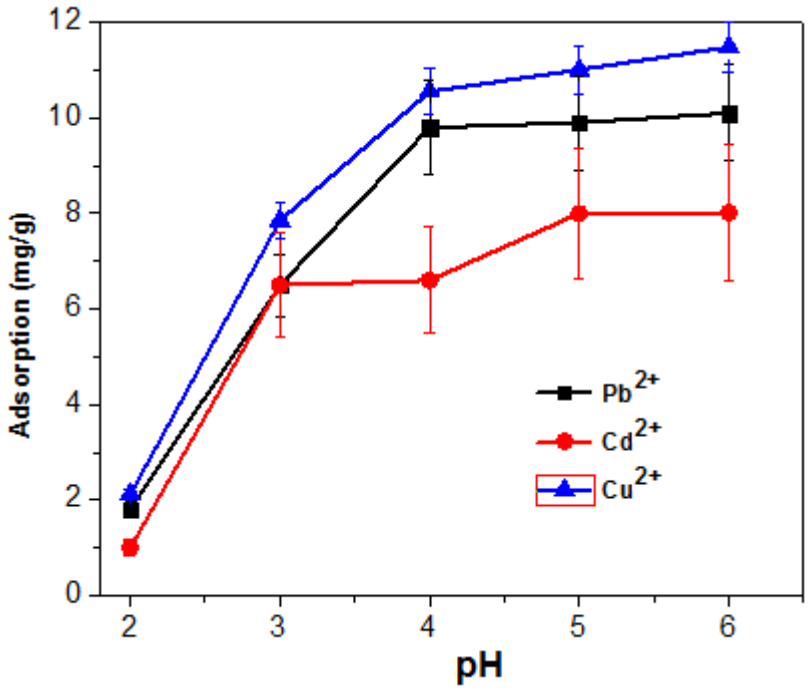

Figure 23 - Effect of pH to the adsorption of Pb^{2+}, Cd^{2+} and Cu^{2+} by BT-PEG (initial metal ions concentration = 100 mg/L; adsorbent's dose = 10 g/L; temperature = 25°C)

The effect of pH on adsorption of heavy metal ions onto pure bentonite was investigated earlier [25]. At pH values ranging from 3 to 6, the adsorption capacity of Cu^{2+} is higher than Pb^{2+} and Cd^{2+}.

At low pH values, which correspond to a high proton concentration, there is competition between the H^{+} and the Pb^{2+}, Cd^{2+} and Cu^{2+} ions for the negatively charged surface of the sorbent [33]. Therefore, as can be seen from Figure 24, at pH 2-3 there is a lower value of adsorption.

The effect of the initial concentration of metal ions on their adsorption was studied at 25 °C in a broad range of 2–270 mg/L. According to the obtained isotherms (Figure 24), the modified sorbent showed maximum adsorption of 22, 18 and 26 mg/g for lead, cadmium and copper ions, respectively, whereas pure bentonite showed considerably lower maximum adsorptions of 13 and 6 mg/g for lead and cadmium, respectively. Sorption isotherms are important for describing the adsorption process, as they show how the metal ions are distributed between the adsorbent and liquid phase at equilibrium depending on the concentration.

In this work, to describe the sorption of heavy metal ions by the investigated sorbent, the two of the most commonly used models were applied –the Langmuir and Freundlich isotherms. The following isotherm constants were calculated: K –

equilibrium constant of the adsorption process, A_∞ – limiting adsorption, β–the Freundlich parameter, and 1/*n* – the heterogeneity factor. As can be seen from Table 14, the Langmuir isotherm does not conform with either of the two metal sorption processes, as evidenced by the values of the R^2 correlation coefficient, which were 0.886 and 0.703 for Pb^{2+} and Cd^{2+} ions, respectively.

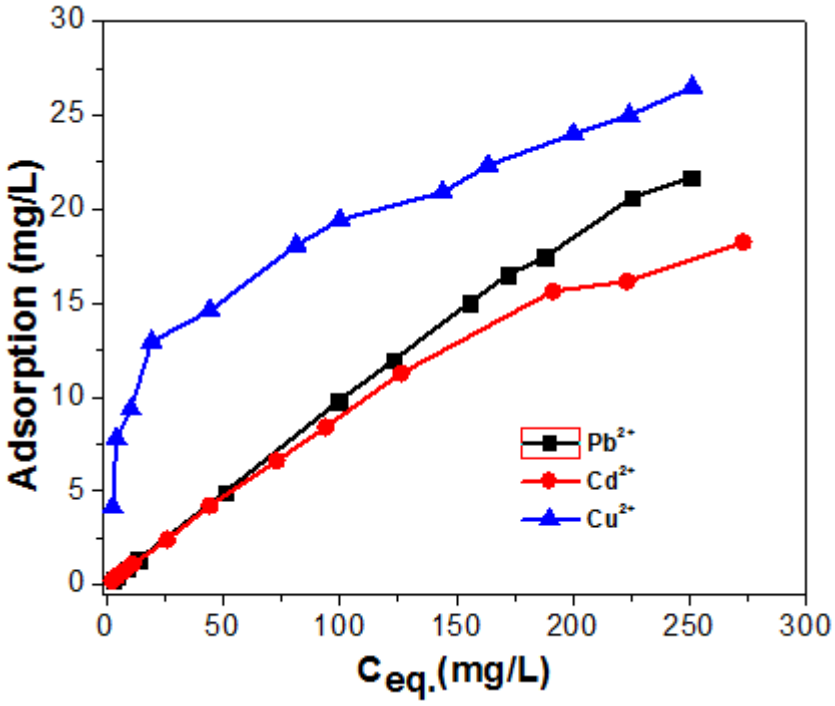

Figure 24 - Adsorption isotherms on Pb^{2+}, Cd^{2+} and Cu^{2+} ions onto BT-PEG (contact time = 180 min; adsorbent dose = 10 g/L; pH = 6.0; temperature = 25°C)

Table 14 - Characterization of adsorption isotherms of metal ions at 25°C

Metal ion	Langmuir model			Freundlich model		
	K, L/mg	A_∞, mg/g	R^2	β	1/n	R^2
BT						
Pb^{2+}	0.05	1.35	0.397	14.45	1.187	0.979
Cd^{2+}	0.18	0.26	0.541	15.35	0.393	0.804
BT-PEG						
Pb^{2+}	1.35	4.46	0.886	3.82	0.91	0.919
Cd^{2+}	2.45	3.34	0.703	2.30	0.53	0.915
Cu^{2+}	0,16	28,57	0,989	10,84	0,184	0,997

The data from adsorption studies is best described by the Freundlich isotherm (Figure 25, R^2 = 0.919 for lead, R^2 = 0.915 for cadmium and R^2 = 0.997 for copper). Therefore, the sorption of metal ions by BT-PEG proceeds in good agreement with the Freundlich isotherm model in which the extraction of metal ions occurs in a

heterogeneous system with uneven filling of the active centers and the visible forces of interaction between the adsorbed particles.

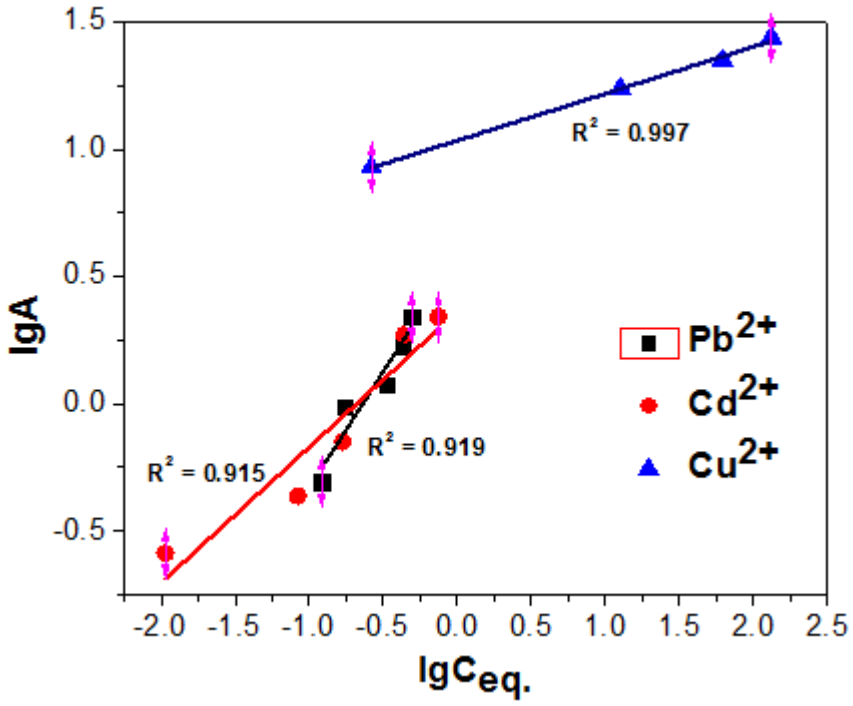

Figure 25 - Freundlich isotherm model of heavy metal ion adsorption onto BT-PEG

In the present study, pseudo-first-order and pseudo-second-order kinetic models were employed to test the experimental data [34]. The pseudo-first-order and pseudo-second-order models are described by the following equations, respectively:

$$\ln(q_e - q_t) = \ln q_e - \mathrm{k}_1 t \quad (15)$$

$$\frac{t}{q_t} = \frac{1}{\mathrm{k}_2 q_e^2} + \frac{t}{q_e} \quad (16)$$

where q_e and q_t are the amounts of adsorbate (mg/g) on the adsorbent at the equilibrium and at time t, and k_1 (min^{-1}) and k_2 (g $\mathrm{mg}^{-1}\mathrm{min}^{-1}$) are the rate constants of the pseudo-first-order and pseudo-second-order models, respectively.

The kinetic data was linearized using the pseudo-first-order and pseudo-second-order models and plotted as $\ln(q_e - q_t)$ versus t and t / q_t versus t, respectively (Figure 28).

The constants were calculated from the slope and intercept of the plots and are given in Table 15 and shown in Figure 26. The results in Table 15 indicate that while the pseudo-first-order model applies for prisrine bentonite (BT), better correlation coefficients were obtained for the composite BT-PEG using the pseudo-second-order model, which thus explains the adsorption process better.

To determine the influence of the temperature, the sorption was carried out at 25 and 35 ^{o}C. Furthermore, the kinetics were characterized and the activation energy

was calculated using the following Arrhenius equation:

$$E_a = \frac{RT_1T_2 ln \frac{k_{T2}}{k_{T1}}}{T_2 - T_1} \quad (17)$$

where R is the gas constant (J mol^{-1} K^{-1}), T_1 and T_2 are the temperatures (K) at which the sorption were carried out, and $k_{T1}$and k_{T2} are the rate constants at temperatures T_1 and T_2.

The obtained results are presented in Table 16, showing that the rise in temperature has negative impact on the rate of sorption of both ions. The physical sorption mechanism is supported by the negative value of the activation energy [157]. In addition, the rapid achievement of the equilibrium state (equilibrium time = 60 minutes) also supports a physical adsorption mechanism.

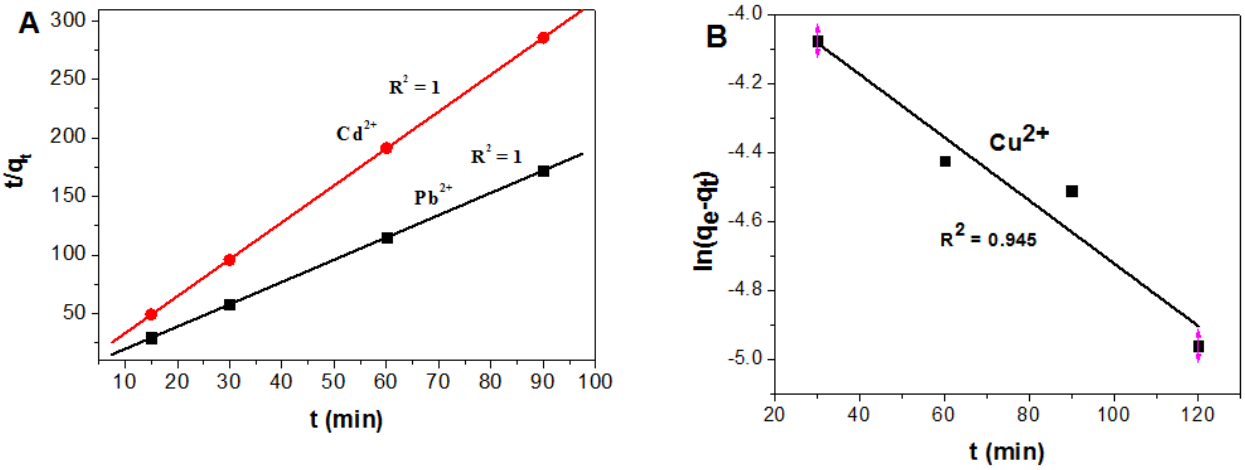

Figure 26 – Plots of kinetics of heavy metal ions (A) Cd^{2+}, Pb^{2+} and (B) Cu^{2+} (initial metal ions concentration = 5 mg/L; adsorbent dose = 10 g/L; pH value = 6.0; temperature = 25 °C)

Consequently, the optimal conditions for the process of sorption of heavy metal ions with the BT-PEG composite material were established. The adsorption depends on the concentration of the PEG modifier, the sorbent dose, pH and temperature.

It was established that the sorption of all ions with modified bentonite clay is described by the Freundlich model, which indicates irregular filling of the active centers of the composite. The maximum sorption capacity of BT-PEG for Pb^{2+}, Cd^{2+} and Cu^{2+} ions are 22 mg/g, 18 mg/g and 26 mg/g, respectively. It is established that the sorption of Pb^{2+} and Cd^{2+} ions by a BT-based composite has a pseudo-second order, indeed sorption of Cu^{2+} ions has pseudo-first order.

Table 15 - Kinetic characterization of Pb^{2+} and Cd^{2+} sorption onto BT-PEG

Metal	C_0, mg/L	A_{max}, mg/L	T, K	Pseudo-first order model		Pseudo-second order model		E_a, kJ/mol
				k, min^{-1}	R^2	k_2 (g mg^{-1} min^{-1})	R^2	
BT								
Pb^{2+}	5	0.16	298	0.015	0.937	0.027	0.919	-
Cd^{2+}	5	0.10	298	0.021	0.976	0.166	0.866	-
BT-PEG								
Pb^{2+}	5	0.52	298	0.065	0.853	6.29	1	-10.38
	5	0.49	308	0.089	0.933	5.49	1	
Cd^{2+}	5	0.46	298	0.036	0.753	6.67	1	-34.21
	5	0.32	308	0.004	0.481	4.26	0.999	
Cu^{2+}	5	0.82	298	0.012	0.945	-	-	-1.67
	5	0.85	308	0.010	0.809	-	-	

It was shown that their rate constants (lead and cadmium ions) decrease with increasing temperature and the processes are characterized by a negative activation energy.

3.2.2 Sorption of Cu^{2+} и Ni^{2+} ions from aqueous solutions with OP-PVP, MP-PVP composite material

Sorption characteristics of the obtained composite materials based on orange peel and mandarin peel were studied with respect to Cu^{2+} и Ni^{2+} ions. Figure 29 presents a comparative analysis of the sorption properties of the initial material (orange and mandarin peel) with respect to copper and nickel ions.

According to the data, it can be concluded that under the same conditions for the sorption of Cu^{2+} and Ni^{2+} ions (temperature, pH, metal ion concentration), the initial materials (OP and MP) have different properties. As can be seen from Figure 27, both materials: OP and MP - are better able to extract nickel ions from an aqueous solution than copper ions.

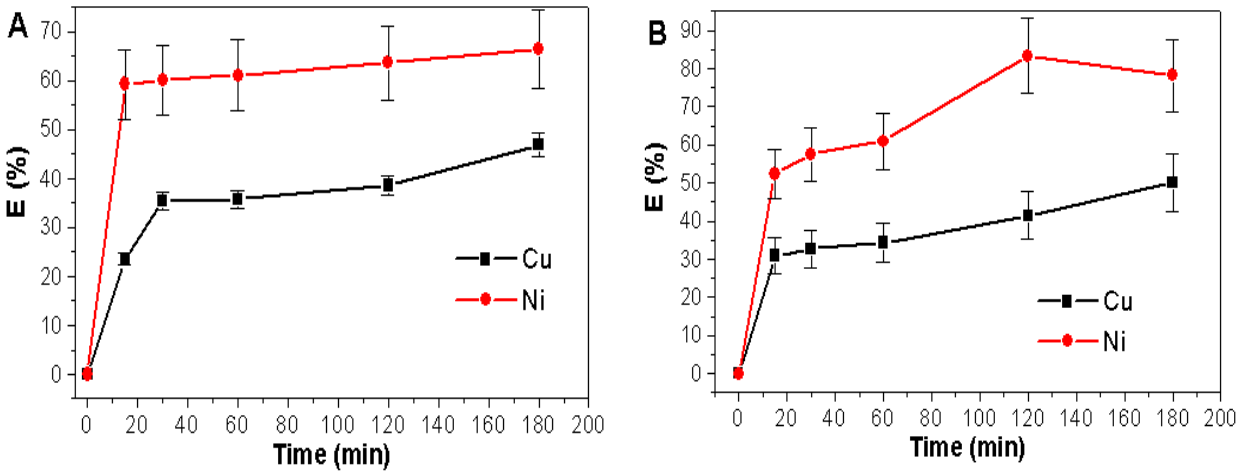

Figure 27 – Dependence of removal degree E (%) of ions Cu^{2+} and Ni^{2+} from time: (A) initial OP; (B) initial MP (temperature = 25°C, C_0= 50 mg/L)

Figure 28 presents the results of sorption of copper (II) and nickel (II) ions by composites - (A) OP-PVP and (B) MP-PVP.

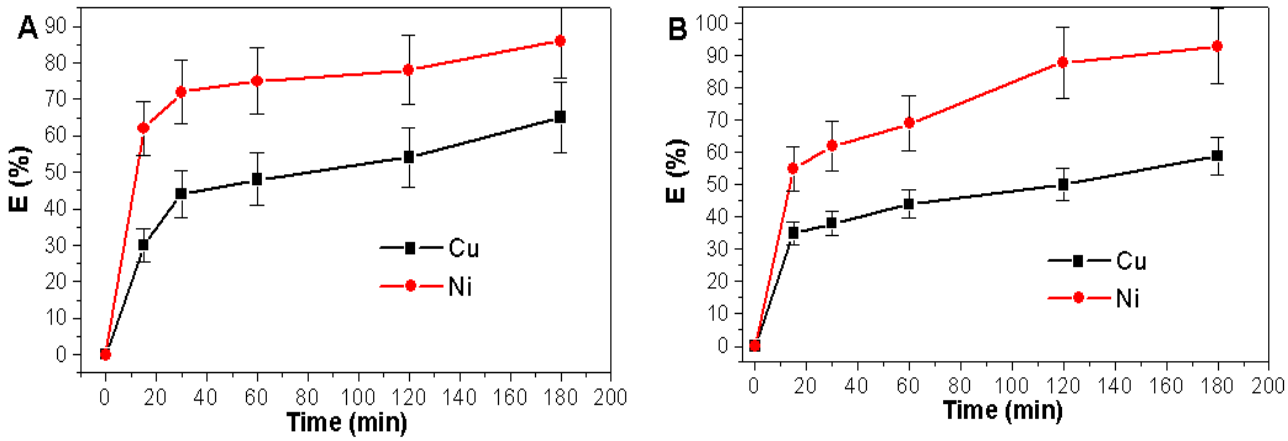

Figure 28 - Dependence of extraction degree E (%) of ions Cu^{2+} and Ni^{2+} from time: (A) OP-PVP; (B) MP-PVP (temperature = 25°C, C_0= 50 mg/L)

Modification of OP and MP with polymer increases the degree of extraction of copper and nickel ions in comparison with the pristine material. The sorption of Cu^{2+} ions OP-PVP reaches about 60 %, while the removal degree of OP has a lower value equal to 40 %. Similar results are typical for the composite MP-PVP. There is a positive effect of modification on the sorption properties of composites based on MP: copper ion sorption increases from 40 % to 55 %. The removal degree of Ni^{2+} ions by synthesized composites lies in the range of 80-90 %, while the initial materials absorb copper and nickel ions in the range of 65-75 %.

Based on the analysis of the kinetic curves of the sorption process, the optimal equilibrium time was established, which is 180 minutes.

There is no single theory that would fairly accurately and fully describe all types of adsorption in a heterogeneous system. In this paper, theories of Langmuir and Freundlich were applied to describe the sorption process of copper and nickel ions with composite materials based on orange and mandarin peel.

According to literature data, within the framework of the Langmuir theory, adsorption proceeds in a homogeneous system with the formation of a monomolecular layer of sorbate without the interaction of the active centers of the sorbent with each other [65]. However, theoretical concepts developed by Lengmuir and Polanyi largely idealize and simplify the true picture of adsorption. In fact, the surface of the adsorbent is heterogeneous, there is an interaction between the adsorbed particles, and active centers are not completely independent of each other. All this complicates the form of the adsorption isotherm equation, which was derived by G. Freundlich [66]. Freundlich's isotherm is empirical and is used to describe heterogeneous systems [157].

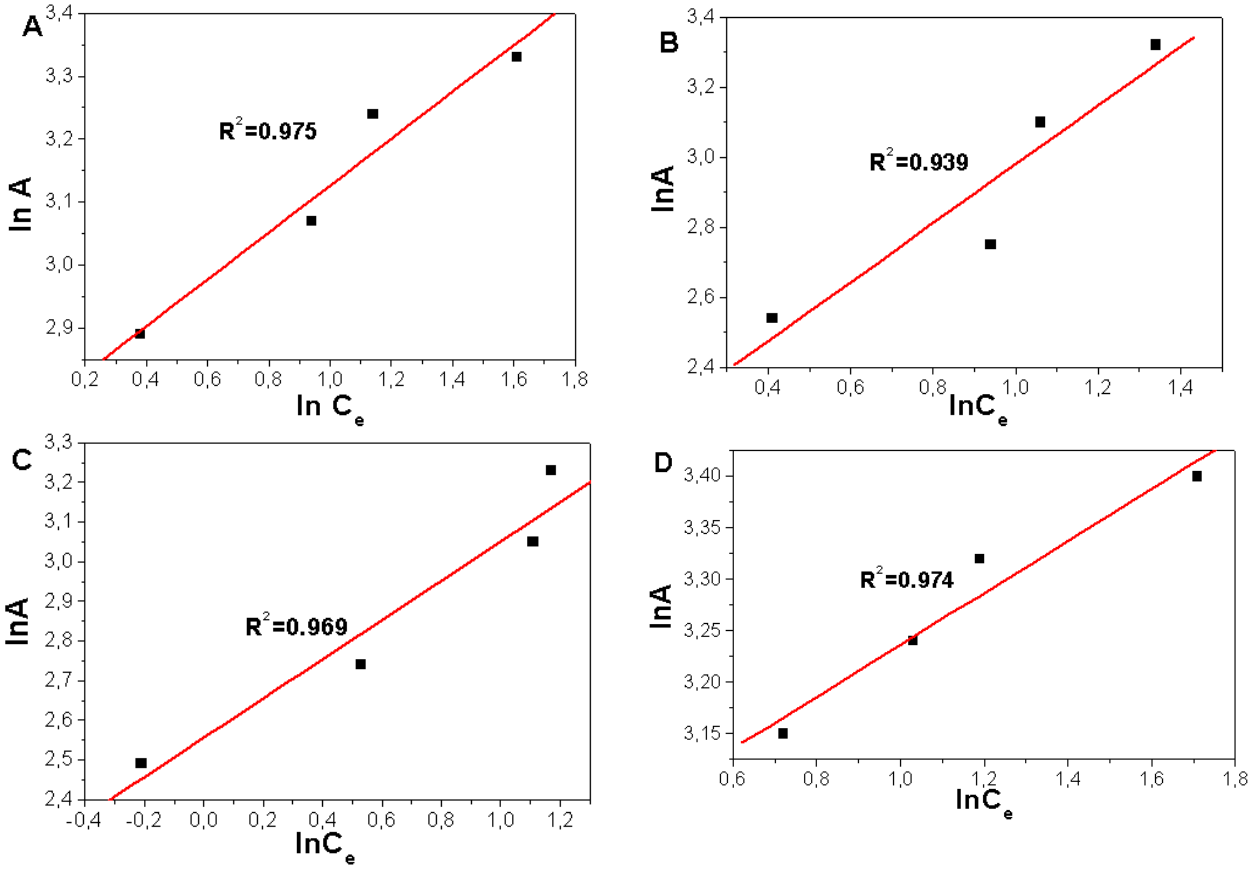

Figure 29 – Freundlich isotherm model of Cu^{2+} OP (A), Ni^{2+} OP (B), Cu^{2+} MP (C) and Ni^{2+} MP (D) ions

Langmuir and Freundlich isotherms constants (K is the adsorption equilibrium constant, A∞ is the limiting adsorption, β and 1/n are the Freundlich isotherms constants) calculated on the basis of experimental data obtained at different initial ion concentrations of investigated metals were shown in Figure 29 and Table 16.

Table 16 - Characterization of adsorption isotherms of metal ions at 25°C

Sorbent	Metal ion	Langmuir model			Freundlich model		
		K	A_∞, mg/L	R^2	β	1/n	R^2
OP	Cu^{2+}	0.0290	4.6082	0.0479	15.3550	0.3702	0.9753
	Ni^{2+}	0.4115	2.5426	0.7512	8.3693	0.8429	0.9391
MP	Cu^{2+}	0.0264	2.0141	0.1710	12.6513	0.4950	0.9694
	Ni^{2+}	0.0554	4.6729	0.3401	2.4480	0.5793	0.9744
OP-PVP	Cu^{2+}	0.0112	6.0423	0,1681	14.5487	0.5602	0.8704
	Ni^{2+}	0.0688	4.8899	0,1327	11.8146	0.5167	0.8595
MP-PVP	Cu^{2+}	0.0103	9.6060	0,2302	11.1062	0.6484	0.9204
	Ni^{2+}	0.0254	4.9358	0,2583	9.3455	0.4233	0.8260

Based on the analysis of the calculated data, it was established that the sorption of copper and nickel ions OP and MP, as well as modified materials: OP-PVP MP-PVP proceeds according to Freundlich's model, i.e. metal ion extraction occurs in a heterogeneous system with uneven filling of the active centers of the sorbent and noticeable interaction forces between the adsorbed particles.

An analysis of the calculated constants of the Freundlich equation showed that the process of sorption of metal ions by the orange peel-based composite is characterized by higher values of the adsorption constant and the degree of extraction as compared to MP-PVP.

To optimize wastewater treatment technology, kinetic studies of the sorption process are of great importance. The sorption processes were carried out with a large excess of the concentration of the sorbent compared with the concentration of metal ions in the solution, therefore, to describe the kinetics, we used the model of the pseudo-first-order reaction. Kinetic studies of the process of metal ion sorption by modified citrus peels were carried out at a temperature 25 °C and are presented in Table 17.

Table 17 - Kinetic characterization of sorption of Cu^{2+} and Ni^{2+} ions at 25 °C

Sorbent	Metal ion	k 10^3, min^{-1}	w, mg/L min
OP-PVP	Cu^{2+}	7.91 ± 0,04	0.167
	Ni^{2+}	3.64 ± 0,02	0.117
MP-PVP	Cu^{2+}	2.91 ± 0,03	0.140
	Ni^{2+}	6.03 ± 0,04	0.207

As can be seen from Table 18, the composite OP-PVP is characterized by a higher rate constant for the sorption of copper ions than MP-PVP. Nickel ions are

sorbed by a mandarin peel based composite with a higher rate constant. From here, taking into account the radii of the TM ions (the radius of the Cu^{2+} ion is from 0.071 nm to 0.087 nm; the radius of the Ni^{2+} ion is from 0.069 nm to 0.083 nm), it can be concluded that the microporous structure prevails on the OP surface compared to the MP.

As part of industrial wastewater there is a whole complex of pollutants, including ions of various metals. As is known, the joint presence of several metal ions in a solution affects the quantitative indicators of adsorption. In this regard, there is a need to study the sorption characteristics of modified materials in these conditions. In order to study the process of sorption, an aqueous solution containing Cu^{2+} and Ni^{2+} ions was simulated. The obtained experimental data are presented in the Table 18.

The obtained experimental data indicate a decrease in the removal degree of copper and nickel ions with their joint presence in solution.

Table 18 – The results of the sorption of Cu^{2+} и Ni^{2+} with their joint presence in an aqueous solution at 25 °C

Sorbent	Metal ion	C_0, mg/L	C_{final}, mg/L	E_1, %	E_2, %
OP-PVP	Cu^{2+}	42±1	23±1	62±3	45±2
	Ni^{2+}	54±2	12±2	80±2	78±4
MP-PVP	Cu^{2+}	49±2	23±2	53±2	52±2
	Ni^{2+}	47±1	18±1	90±2	62±2
E_1 – removal degree from solutions in the presence of one type of metal ion; E_2 – removal degree from solutions with the joint presence of metal ions.					

In conclusion, we can settle that the sorption of copper and nickel ions by composites based on orange and mandarin peel was described by the Freundlich model; modification with PVP leads to an increase in their sorption properties. Sorption kinetics described by the pseudo-first order model.

3.3 Catalytic characteristics of composite materials based on natural raw materials

3.3.1 Catalytic reaction of 4-nitrophenol reduction by in situ Cu_2O nanocomposite based on clay materials and PEG

The reduction reaction of 4-NP to 4-aminiphenol in the presence of $NaBH_4$ was considered for the evaluation of the catalytic activities of the obtained composites (Figure 30).

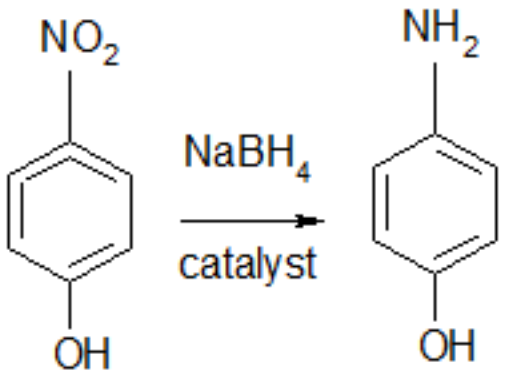

Figure 30 – Reaction of 4-nitrophenol reduction

The reaction was monitored by UV-Vis spectroscopy. Solutions of 4-NP have a strong peak at 317 nm which shifts to 400 nm when $NaBH_4$ is added, due to the formation of 4-nitrophenolate ions. This process is characterized by a change in the color from pale yellow to deep yellow. The UV-Vis absorption spectra of 4-NP and 4-NP + $NaBH_4$ with different composites and at several time intervals are shown in Figure 31. As seen in Figure 31 (B, D), the peaks at 400 nm completely disappeared after 180 s and 240 s in the presence 15 mg composites Cu^{2+}/PEG-BT and Cu^{2+}/PEG-ZT, respectively.

The influence of the PEG content in the composition of the catalysts was also investigated. As shown in Fig. 31 (A, C), the reaction is going more slowly and the peaks at 400 nm completely disappeared only after 10 min and 20 min respectively for Cu_2O /BT and Cu_2O /ZT. This is possibly caused by the properties of PEG such as its compatibility with aqueous mixtures of clay materials and its ability to interact at the molecular level, thereby increasing the chemical activity of the substrate. Moreover, this can be related to the aggregation of active particles of copper oxide (I) in the absence of the dispersive polymer. Black precipitates immediately appeared after the contact between 4-NP and catalysts with $NaBH_4$ in the vessel. This can be related to the precipitation of Cu_2O, which promotes the decomposition of sodium borohydride and the adsorption of nitro-phenols onto the surface of copper oxide (I) and so activates the reduction of 4-NP by $NaBH_4$ (eq. 18-21):

$$NaBH_4 + 2H_2O \rightarrow NaBO_2 + 4H_2 \quad (18)$$

$$Cu^{2+} + H_2 \rightarrow Cu^0 + 2H^+ \quad (19)$$

$$4Cu^0 + O_2 \rightarrow 2Cu_2O \quad (20)$$

$$R\text{-}NO_2 + 3H_2 \rightarrow R\text{-}NH_2 + 2H_2O \quad (21)$$

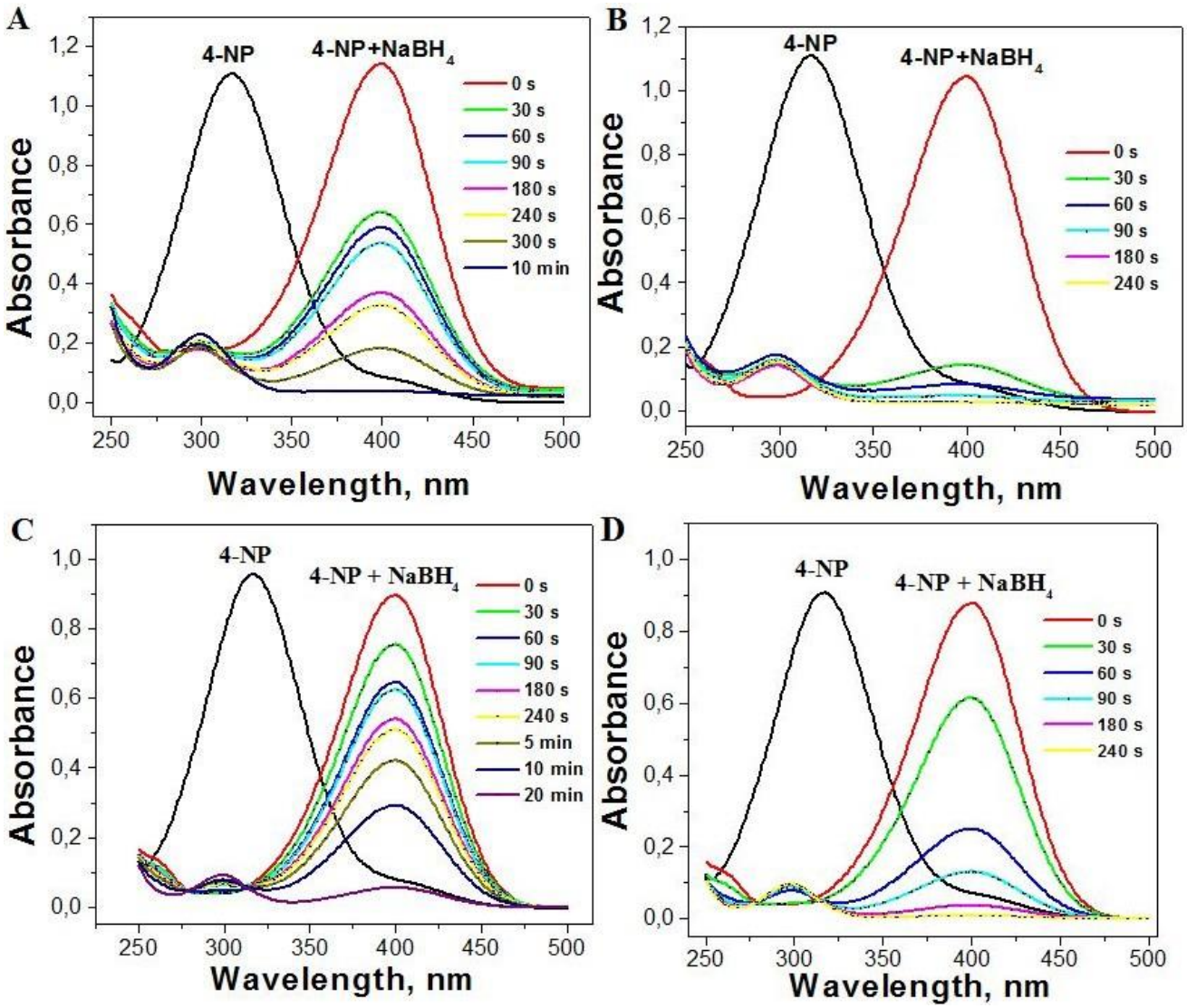

Conditions: C (4-NP) = 2.5×10^{-3} M, C ($NaBH_4$) = 0.25 M, catalyst weight = 15 mg

Figure 31 – UV-Vis absorption spectra of 4-NP and 4-NP+$NaBH_4$ in the presence (A) Cu_2O/BT, (B) Cu_2O/PEG-BT and (C) Cu_2O/ZT, (D) Cu_2O/PEG-ZT composites at several time intervals

Due to the large excess of $NaBH_4$ compared to 4-NP, the kinetics characteristics were investigated using the pseudo-first-order equation:

$$\ln\left(\frac{C_t}{C_0}\right) = \ln\left(\frac{A_t}{A_0}\right) = -k_1 t \tag{22}$$

where C_t is the concentration of 4-NP at a reaction time t, C_0 initial concentration of 4-NP, A_t is the absorbance of 4-NP at a reaction time t and A_0 is the absorbance at time zero. The calculated rate constants (k) from the slopes and intercept of the plots are given in Figure 32 and are equal to 1.22×10^{-2} s^{-1} for Cu_2O/PEG-BT and 1.79×10^{-2} s^{-1} for Cu_2O/PEG-ZT.

The rate of the reaction catalyzed by Cu_2O/PEG-ZT is higher in comparison with Cu_2O/PEG-BT. This can be explained by the results in Table 10, where the surface area of Cu_2O/PEG-ZT is 4.5 times higher than the surface area of Cu_2O/PEG-BT. Also, the difference in rate constants can be explained by the differences in the structure of the pores between bentonite and zeolite. The structure of bentonite clays is characterized by sliced pores of variable sizes in plate-form particles. On the other hand, a characteristic of the frame of zeolites is the presence of regular and communicating cavities capable of retaining more molecules of copper oxide (I).

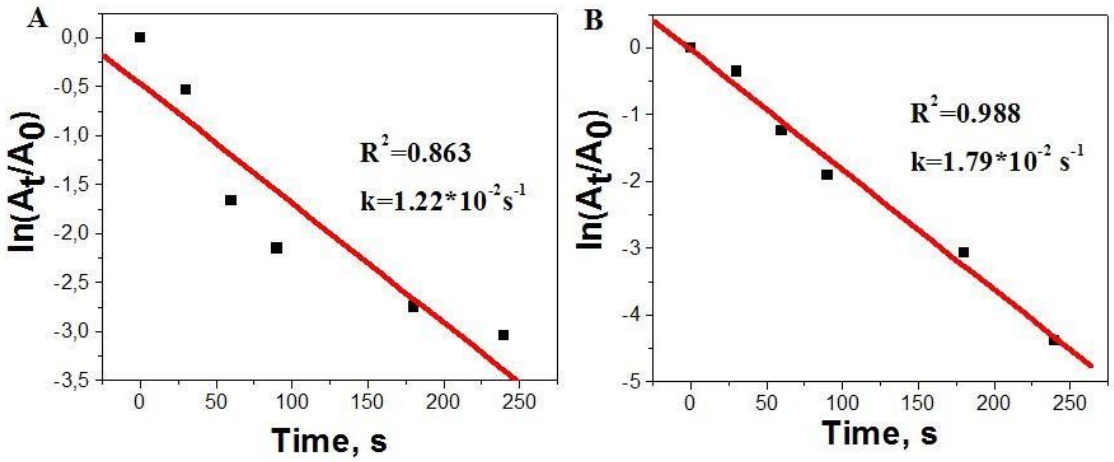

Conditions: [4-NP] = 2.5×10^{-3} M, [$NaBH_4$] = 0.25 M, catalyst weight=15 mg

Figure 32 - Kinetics of the reduction by Cu_2O/PEG-BT (A) and Cu_2O/PEG-ZT (B)

Quantitative comparison was performed using AAS analysis and the activity parameters of the catalysts were calculated as k/M_{Cu}, where k is the rate constant and M_{Cu} is the mass of the impregnated copper. These activity parameters are given in table 20. The results revealed that the copper amounts in catalyst were equal to 1.18 mg Cu for Cu_2O/PEG-BT and 1.05 mg Cu for Cu_2O/PEG-ZT, which represents respectively 7.9 % and 7.0 % of the mass of catalyst. The reaction rate constant per unit of mass (M_{Cu}) was calculated to be 10.37 $s^{-1}g^{-1}$ and 17.02 $s^{-1}g^{-1}$ respectively for Cu_2O/PEG-BT and Cu_2O/PEG-ZT catalysts. The calculated reaction rate constants were also comparable to other reported catalysts (Table 19). Finally, second cycle reduction reaction by both catalysts were performed in the same conditions. The rates of the reaction are presented in the Figure 33 and were equal to 0.15×10^{-2} s^{-1} and 0.62×10^{-2} s^{-1} for Cu_2O/PEG-BT and Cu_2O/PEG-ZT respectively. The lower values obtained for the second cycle reduction kinetics can be related to the decreasing number of active sites in connection with the elution of the active catalyst component Cu_2O.

Thus, a novel, simple and cost-effective *in-situ* method of preparation copper oxide (I) NPs showing high catalytic activity was demonstrated. The copper oxide (I) NPs were supported onto natural bentonite and zeolite using PEG as a stabilizing agent in the course of the 4-NP reduction reaction.

Table 19 – Comparison of the rate characteristics obtained for different catalysts

№	Catalyst	m_{cat}, mg	$C_{4\text{-}NP}\times10^3$, M	C_{NaBH4}, M	t, °C	$k\times10^2$, s^{-1}	k/M^a, $s^{-1}g_{Cu}^{-1}$	Ref
1	Cu_2O/PEG-BT	15.00	2.50	0.25	25	1.22	10.37[b]	*
2	Cu_2O/PEG-ZT	15.00	2.50	0.25	25	1.79	17.02[b]	*
3	Cu_2O/BT	15.00	2,50	0.25	25	0.40	2.92[b]	*
4	Cu_2O/ZT	15.00	2.50	0.25	25	0.20	1.94[b]	*
5	Cu NPs/bentonite	15.00	2.50	0.25	-	4.10	-	[138]
6	Cu_2O@CMK-8	0.20	0.09	0.05	-	2.20	203	[151]
7	Cu@CMK-8	0.20	0.09	0.05	-	1.49	114	[151]
8	CuO@CMK-8	0.20	0.09	0.05	-	0.58	50	[151]
9	Flower-CuO	10.00	0.25	0.20	-	0.31	-	[109]
10	Ni Ps in p(AMPS)	5.92	14.4	0.29	30	0.09	0.15	[128]
11	Ni@Pd/KCC	0.067	0.12	0.50	-	2.04	510	[150]
12	Pd-FG	1.00	0.10	0.01	-	0.24	480	[196]
13	@Pd/CeO_2	-	-	-	-	0.80	-	[197]
14	@Au/CeO_2	-	-	-	25	1.30	-	[197]
15	Au@SiO_2	0.32	3.40	1.20	25	1.40	44.44	[141]
16	Ag NPs/PD/PANFP	0.17	0.10	0.10	25	0.23	16.31	[146]
17	PPy-MAA/Ag	49.00	1.00	0.01	55	0.23	42.13	[145]

[*] – the catalysts obtained in this work
[a] – Only the mass of the Cu amount in the catalyst was counted
[b] –Determined by AAS.

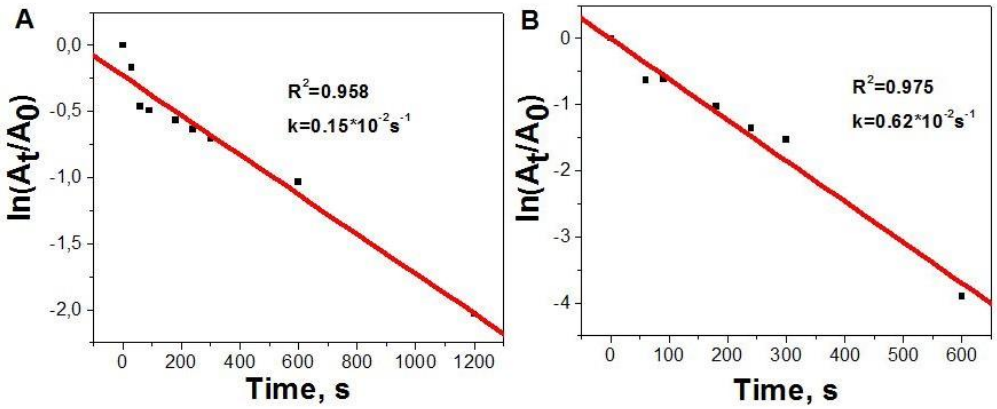

Figure 33 - Kinetics of 2nd cycle reduction process by Cu_2O/PEG-BT (A), Cu_2O/PEG-ZT (B)

The composites before and after reaction were characterized by various methods. The XRD analysis indicated the formation of cubic-phase Cu_2O. The existence of NPs with sizes of about 20 nm was further confirmed by HR-SEM and EDS analysis. These catalysts showed high catalytic activities in the model reduction

reaction of 4-NP to 4-AP using mild conditions. Zeolite was more effective than bentonite as a support material for the catalytic and kinetic characteristics. Comparative analysis of various works illustrated the superiority of this method thanks to the use of inexpensive materials and high catalytic efficiency.

3.3.2 Oxidative hydrolysis of yellow phosphorus to phosphoric acid in the presence of a copper-polymer catalyst $[Cu(PEG)_2Cl_2]$

Synthesized copper-polymer complex based on copper (II) chloride and PEG ($[Cu(PEG)_2Cl_2]$) was used as a catalyst in the oxidative hydroxylation of yellow phosphorus (P_4). Reactions were performed under mild conditions (50-70 °C, P_{O2} = 1 atm). The final product was phosphoric acid.

$$P_4 + 6H_2O + 5O_2 \rightarrow 4P(O)(OH)_3 \quad (23)$$

Table 20 - Oxidative hydrolysis of yellow phosphorus in the presence of $[Cu(PEG)_2Cl_2]$ with a molar ratio of reagents [Cat]:[P_4] = (6-11):1

№	Composition of solution, mol/L				t, °C	C_{O2}, %	The product yield, %		TON, mole acid / (mol Cat)	TOF, mole acid / (mol Cat ·h)
	Cat	$P_4 \cdot 10^2$	C_7H_8	H_2O			H_3PO_3	H_3PO_4		
Temperature variation										
1	0,12	1,06	0,94	50,0	50	100	24	76	1,24	4,96
2	0,12	1,06	0,94	50,0	60	100	55	45	1,24	3,76
3	0,12	1,06	0,94	50,0	70	100	13	87	1,24	2,95
Varying the concentration of catalyst										
4	0,06	1,06	0,94	50,0	70	100	38	62	2,48	3,70
5	0,12	1,06	0,94	50,0	70	100	13	87	1,24	3,76
6	0,24	1,06	0,94	50,0	70	100	47	53	0,62	1,24
Varying the concentration of yellow phosphorus										
7	0,12	0,53	0,47	52,8	70	100	18	82	0,62	1,88
8	0,12	1,06	0,94	50,0	70	100	13	87	1,24	3,76
9	0,12	2,12	1,88	44,4	70	100	64	36	2,47	1,65
Stability of the catalyst										
10	0,12	1,06	0,94	50,0	70	100	51	49	1,24	2,14
		1,06	0,94							
		1,06	0,94							

As intermediate compounds, a complex of copper (I) with phosphorous acid of the type $[Cu_2(PEG)_2P(OH)_3\ Cl^-_2]$ was appeared. This complex is easily destroyed by chlorine at 70 ° C to phosphoric acid [198-199].

$$[Cu_2(PEG)_2P(OH)_3\ Cl^-_2]+2Cl_2+H_2O \rightarrow 2[Cu(PEG)_2Cl^-_2]+P(O)(OH)_3+2HCl \quad (24)$$

The reaction in the presence of a catalyst (Cat) was studied at a molar ratio of reagents [Cat]:[P_4] = (6-11):1. The use of an excess of copper-polymer complexes as

catalysts allows suppressing the side reaction between P_4 and O_2 and shifting the process towards a direct reaction, the formation of phosphoric acids.

In order to establish the kinetics, key stages and optimal reaction conditions, the effect of the concentration of reactants, catalyst, and temperature on the process rate was studied. The reaction conditions and the yields of the oxidation products of yellow phosphorus with oxygen in an aqueous solution of [Cu $(PEG)_2Cl_2$] are presented in the Table 20. The typical kinetic, conversion, and potentiometric curves of the process of oxidative hydroxylation of P4 in solutions $[Cu(PEG)_2Cl_2]$-C_7H_8-P_4-H_2O is shown in Figure 38-40.

An increase in temperature in the range of 50-70 °C has a positive effect on the reaction rate (1) and the yield of the target product (Figure 34, Table 21). The maximum rate of oxygen absorption is observed at 70 °C.

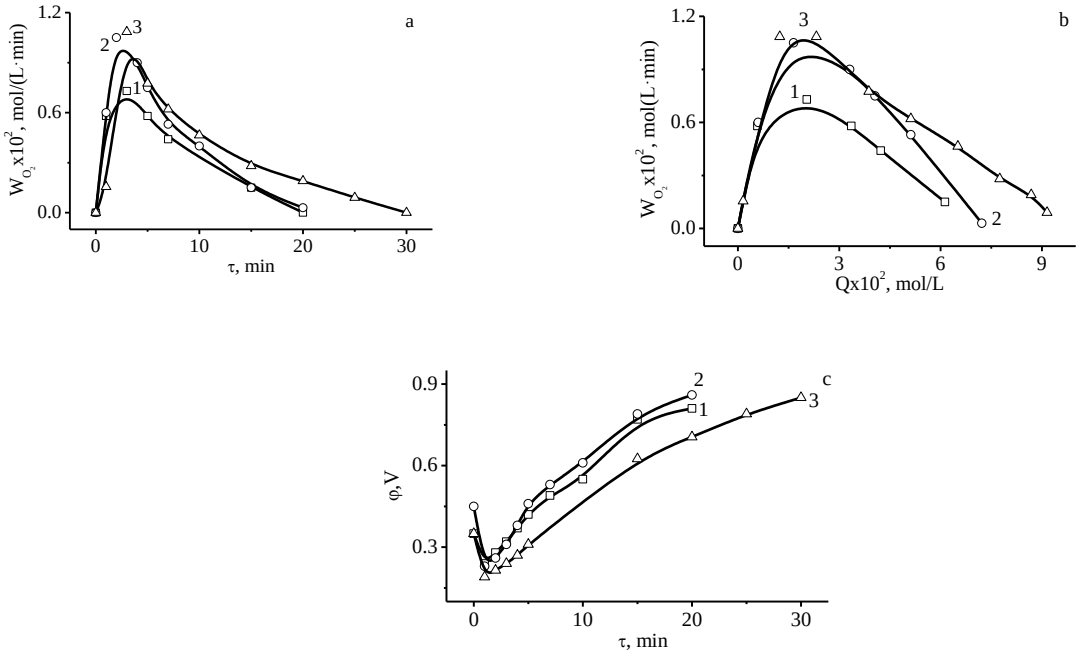

Effect of temperature

Conditions: concentration, mol/L: $[Cu(PEG)_2Cl_2]$ - 0,12; $[P_4]$ - $1{,}06\cdot10^{-2}$; $[H_2O]$ - 50; $[C_7H_8]$ 0,94; $[O_2]$ $(1{,}18\text{-}1{,}66)\cdot10^{-3}$; temperature, °C: 1 – 50; 2 – 60; 3 – 70.

Figure 34 - Kinetic (a), conversion (b) and potentiometric (c) curves of P_4 oxidation with oxygen in an aqueous medium in the presence of $[Cu(PEG)_2Cl_2]$

The average duration of the experiments was 20-30 minutes. Depending on the process conditions, the number of catalytic cycles TON (or catalyst productivity) carried out by one catalyst molecule lies in the limit of 0.62-2.48 mol acid/(mol Cat). Besides the number of revolutions per unit time (1 hour) TOF, carried out by one molecule of catalyst amounted to 1.24 – 4.96 mol of acids/(mol Cat ·h) (Table 21).

Increasing the catalyst concentration from 0.06 to 0.24 mol/L in the system in H_2O-P_4-C_7H_8-O_2 leads first to an increase in the rate of oxygen absorption (Figure 35), and then to its decrease. The amount of absorbed oxygen does not depend on the concentration of the catalyst.

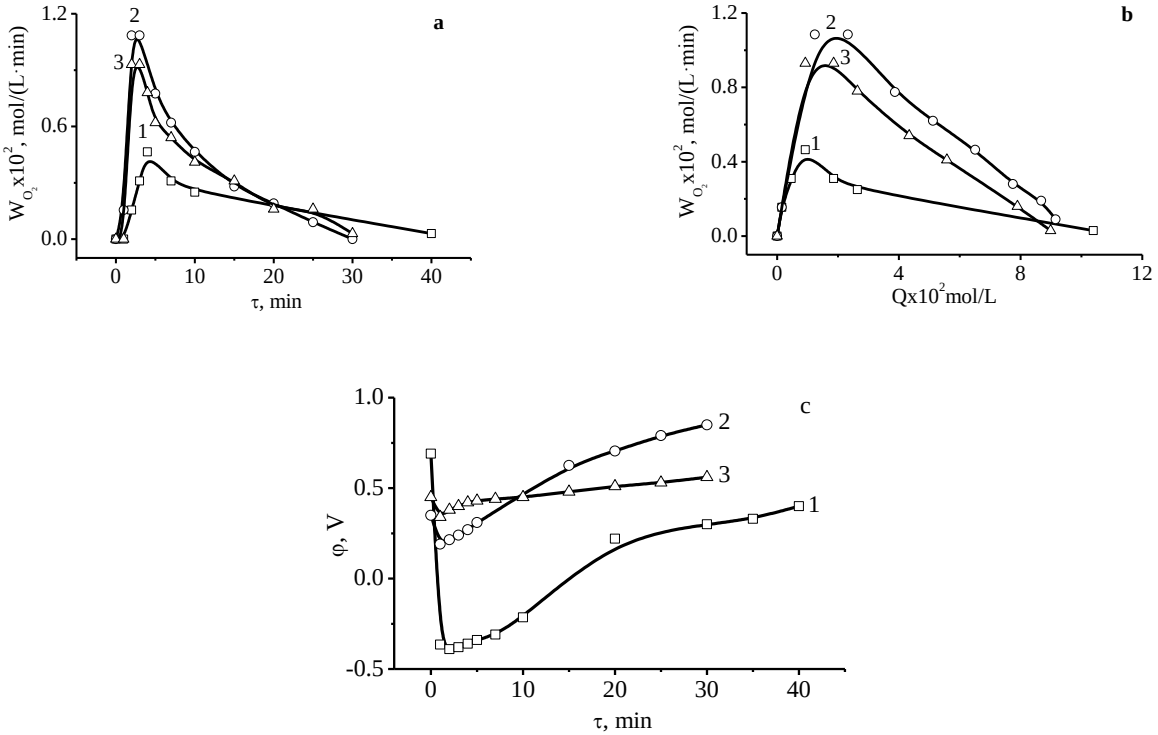

Effect of the catalyst concentration

Conditions: concentration, mol/L: [P_4] - 1,06·10^{-2}; [H_2O] - 50; [C_7H_8] - 0,94; [O_2] - 1,18·10^{-3}; 70 °C; [$Cu(PEG)_2Cl_2$]: 1 – 0,06; 2 – 0,12; 3 – 0,24.

Figure 35 - Kinetic (a), conversion (b) and potentiometric (c) curves of P_4 oxidation with oxygen in an aqueous medium in the presence of [$Cu(PEG)_2Cl_2$]

The maximum rate of oxygen absorption is observed at a catalyst concentration of 0.12 mol/L. The rate of the oxidation of yellow phosphorus with oxygen passes through a maximum at varying the concentration of yellow phosphorus from 0,53·10^{-2} до 2,12·10^{-} mol/L and the maximum rate of oxygen absorption is observed at (Figure 36).

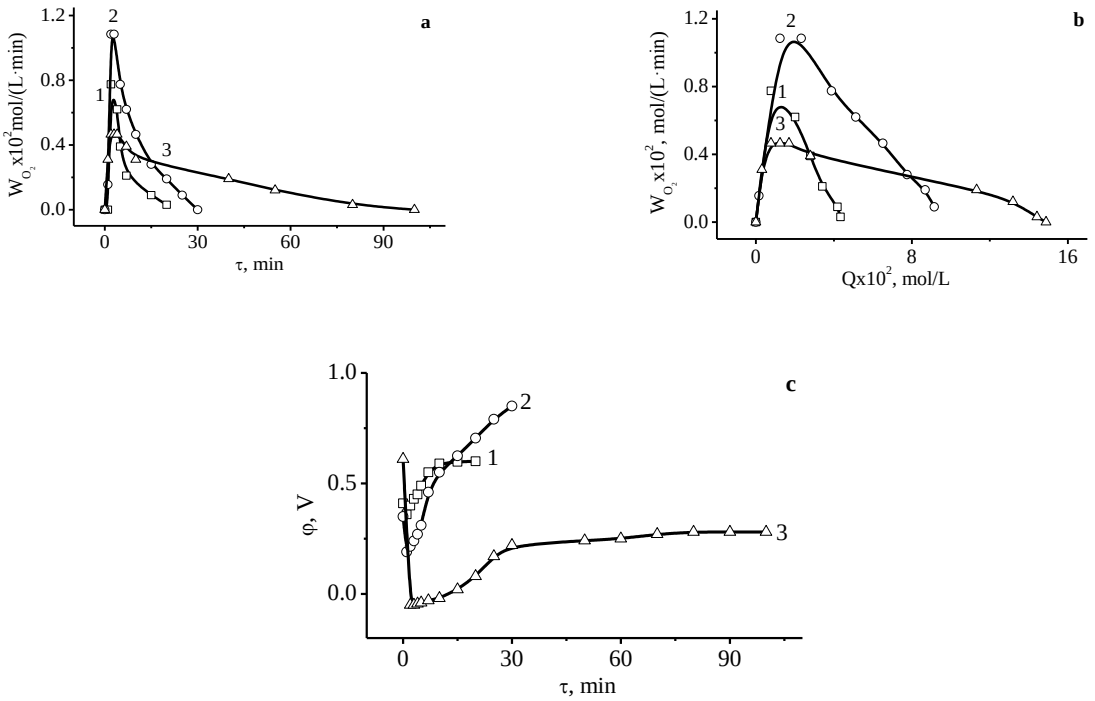

Effect of the phosphorus (P_4) concentration

Conditions: concentration, mol/L: [$Cu(PEG)_2Cl_2$] - 0,12; [P_4] - $1,06 \cdot 10^{-2}$; [H_2O] - 44,4-52,8; [C_7H_8] - 0,47-1,88; [O_2] - $1,18 \cdot 10^{-3}$; 70 °C; [P_4]: 1 – 0,53; 2 – 1,06; 3 – 2,12.

Figure 36 - Kinetic (a), conversion (b) and potentiometric (c) curves of P_4 oxidation with oxygen in an aqueous medium in the presence of [$Cu(PEG)_2Cl_2$]

As a result, it was found that yellow phosphorus in aqueous solutions with the polymer-metal complex [$Cu(PEG)_2Cl_2$] at 70 °C and P_{O2} = 1 atm is oxidized by oxygen to form phosphorous (13-64 %) and phosphoric acid (36-87 %). Optimum reaction conditions and a good yield of phosphoric acid are achieved at 70 °C and P_{O2} = 1 atm with a molar ratio of reagents [$Cu(PEG)_2Cl_2$]:[P_4] = 11:1. The maximum catalyst productivity at a molar ratio of reagents [Cu $(PEG)_2Cl_2$]:[P_4] = (6-11): 1 was TON = 2,48 mol acid/(mol Cat); TOF = 4,96 mol acid/(mol Cat·h)).

3.3.3 Oxidizing butoxylation of yellow phosphorus in the presence of catalysts - supported $CuCl_2$-PVP

Synthesized catalysts were tested in the reaction of oxidative butoxylation of yellow phosphorus. It was established that P_4 in the presence of supported copper-polymer catalysts at 60 °C is oxidized by carbon tetrachloride in alcohol-pyridine solutions with the formation of tributyl phosphite.

$$P_4 + 12Cl^- + 12BuOH \xrightarrow{cat} 4P(OBu)_3 + 12HCl \quad (25)$$

cat – 10% Cu(II)(PVP)/substrate

To study this reaction, the methods of redox potentiometry, gas chromatography analysis, IR spectroscopy and optical microscopy were used.

Table 21 presents the values of the specific surface of the carriers — substrates of the synthesized catalysts. The highest specific surface area is characterized by γ-Al_2O_3, and the smallest - natural zeolite. The largest specific pore volume corresponds to γ-Al_2O_3, and the smallest corresponds to walnut coal.

Table 21 – Surface Characteristics of Catalyst Supports

Carrier	Specific surface area, m^2/g	Average pore size, nm	Specific pore volume, cm^3/g
γ-Al_2O_3	135,771	1,713	0,058
SiO_2	76,669	1,713	0,033
Natural zeolite	0,810	-	-
Kieselguhr	24,180	1,713	0,010
Cellulose	-	-	-
Chitosan	-	-	-
Thistle meal	-	-	-
Walnut Coal	5,233	-	0,002

In the absence of a catalyst, the reaction of the oxidative butoxylation of yellow phosphorus proceeds very slowly [163]. The reaction was carried out in the presence of catalysts. Initially, a mixed solution containing tetrachloromethane, pyridine, n-butanol, quickly acquires a redox potential determined by the pair Cu (II)/Cu (I) (φ_{Cu}) and equal to 0.4-0.6 V. After addition of the P_4 solution in toluene to the butanol-pyridine solution with 10% Cu(II)-PVP/carrier in N_2 atmosphere in the absence of pyridine, the redox potential of the catalytic solution is shifted to the cathode side by $\Delta\varphi$ = 0.2-0.25 V within 5-10 minutes, then gradually returns to the anode (Figure 37, 38).

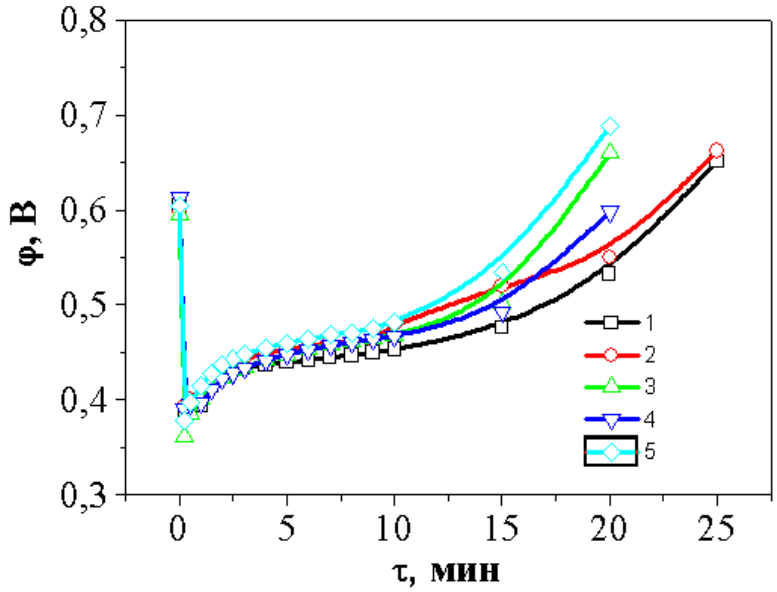

1 – 10% Cu(II)-PVP/zeolite; 2 –10% Cu(II)-PVP/Al_2O_3; 3 – 10% Cu(II)-PVP/SiO_2; 4 – 10% Cu(II)-PVP/kieselguhr; 5 – 10% Cu(II)-PVP/cellulose

Figure 37 – Potentiometric curves of oxidative butoxylation of P_4 with carbon tetrachloride in butanol solutions in the presence of catalysts

Pyridine is a necessary component of the reaction solution, since it promotes the dissociation of alcohol and catalyst regeneration. The duration of the experiments is within 20-30 minutes.

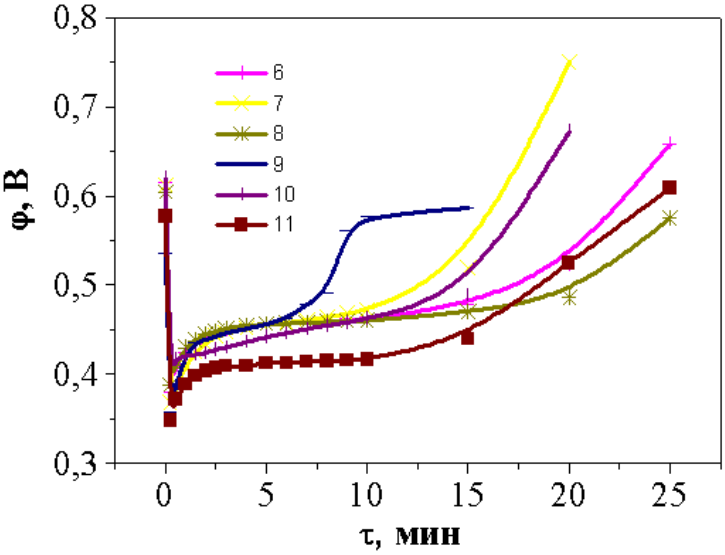

6 – 10% Cu(II)-PVP/walnut coal; 7 – 10% Cu(II)-PVP/thistle meal; 8 – 10% Cu(II)/PVP-chitosan; 9 – blank test; 10 – Cu(II) - fullerene ; 11 – $Cu(PVP)_3Cl_2$

Figure 38 – Potentiometric curves of oxidative butoxylation of P_4 with carbon tetrachloride in butanol solutions in the presence of catalysts

The reaction conditions and the yields of tetraphosphorus oxidation products by carbon tetrachloride in butanol-pyridine solutions in the presence of 10 % Cu(II)-PVP/catalyst support are presented in Table 22.

The total yield of organophosphorus compounds after the experiment is close to 100 %. The main products are tributyl phosphite (46-71%) and dibutyl phosphite (14-54%). Tributyl phosphate is formed with a lower yield (0,8-8,0%).

Table 22 – The oxidative butoxylation of P_4 in the presence of 10% Cu(II)-PVP/carrier

№	Catalyst	η∑ (%)	$(BuO)_3P$, %	$P(O)H(OBu)_2$, %	$PO(OBu)_3$, %
1[a]	$[Cu(PVP)_2Cl_2]$	100	66,1	30,5	3,4
2	10% Cu(II)-PVP/SiO_2	100	64,7	29,7	5,6
3	10% Cu(II)-PVP/γ-Al_2O_3	100	71,0	14,3	4,7
4	10% Cu(II)-PVP/kieselguhr	100	63,4	31,1	5,5
5	10% Cu(II)-PVP/Zeolite	100	46,7	53,3	-
6	10% Cu(II)-PVP/ cellulose	100	63,4	31,1	5,5
7	10% Cu(II)-PVP/walnut coal	100	56,3	36,3	7,4
8	10% Cu(II)-PVP/thistle meal	100	66,2	33,0	0,8
9	10% Cu(II)/PVP-chitosan	100	61,6	37,1	1,3
10	Cu(II)-fullerene	100	61,5	32,7	5,8
11	Blank test	47,9	0	36,4	1,5
Note - Reaction conditions, mol/L: m_{cat} 0,1 g; [BuOH] 7,70; $[CCl_4]$ 2,1; [Py] 0,16; $[P_4]$ $1{,}63\cdot10^{-2}$; $[C_7H_8]$ 0,90; 60 °C; Ar, reaction duration 25-40 min. a - m_{cat} 0,561 (0,16 mol) g.					

Chromatographic analysis of the reaction solutions confirms that under anaerobic conditions $P(O)H(OBu)_3$ and $P(O)(OBu)_3$ are formed (Table 22, Figure 39). Trialkylphosphites are characterized in the ^{31}P-NMR spectra by a chemical shift of 130-140 ppm, are not observed in the free state on chromatograms. In solution, they form strong complexes with Cu (I) ions of the $Cu[P(OR)_3]Y$ and $Cu[P(OR)_3]Y_2$ type, which are well manifested in the ^{31}P NMR spectra in the range of 6-10 ppm [200]. The trialkylphosphite complexes of Cu (I) are white substances with a consistency of ointment with a melting point depending on the nature of the alkoxy group from 90 to 180 °C. They are soluble in ether, arena, acetone, alcohols, easily destroyed by chlorine [201].

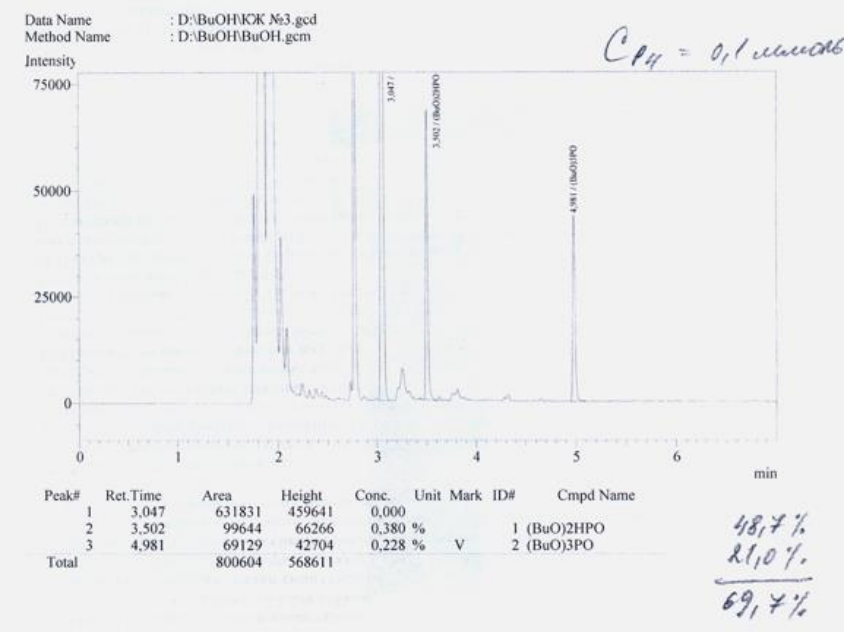

Figure 39 – Chromatogram of products obtained in the system 10% Cu (II)-PVP/kieselguhr-BuOH-C_5H_5N-CCl_4-P_4-C_7H_8 at 60 °C and the following component concentrations, mol/L:
[BuOH] 6,50; [C_5H_5N] 1,24; [CCl_4] 2,1; [P_4] $1{,}63 \cdot 10^{-2}$; [C_7H_8] 0,90; P_{N2} =1 atm

The obtained data indicate the formation of polymer films in the solution. The dense particles with a size of about 10 nm are observed (Figure 40).

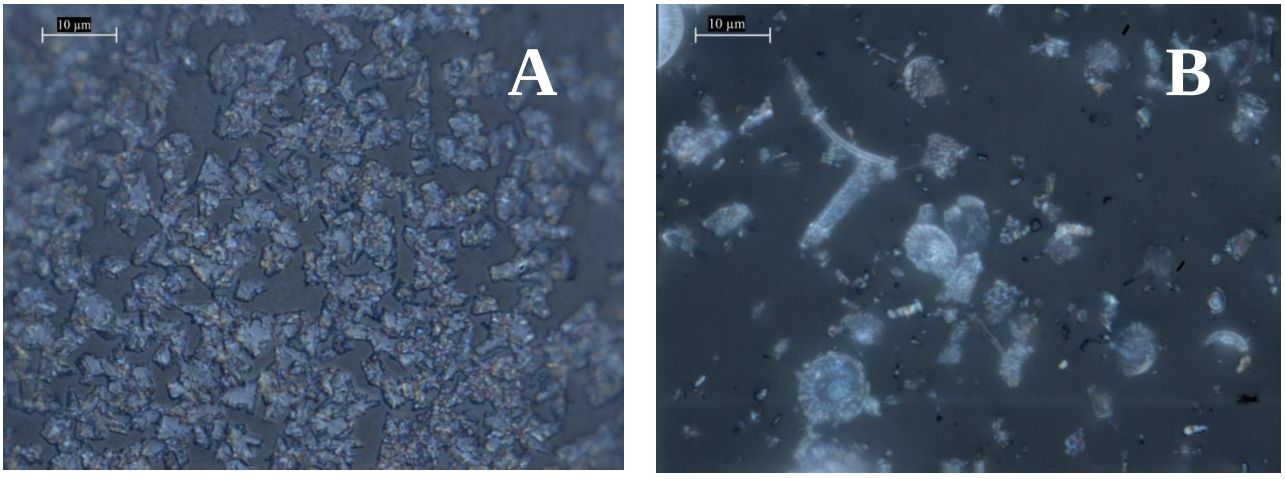

Figure 40 - Electron microphotographs of (A) [$Cu(PVP)_2Cl_2$] and the supported catalyst (B) 10% Cu(II)-PVP/kieselguhr

The clusters of various forms of translucent aggregates are formed on amorphous particles of kieselguhr-PVP due to deposition of copper chloride on its surface. The size of composed of particles about 10 nm, which apparently indicates copper fixation (Figure 40).

As a result, new catalysts have been obtained. These catalysts combine the activity of a homogeneous catalyst as well as the stability of heterogeneous catalysts

due to the deposition of the active phase on an inorganic carrier. At the same time, the fixation of the metal by bonding with the polymer greatly simplifies the preparation process. Also, provides the formation of a structure that improves the catalytic properties.

The extreme nature of the potentiometric curves allow us to conclude that the first key reaction of the oxidative butanolysis process of yellow phosphorus is the reduction of the in situ copper-polymer catalyst Cu(II)(PVP) to the elemental copper sols. These sols are stabilized by polyvinylpyrrolidone and catalysized the formation of intermediate tributyl phosphite (26). In the presence of the unstable acid evolved by equation (27), $P(OBu)_3$ is easily subjected to acidolysis by reaction (28) with the formation of dibutylphosphite. Tributyl phosphate is formed as a result of the oxidation of $P(OBu)_3$ with carbon tetrachloride in alcohol (29). The second key stage of the reaction process is the oxidation of copper-polymer Cu(0)sol(PVP) with carbon tetrachloride (28), which returns the complex Cu (II)(PVP) to the catalytic cycle.

$$P_4+6Cu(II)(PVP)/S+12Cl^-+12BuOH \rightarrow 4P(OBu)_3+6Cu(0)(PVP)/S+12HCl \quad (26)$$

$$P(OBu)_3 + HCl \rightarrow P(O)H(OBu)_2 + BuCl \quad (27)$$

$$P(OBu)_3 + CCl_4 + BuOH \rightarrow 4P(O)(OBu)_3 + CHCl_3 + BuCl \quad (28)$$

$$Cu(0)(PVP)/S+CCl_4+2HCl \rightarrow Cu(II)(PVP)/S+CHCl_3+2Cl^-+HCl \quad (29)$$

where S - substrate

The rate of the total catalytic process is determined by the rate of the slowest reaction and is characterized by the presence of a minimum on the potentiometric curves.

The thermodynamic probability of the occurrence of redox stages (26-29) was estimated from the values of the standard potentials of oxidizers and reducing agents and the change in the free energies of these processes.

P_4 molecule, its inorganic and organic derivatives are prone to two-electron oxidation in aqueous solutions: $P_4 \rightarrow 4P^+$; $P^+ \rightarrow P^{3+}$; $P^{3+} \rightarrow P^{5+}$. It is known that the products of two-electron oxidation of P_4 are stable compounds $P_4(OR)_2$, $P_4(OR)_4$, $P_2(OR)_4$, $P(OR)_3$, $P(OR)_5$, whereas the single-electron oxidation products of P_4 are unstable radicals [202, 203]. In organic media P_4 and its derivatives P(I) ($P_4(OR)_2$), P(III) ($P(OR)_3$) and P(V) ($P(O)(OR)_3$) are characterized by similar values of redox two-electron transition potentials. They are strong two-electron reducing agents, imposing on Cu (II) complexes the role of a two-electron oxidant [201]. Standard Cu (II) reduction potentials indicate that, depending on the redox partner, Cu (II) can be reduced to Cu (I) or Cu (0). The Cu (II) ion is prone to both one-electron ($E°_{Cu(II)/Cu(I)}$ = 0,538 V) and two-electron reduction ($E°_{Cu(II)/Cu(0)}$ = 0,337 V).

The calculated values of the electromotive force and the free energy of the Cu (II) reduction reactions with yellow phosphorus and its derivatives indicate that they are resolved thermodynamically. This suggests that the two-electron oxidation of P_4 into $P_4(OR)_2$, then $P_4(OR)_2$ into $P(OR)_3$ and $P(OR)_3$ into $P(O)(OR)_3$, proceeds rapidly in the coordination sphere of Cu (II) (Table 23).

Table 23 – Possible electrode processes in the system P_4-$CuCl_2$-ROH-O_2

Redox half reaction	E^o, V#	Redox reaction	z_e	E, V	$\Delta G°$, kJ
Reducing agent					
$P_4 - 2e \rightarrow P_4^{2+}$	-0.508				
$P^+ - 2e \rightarrow P^{3+}$	-0.499				
$P^{3+} - 2e \rightarrow P^{5+}$	-0.276				
Catalyst CuX_2					
Oxidizing agent Cu(II)		Reduction Cu(II)			
$Cu^{2+} + 2e \rightarrow Cu$	0.337	$P_4 + Cu^{2+} \rightarrow P_4(OR)_2 + Cu$	2	0.845	-163
		$P_4(OR)_2 + Cu^{2+} \rightarrow P(OR)_3 + Cu$	2	0.836	-161
		$P(OR)_3 + Cu^{2+} \rightarrow P(O)(OR)_3 + Cu$	2	0.613	-118
		Oxidation of Cu and Cu (I)			
$Cu^{2+} + e \rightarrow Cu^+$	0.538	$Cu + Cu^{2+} \rightarrow 2Cu^+$	1	0.401	-38
$Cu^+ + e \rightarrow Cu$	0.137				

Accordingly, it was established that the studied processes proceed by the redox mechanism and consist of two key reactions: reduction of Cu (II) with yellow phosphorus to Cu (I) to form tributyl phosphite and oxidation of Cu (I) to Cu (II) with carbon tetrachloride.

4 APPLIED ASPECTS

4.1 The development of the principle technological scheme and cost estimates of the synthesis of sorbents based on clay and plant materials

The use of clays as adsorbent have advantages upon many other commercially available adsorbents in terms of low-cost, an abundant availability, high specific surface area, excellent adsorption properties, non-toxic nature, and large potential for ion exchange [20-21]. The most of the clay minerals are negatively charged and very effective and extensively used to adsorb metal cations from the solution; due to their high cation exchange capacity, high surface area, a pore volume [22]. In addition, due to the low cost of clay there is no need to regenerate them. Therefore, the use of clay and materials based on it would solve the problem of waste disposal, as well as access to less expensive material for wastewater treatment.

High content of quartz, as well as ferrous minerals and other impurities reduce the quality of bentonite clays, which makes it necessary to enrich. The amount of montmorillonite in the feedstock after enrichment is 95 %.

The principal technological scheme for the synthesis of composite materials based on bentonite comprises the following steps (Figure 41):

1 Unloading of bentonite clay from the Dinosaur deposit (reserves of 4 million tons) to the warehouse;

2 The process of crushing large pieces of raw materials in a jaw crusher until size 50 mm;

3 After crushing, the clay pieces are sent to the gross mill feed bin, where they are ground to a fraction of <0.1 mm;

4 Simultaneously with the grinding process, bentonite is dried in drum-type furnaces with hot air at a temperature of 80-300 °C to a residual moisture content of clay 6-15 %;

5 The raw material obtained after grinding, in the form of a mixture of granules of various sizes, has to be send to an air granulator for particle size distribution. Particles of 0.07 mm sent for further modification. Larger particles removed from the environment for further use in the production of building materials;

6 To obtain the final product, modifying the PEG polymer with a concentration of 0.1 % added to the crushed clay. The mixing process carried out for one hour, followed by settling during the day;

7 The obtained composition subjected to washing with distilled water, filtering and drying at 100 °C for 6 hours;

8 The obtained composition is subjected to grinding to size <0.1 mm;

9 The final product weighed and packaged in paper bags.

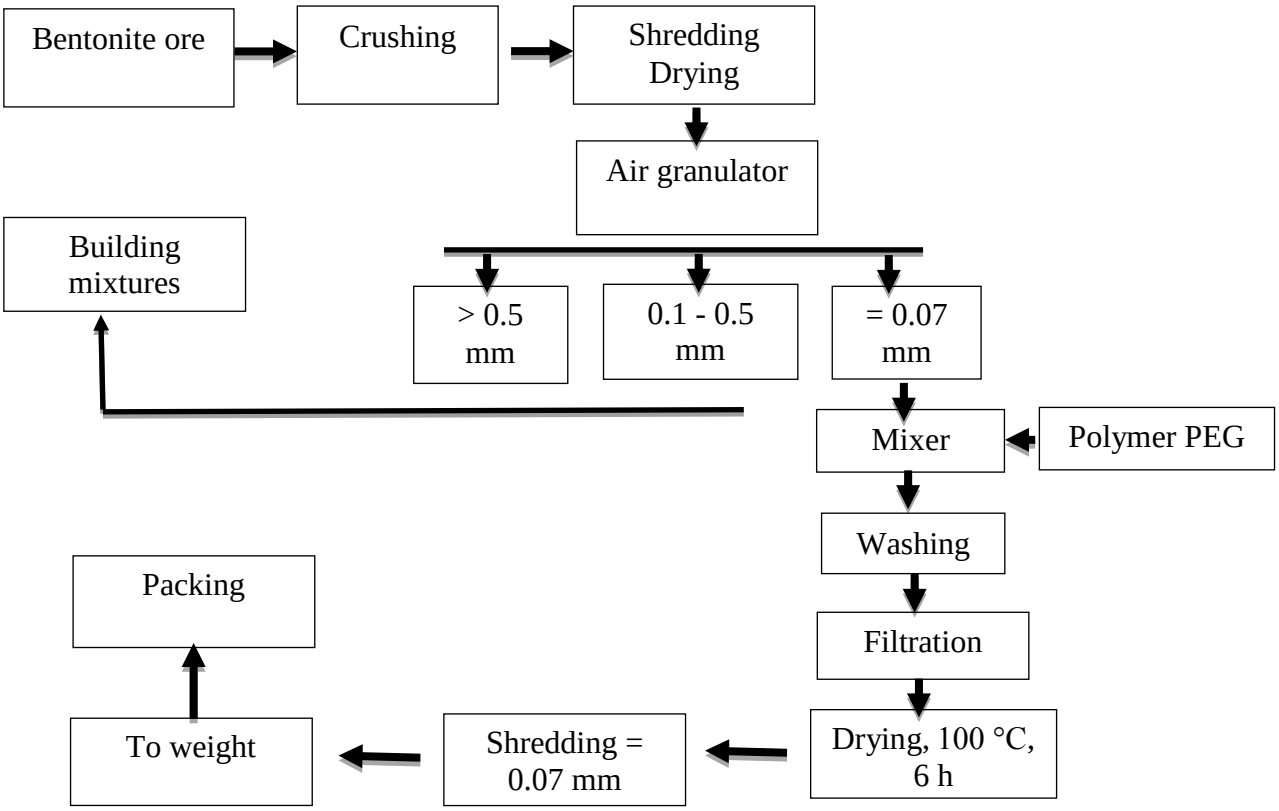

Figure 41 – Schematic diagram of the synthesis of composite materials based on bentonite

Taking into account that the specific consumption of water in the processing plants of ferrous and nonferrous metallurgy depends on a number of factors such as the composition of the ore, technological processes and productivity of factories, its amount is hundreds of cubic meters of water per day. To calculate the material balance of the synthesis of the sorbent, the amount of wastewater was chosen equal to 100 m^3. In this work, it was found that the optimal dose of sorbent for treatment aqueous solutions of copper (II), lead (II), cadmium (II) ions is 10 g/L, therefore, 1000 kg of sorbent is required for cleaning 100 m^3. In view of the sorbent yield equal to 90 %, the estimated cost of raw materials was calculated without taking into account the amount of electricity, the cost of equipment and wages to employees. For 1 kg of sorbent the price is 196.4 tenge. While the average price of sorbents for 1 kg on the market is 1132.4 tenge. Table 24 shows calculated cost estimates for getting 1000 kg of BT-PEG sorbent.

Table 24 – Estimated cost of BT-PEG

Nomination	Quantity (kg)	Cost for 1 kg (tg)	Costs (tg)
Bentonite	1106.1	60	66 366
Polyethylene glycol (6000)	5.0	26 000	130000
Total			196366

In a number of studies, due to such characteristics as uniform distribution of pore size, sufficient surface area and the presence of active functional groups, biosorbents are considered as promising materials for wastewater treatment [61-96].

Confectionery waste can be used to produce new CM with sorption properties. The principal technological scheme for the synthesis of composite materials based on orange and mandarin peels comprises the following steps (Figure 42):

1 Unloading of oranges' peel to the warehouse. Fruits' peel delivered in boxes to the factory are stored on the raw materials sites for no more than 3 days, and in refrigerated rooms no more than 1 month;

2 Washing with hot water (40-50 °C);

3 The resulting peel is sent to the reagent vessel, where a solution of 1 M NaOH is added for chemical activation. The process is accompanied by stirring for an hour and settled for 24 hours for effective modification;

4. Next, rinsing with distilled water to a neutral environment, filtering and drying at 100 ° C for 2 hours;

5 To obtain the final product, the modifying PVP polymer with concentration 2.5 10^{-2} M is added to the activated orange peel. The mixing process is carried out for one hour, followed by settling during the day;

6 The resulting composition is subjected to washing with distilled water, filtering and drying at 80 - 100 °C for 2 hours;

7 The resulting composition is subjected to grinding to size <0.1 mm;

8 The resulting product was weighed and packaged in paper bags.

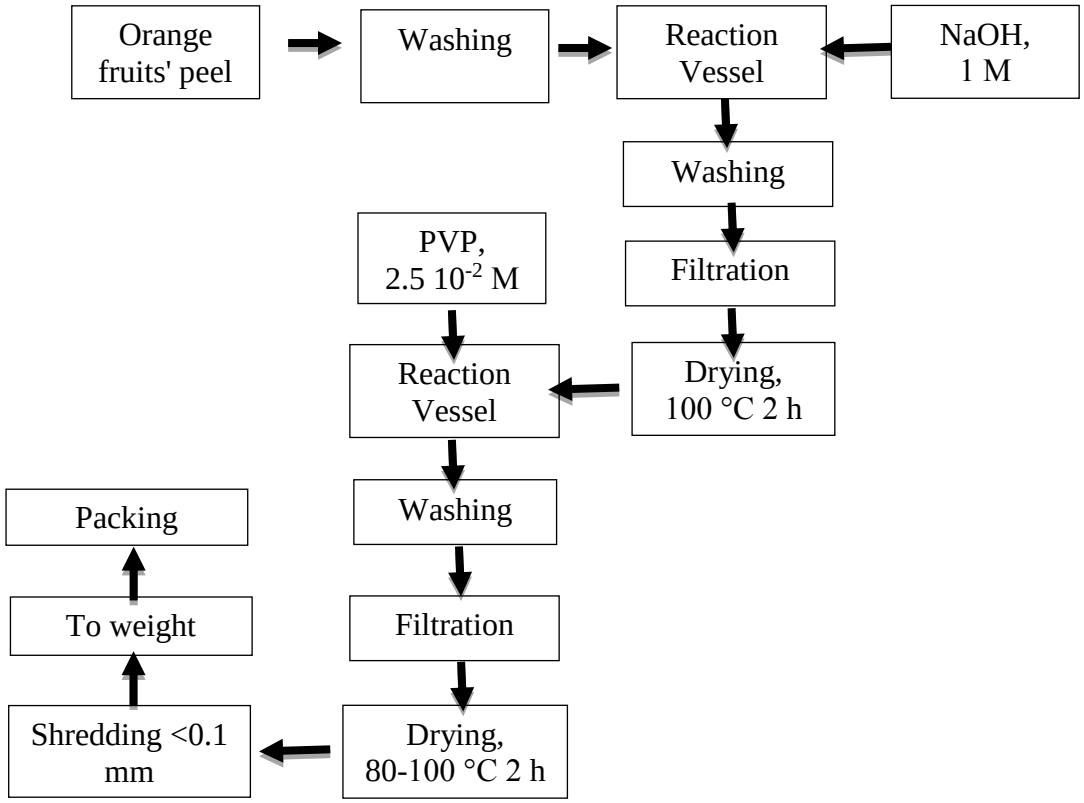

Figure 42 – Schematic diagram of the synthesis of composite materials based on orange/mandarin peels

A similar scheme is suitable for obtaining a composite material from mandarin peel.

An estimate of the cost of raw materials per 1000 kg of sorbent based on orange/mandarin peel was also calculated. The results are presented in Table 25. Considering the sorbent yield equal to 85 %, the estimated cost of raw materials was calculated without taking into account the amount of electricity, the cost of equipment and wages to employees and it was found that for 1 kg of sorbent the cost is 523.3 tenge. While the average price of sorbents for 1 kg on the market is 1132.4 tenge.

Table 25 – Estimated cost of obtaining OP(MP)-PVP

Nomination	Quantity (kg)	Cost for 1 kg (tg)	Costs (tg)
Orange/Mandarin peel	1176.5	-	-
NaOH (pure)	400.0	894	357600
Polyvinylpyrrolidone (K30)	27.8	5960	165688
Total			523288

So, a conceptual scheme for the synthesis of CM based on bentonite clay and citrus peel (orange, mandarin) is proposed. The procedure is characterized by simplicity of synthesis and a small number of stages.

4.2 The development of the principle technological scheme and cost estimates of the synthesis of catalysts

Synthesis of catalyst for reduction processes - Cu^{2+}/PEG-BT and Cu^{2+}/PEG-ZT: The catalytic properties of these composites were tested on the reduction reaction of p-nitrophenols. Reduction process of nitro groups into amines plays an essential role in organic, medicinal and synthetic chemistry [128]. Substituted aromatic amines are indeed widely used as dyes [129], agrochemical and pharmaceutical products [130], and as intermediates for the production of diazonium salts, acylated aminophenols, quinones, and many other compounds.

One of the most effective methods for the transformation of nitro groups into amino groups is hydrogenation catalyzed by precious or transition metals.

For the purpose of efficient utilization of the consumed sorbents and further use as catalysts, the following method is proposed (Figure 5). The maximum copper adsorption on the BT-PEG sorbent reaches 26 mg/g with an initial copper concentration of 270 mg/L. That is, 1 g of sorbent contains 26 mg of copper ions. After pre-precipitation with 0.2 M CuSO4 solution, the mass of Cu (II) in 1 g of the sorbent was 91.47 mg, that is, the ratio of copper into the sorbent after sorption and after pre-precipitation is 0.4.

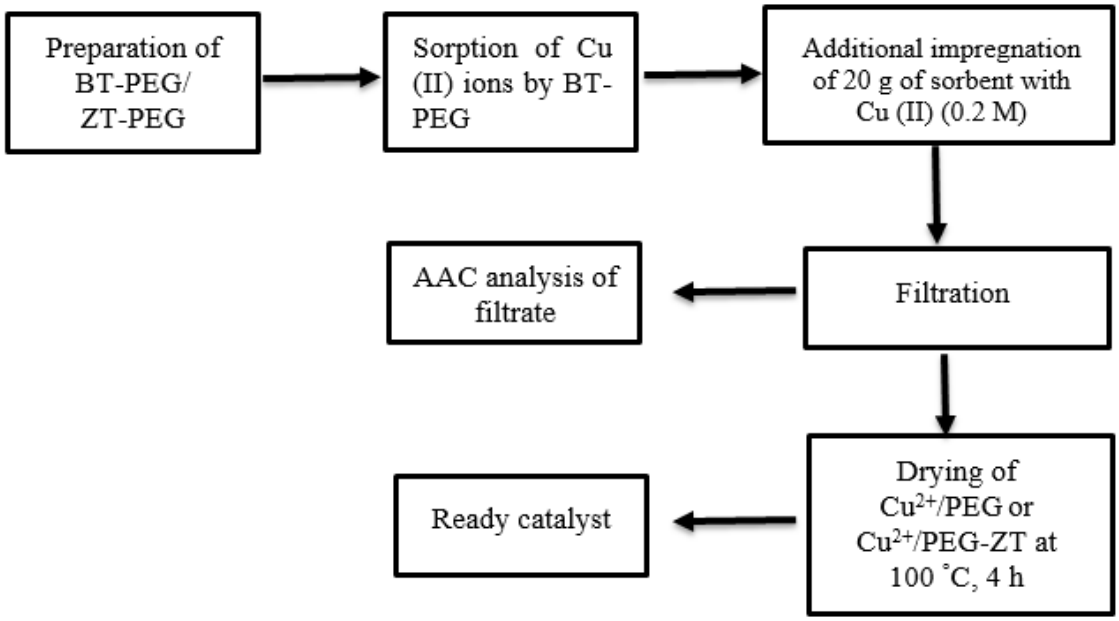

Figure 43 - The scheme of synthesis of CM (Cu^{2+}/PEG-BT and Cu^{2+}/PEG-ZT) based on clay raw materials with catalytic characteristics

Currently, the industrial method of obtaining p-aminophenol is the electrolytic reduction of nitrobenzene in the presence of concentrated sulfuric acid. The disadvantage of this method is the large number of generated acidic waste. New procedure of catalyst's synthesis to decrease the waste production was shown. This process is characterized, by rapid and environmental friendly properties.

The estimated cost of the raw materials for 1 kg of catalyst are shown in Table 26.

Table 26 – Estimated cost of Cu^{2+}/PEG-BT(ZT)

Nomination	Quantity (kg)	Cost for 1 kg (tg)	Costs (tg)
PEG-BT(ZT) sorbent after sorption of copper-containing solutions	1.00	-	-
$CuSO_4\,10H_2O$ (pure)	0.16	720	115.2
Total			115.2

Synthesis of catalyst for hydroxylation processes – $[Cu(PEG)_2Cl_2]$: Catalytically active metal complexes fixed on polymer substrates have great prospects in chemical technology of inorganic and organic materials to solve problems in the field of phosphor chemical production. The study of the complexation processes of the latter with the polymer ligand is not only of theoretical interest for expanding the field of coordination chemistry of polymers, but also has a practical direction. Polymeric compounds containing functional groups are suitable carriers of metal ions. In the

interaction of polymers with metal ions, new coordination compounds are formed, combining the properties of the initial components, as well as possessing a number of unique properties, in particular, high catalytic activity. In this regard, principal technological scheme for the synthesis of catalyst [$Cu(PEG)_2Cl_2$] are presented in Figure 44.

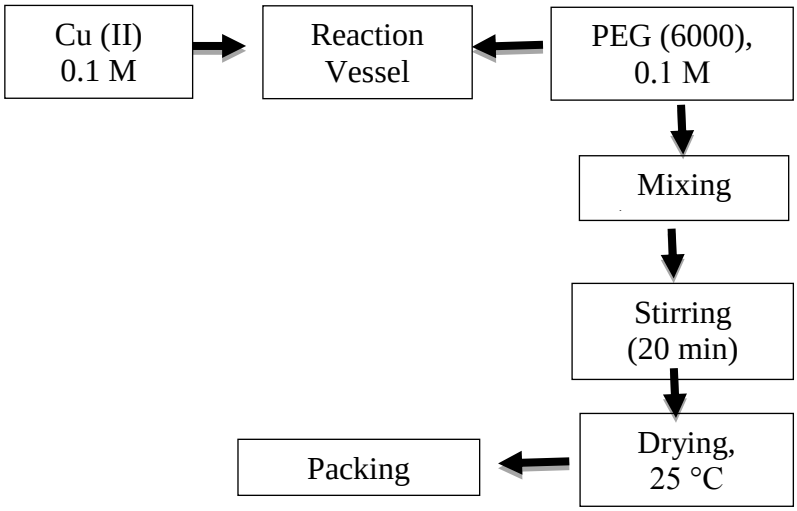

Figure 44 - The scheme of synthesis of CM: [$Cu(PEG)_2Cl_2$]

The estimated cost of the raw materials for 1 kg of catalyst was shown in Table 27.

Table 27 – Estimated cost of [$Cu(PEG)_2Cl_2$]

Nomination	Quantity (kg)	Cost for 1 kg (tg)	Costs (tg)
Polyethylene glycol (6000)	0.341	26 000	8866
$CuCl_2\,2H_2O$ (pure)	0.740	2620	419.1
Total			9285.1

Thus, the cost of the catalyst was 9285.1 tenge per 1 kg. However, it is known that in the price of the product also need to add energy, employee wages, transportation and equipment. Despite this, due to its high catalytic performance, this catalyst can be a commercial product.

Synthesis of catalyst for butoxilation processes – Substrate/$CuCl_2$-PVP: The use of metal complexes, fixed on organic and inorganic carriers, creates prospects for the rejection of expensive materials such as platinum, palladium and others. In this regard, the synthesis of new metal-polyelectrolyte catalysts supported on solid substrates opens up a wide range of their applications, ranging from simple exchange reactions in inorganic chemistry to the most complex transformations of substances in organic synthesis.

As a substrate in this paper were investigated: γ-Al_2O_3, SiO_2, Natural zeolite, Kieselguhr, Cellulose, Chitosan, Thistle meal, Walnut Coal. The principlal technological scheme for the synthesis of composite materials based on bentonite comprises the following steps (Figure 45).

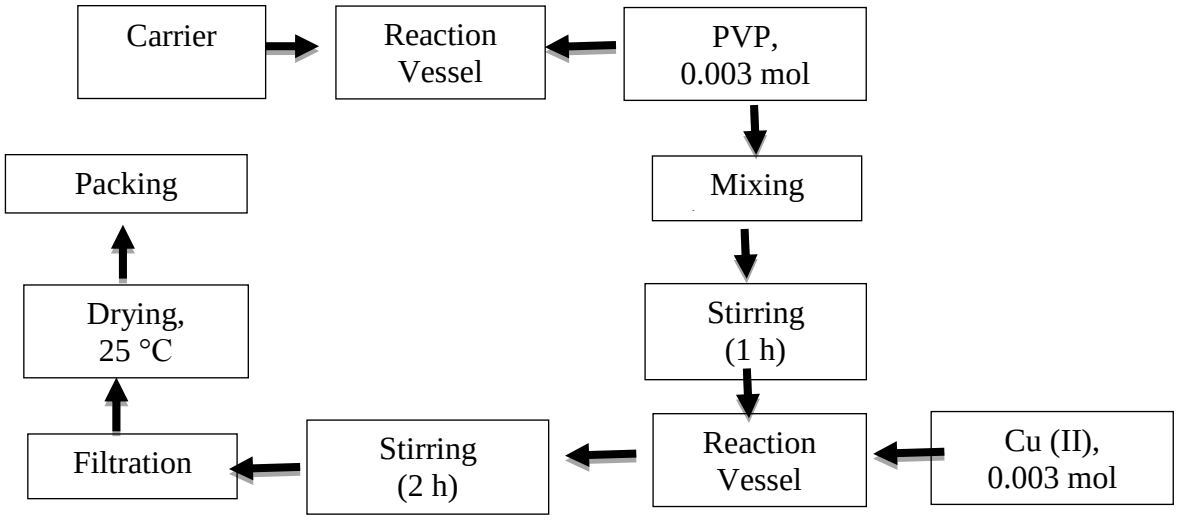

Figure 45 - The scheme of synthesis of CM: Substrate/$CuCl_2$-PVP

Table 28 shows the estimated cost of the raw materials for 1 kg of catalyst.

Table 28 – Estimated cost of Substrate/$CuCl_2$-PVP

Nomination	Quantity (kg)	Cost for 1 kg (tg)	Costs (tg)	The cost of the catalyst depending on the substrate (tg)
γ-Al_2O_3*	1.000	516.8	516.8	3288.6
SiO_2*	1.000	475.2	475.2	3246.8
Natural zeolite*	1.000	100.0	100.0	2872.0
Kieselguhr*	1.000	750.0	750.0	3521.8
Cellulose*	1.000	1850.0	1850.0	4621.8
Thistle meal*	1.000	450.0	450.0	3221.8
Polyvinylpyrrolidone	0.333	7065	2352.7	-
$CuCl_2$ $2H_2O$ (pure)	0.404	2620	419.1	-
*Carrier				

Hence, the cost of the catalyst varies from 2872 to 4621 tenge per 1 kg. In the future, the catalytic activity of the obtained catalysts in industrial plants has to be checked for testing with commercial analogues.

CONCLUSION

During performing this thesis, new composite materials based on mineral and plant materials were obtained, their physicochemical, sorption and catalytic properties were established.

Based on the analysis of the new results, the following conclusions were made:

1. In summary, BT-PEG sorbent was prepared successfully from bentonite of the Dinozaur field and used as an adsorbent for removing Pb^{2+} and Cd^{2+} from aqueous solutions. SEM, XRD and BET analysis indicate intercalation of the PEG polymer into the initial structure of the bentonite. The surface area, total pore volume and average pore diameter of BT-PEG were calculated to be 3.67 m^2/g, 0.0082 cm^3/g and 186.3 nm.

2. Composite materials - OP-PVP and MP-PVP based on orange and mandarin peel were obtained. According to the data of IR spectroscopy, it was found that the composites contain functional groups (=C-H, Ar-N=O), which can effectively be replaced and interact with metal ions.

3. The copper oxide (I) NPs were supported onto natural bentonite and zeolite using PEG as a stabilizing agent in the course of the 4-NP reduction reaction. The method consists in the sequential deposition of the polymer, and then copper (II) ions on the carrier, followed by reduction of the metal by $NaBH_4$ in the process of reduction of 4-nitrophenol. The XRD analysis indicated the formation of cubic-phase of Cu_2O. The existence of NPs with sizes of about 20 nm was further confirmed by HR-SEM and EDS analysis.

4. New polymer-metal heterogeneous catalysts based on copper (II) ions and polyvinylpyrrolidone (PVP) and polyethylene glycol (PEG), supported on a carrier, for the oxidation of yellow phosphorus were obtained. The compositions of polymer-metal complexes is PEG-Cu^{2+}=2:1 were established based on the analysis of the physico-chemical studies.

The optimal conditions for the sorption process of lead (I) and cadmium (II) and copper (II) ions with BT-PEG composite material were established. The adsorption of Pb^{2+} and Cd^{2+} was found to be dependent on the metal ion concentration, pH and temperature. The adsorbed amounts of both metal ions increased with increasing PEG concentration, pH. The adsorption equilibrium for all metal ions can be described by the Freundlich model, which confirmed the presence of a heterogeneous system with irregular filling of the active centers. The maximum sorption capacities for Pb^{2+}, Cd^{2+} and Cu^{2+} shown by BT-PEG were 22, 18 and 26 mg/g, respectively. The rate constants for Pb^{2+} and Cd^{2+} sorption were found to be 6.29 and 6.67 g mg^{-1} min^{-1}, respectively, at 25°C. It is established that the sorption of Pb^{2+} and Cd^{2+} ions by a BT-based composite has a pseudo-second order, indeed sorption of Cu^{2+} ions has pseudo-first order ($k = 0.01$ min^{-1}). It is shown that their rate constants decrease with increasing temperature and the processes are characterized by a negative activation energy.

5. The optimal conditions for the sorption process of copper (II) and nickel (II) ions with OP-PVP and MP-PVP composite material were established. The adsorption equilibrium for both Cu^{2+} and Ni^{2+} can be described by the Freundlich

model. Modification of peel with PVP polymer leads to an increase in their sorption properties. Sorption kinetics described by the pseudo-first order model.

6. Composites Cu_2O/PEG-BT and Cu_2O/PEG-ZT showed high catalytic activities in the model reduction reaction of 4-NP to 4-AP using mild conditions. Zeolite was more effective than bentonite as a support material for the catalytic and kinetic characteristics. 4-NP reduction reaction rate constants are equal 1.22×10^{-2} s^{-1} and 1.79×10^{-2} s^{-1} in the presence of Cu_2O/PEG-BT and Cu_2O/PEG-ZT accordingly.

7. It was established that yellow phosphorus in aqueous solutions in the presence of a polymer-metal complex $[Cu(PEG)_2Cl_2]$ at 70 °C and P_{O2} = 1 atm is oxidized by oxygen to form phosphorous (13-64 %) and phosphoric acid (36-87 %). Optimal reaction conditions and a good yield of phosphoric acid are achieved at 70 °C and P_{O2} = 1 atm with a molar ratio of reagents $[Cu(PEG)_2Cl_2]$:$[P_4]$ = 11:1. The maximum catalyst productivity at a molar ratio of reagents $[Cu(PEG)_2Cl_2]$:[P4]=(6-11):1 was TON = 2,48 mol acid/(mol Cat); TOF = 4,96 mol acid/(mol Cat ·h)).

8. The optimal conditions for the reaction of oxidation of yellow phosphorus in an organic medium in the presence of a polymer-metal complex of copper (II) supported on carriers are established. It was found: temperature 60°C in the presence of catalyst 10% Cu(II)-PVP/γ-Al_2O_3 and molar ratio of reagents is $[BuOH]:[C_5H_5N]:[CCl_4]:[P_4]:[C_7H_8]$ = (7,7:1,2:2:0,06:0,9).

9. Concepts of synthesis of composite materials based on natural raw materials have been developed. A preliminary assessment of the economic efficiency of obtaining composite materials with sorption and catalytic properties in comparison with known sorbents and catalysts were carried out.

REFERENCES

1 Ali I., Gupta V.K. Advances in water treatment by adsorption technology // Nat. Protoc. – 2007. - №1. – P. 2661-2667.

2 Gupta V.K., Carrott P.J.M., Carrott M.M.L. Low-cost adsorbents: growing approach to wastewater treatment – a review // Crit. Rev. Environ. Sci. Technol. – 2009. - №39. – P. 783-842.

3 Rao R.A.K., Kashifuddin M. Kinetics and isotherm studies of Cd (II) adsorption from aqueous solution utilizing seeds of bottlebrush plant (Callistemon chisholmii) // Appl. Water Sci. – 2014. - №4. – P. 371-383.

4 Halim M., Conte P., Piccolo A. Potential availability of heavy metals to phytoextraction from contaminated soils induced by exogenous humic substances // Chemosphere. – 2002. - №52. – P. 26–75.

5 Balasubramanian R., Perumal S.V., Vijayaraghavan K. Equilibrium isotherm studies for the multicomponent adsorption of lead, zinc, and cadmium onto Indonesian peat // Ind. Eng. Chem. Res. – 2009. - №48. – P. 2093–2099.

6 Gupta V.K., Ali I. Removal of lead and chromium from wastewater using bagasse fly ash – a sugar industry waste // J. Colloid Interface Sci. – 2004. - №271. – P. 321–328.

7 Howard H., Michael M.C. Human health and heavy metals exposure. - Life Support: The Environment and Human Health, MIT Press, 2002. -383 p.

8 Ahmaruzzaman M. Industrial wastes as low-cost potential adsorbents for the treatment of wastewater laden with heavy metals // Adv. Colloid Interface Sci. – 2011. - №116. – P. 36–59.

9 Cempel M., Nikel G. Nickel: a review of its sources and environmental Toxicology // Pol. J. Environ. Stud. -2006. - №15. – P. 375–382.

10 EPA-450/4-84-007f. Locating and Estimating air Emissions from Sources of Nickel, U.S. Environmental Protection Agency, 1984.

11 Venugopal B., Luckey T.D. Toxicity of group VII metals, in: Metal Toxicity in Mammals. - Chemical Toxicity of Metals and Metalloids, Plenum Press, 1978. - pp. 261–271.

12 Schroeder W.H., Dobson M., Kane D.M. Toxic trace elements associated with airborne particulate matter: a review // J. Air Pollut. Control Assoc. -1987. - №37. – P. 1267–1285.

13 Siahkamari M., Jamali A., Sabzevari A., Shakeri A. Removal of Lead (II) ions from aqueous solutions using biocompatible polymeric nano-adsorbents: A comparative study // Carbohydr. Polym. – 2017. - №157. – P.1180-1189.

14 Rao R.A.K., Kashifuddin M. Adsorption properties of coriander seed powder (Coriandrum sativum): extraction and pre-concentration of Pb (II), Cu (II) and Zn (II) ions from aqueous solution // Adsorpt. Sci. Technol. – 2012. - №30. – P. 127–146.

15 Gisi S.D., Lofrano G., Grassi M., Notarnicola M. Characteristics and adsorption capacities of low-cost sorbents for wastewater treatment: A review // Sustainable Materials and Technologies. – 2016. - №9. - P. 10-40.

16 Belarbi H., Al-Malack M. H. Adsorption and stabilization of phenol by modified local clay // Int. J. Environ. Res. – 2010. - №4. – P. 855–860.

17 Ahmad R., Mirza A. Facile one pot green synthesis of Chitosan-Iron oxide (CS-Fe_2O_3) nanocomposite: Removal of Pb(II) and Cd(II) from synthetic and industrial wastewater // Journal of Cleaner Production Volume. – 2018. - №186. – P. 342-352.

18 Ali I., Ashim M., Khan T.A. Low cost adsorbents for the removal of organic pollutants from wastewater // J. Environ. Manag. – 2012. - №113. – P.170-183.

19 Das B.M. Introduction to Geotechnical Engineering. - Cram101 Inc., Publication and services, 2012. – 375 p.

20 Crini G., Badot P-M. Sorption Process and Pollution, Conventional and Non-Conventional Sorbents for Pollutant Removal from Wastewaters. - Presses Univ. Franche-Comté, 2010. – 499 p.

21 Srinivasan R. Advances in application of natural clay and its composites in removal of biological, organic, and inorganic contaminants from drinking water // Adv. Mater. Sci. Eng. – 2011. – Vol. 2011. – P. 1–17.

22 Churchman G.J., Gates W.P., Theng B.K.G., Yuan G. Clays and Clay Minerals for Pollution Control. - Development in Clay Science, vol. 1, Elsevier Press, 2006.

23 Odoma A.N., Obaje N.G., Omada J.I., Idakwo S.O., Erbacher J. Paleoclimate reconstruction during Mamu formation (cretaceous) based on clay mineral distributions // J. Appl. Geol. Geophys. – 2013. - №1. – P. 40–46.

24 Ross C.S. The mineralogy of clays // Transactions of the 1st International Congress of Soil Science. - Washington, D.C., 1999. - P. 555–561.

25 Hendricks S.B. Diffraction of X-ray radiation from crystalline aggregates // Z. Phys. – 1929. - №4. – P. 1058–1072.

26 Hendricks S.B., Fry W.H. The results of X-ray and microscopal examinations of soil colloids // Soil Sci. – 1930. - №29. – P. 457–478.

27. Pauling L. Structure of the chlorites // Proc. Natl. Acad. Sci. USA. -1930. - №16. – P.578–582.

28 Grim R.E. Mineralogy, second ed. - McGraw-Hill Press, 1968. - 596 p.

29 Weaver C.E., Pollard L.D. Developments in Sedimentology, The Chemistry of Clay Minerals, vol. 15. - Elsevier Scientific Publishing Company, 1973. - 213 p.

30 Miranda-Trevino J.C., Coles C.A. Kaolinite properties, structure and influence of metal retention on pH // Appl. Clay Sci. – 2003. - №23. - P. 133–139.

31 Brigatti M.F., Galan E., Theng B.K.G. Structure and Mineralogy of Clay Minerals, Developments in Clay Science. - Elsevier Press, 2013. - Vol. 5A. -P. 21–68.

32 Fjar E., Holt R.M., Raaen A.M., Risnes R., Horsrud P. Petroleum Related Rock Mechanics, Developments in Petroleum Science, second ed. -Elsevier Press, 2008. - Vol. 53. – 514 p.

33 Bear F.E. Chemistry of the Soil, second ed. - Reinhold Publishing, 1965.

34 Имангалиева А.Н., Сейлханова Г.А., Акбаева Д.Н., Рахым А.Б., Кенжалина Ж.Ж. Модифицированный сорбент на основе бентонитовой глины

для извлечения ионов кадмия (II) из водных растворов // Комплексное использование минерального сырья. - 2016. - №3. - С. 57-62.

35 Abou-El-Sherbini K., Hassanien M.M. Study of organically-modified montmorillonite clay for the removal of copper(II) // J. Hazard. Mater. – 2010. - № 184. - P. 654–661.

36 Ma L., Chen Q., Zhu J., Xi Y., He H., Zhu R., Q. Tao Q., Ayoko G.A. Adsorption of phenol and Cu(II) onto cationic and zwitterionic surfactant modified montmorillonite in single and binary systems // Chem. Eng. J. – 2016. - №283. – P. 880–888.

37 Yu R., Wang S., Wang D., Ke J., Xing X., Kumada N., Kinomura N. Removal of Cd^{2+} from aqueous solution with carbon modified aluminum-pillared montmorillonite // Catal. Today. – 2008. - №139. – P. 135–139.

38 Ma L., Zhu J., Xi Y., Zhu R., He H., Liang X., Ayoko G.A. Simultaneous adsorption of Cd (II) and phosphate on Al_{13} pillared montmorillonite // RSC Adv. - 2015. - №5. – P. 77227–77234.

39 Karamanis D., Assimakopoulos P.A. Efficiency of aluminum-pillared montmorillonite on the removal of cesium and copper from aqueous solutions // Water Res. - 2007. - №41. – P. 1897–1906.

40 Gupta S.S., Bhattacharya K.G. Treatment of water contaminated with Pb(II) and Cd(II) by adsorption on Kaolinite and Montmorillonite and their acid activated forms // Ind. J. Chem. Technol. – 2009. - №16. – P. 457–470.

41 Ma B., Oh S., Shin W.S., Choi S.J. Removal of Co^{2+}, Sr^{2+} and Cs^{+} from aqueous solution by phosphate-modified montmorillonite (PMM) // Desalination. – 2011. - №276. – P. 336–346.

42 Goncharuk V.V., Puzyrnaya L.N., Pshinko G.N., Bogolepov A.A., Demchenko V.Y. The removal of heavy metals from aqueous solutions by montmorillonite modified with polyethylenimine // J. Water Chem. Technol. – 2010. -№32. – P. 67–72.

43 Xu D., Zhou X., Wang X. Adsorption and desorption of Ni^{2+} on Na-montmorillonite: effect of pH, ionic strength, fulvic acid, humic acid and addition sequences // Appl. Clay Sci.-2008. – №39. – P.133-141.

44 Aziz I., Sirajuddin M., Khan M.H., Nadeem S., Tirmizi S.A., Khan R.A., Investigation of adsorption of lead (II) onto a montmorillonite clay modified by humic acid // J. Chem. Soc. Pak. – 2015. - №37. – P. 894–902.

45 Pereira F.A.R., Sousa K.S., Cavalcanti G.R.S., Fonseca M.G., de-Souza A.G, Alves A.P. M. Chitosan-montmorillonite biocomposite as an adsorbent for copper (II) cations from aqueous solutions // Int. J. Biol. Macromol. – 2013. - №61. – P. 471–478.

46 Soltermann D., Fernandes M.M., Baeyens B., Dahn R., Miehe-Brendle J., Wehrli B., Bradbury M.H. Fe(II) sorption on a synthetic montmorillonite. A combined macroscopic and spectroscopic study // Environ. Sci. Technol. – 2013. - №47. – P. 6978–6986.

47 Zhu J., Cozzolino V., Pigna M., Huang Q., Caporale A.G., Violante A. Sorption of Cu, Pb and Cr on Na-montmorillonite: competition and effect of major elements // Chemosphere. – 2011. - №84. – P. 484–489.

48 Chen C., Liu H., Chen T., Chen D., Frost R.L. An insight into the removal of Pb (II), Cu(II), Co(II), Cd(II), Zn(II), Ag(I), Hg(I), Cr(VI) by Na(I)-montmorillonite and Ca(II)-montmorillonite // Appl. Clay Sci. – 2015. - №118. – P. 239–247.

49 De-Pablo L., Chavez M.L., Abatal M. Adsorption of heavy metals in acid to alkaline environments by montmorillonite and Ca-montmorillonite // Chem. Eng. J. – 2011. -№171. - P. 1276–1286.

50 Lutz W. Zeolite Y: Synthesis, modification, and properties-a case revisited // Adv. Mater. Sci. Eng. – 2014. – Vol. 2014. –P. 1-20.

51 Faghihian H., Iravani M., Moayed M., Ghannadi-Maragheh M. Preparation of a novel PAN-zeolite nanocomposite for removal of Cs^{+} and Sr^{2+} from aqueous solutions: Kinetic, equilibrium, and thermodynamic studies // Chem. Eng. J. -2013. - №222. – P. 41-48.

52 Kaygun A.K., Akyil S. Study of the behaviour of thoriurn adsorption on PAN/zeolite composite adsorbent // J. Hazard. Mater. – 2007. - №147. – P. 357–362.

53 Elwakeel K.Z., El-Bindary A.A., Kouta E.Y., Guibal E. Functionalization of polyacrylonitrile/Na-Y-zeolite composite with amidoxime groups for the sorption of Cu(II), Cd(II) and Pb(II) metal ions // Chem. Eng. J. – 2018. - №332. - P. 727-736.

54 Elwakeel K.Z., El-Bindary A.A., Kouta E.Y. Retention of copper, cadmium and lead from water by Na-Y-Zeolite confined in methyl methacrylate shell // J. of Envir. Chem. Eng. – 2017. - № 5. – P. 3698-3710.

55 Ma L., Chen Q., Zhu J., Xi Y., He H., Zhu R., Tao Q., Ayoko G.A. Adsorption of phenol and Cu(II) onto cationic and zwitterionic surfactant modified montmorillonite in single and binary systems // Chem. Eng. J.- 2016. -№ 283. – P. 880–888.

56 Yu R., Wang S., Wang D., Ke J., Xing X., Kumada N., Kinomura N. Removal of Cd^{2+} from aqueous solution with carbon modified aluminum-pillared montmorillonite // Catal. Today. – 2008. - №139. – P. 135–139.

57 Ma L., Zhu J., Xi Y., Zhu R., He H., Liang X., Ayoko G.A. Simultaneous adsorption of Cd(II) and phosphate on Al_{13} pillared montmorillonite // RSC Adv. – 2015. - № 5. – P. 77227–77234.

58 Gupta S.S., Bhattacharya K.G. Treatment of water contaminated with Pb (II) and Cd (II) by adsorption on Kaolinite and Montmorillonite and their acid activated forms // Ind. J. Chem. Technol. – 2009. - №16. – P. 457–470.

59 Pereira F.A.R., Sousa K.S., Cavalcanti G.R.S., Fonseca M.G., de-Souza A.G, Alves A.P. M. Chitosan-montmorillonite biocomposite as an adsorbent for copper (II) cations from aqueous solutions // Int. J. Biol. Macromol. – 2013. - №61. – P. 471–478.

60 Chen C., Liu H., Chen T., Chen D., Frost R.L. An insight into the removal of Pb (II), Cu(II), Co(II), Cd(II), Zn(II), Ag(I), Hg(I), Cr(VI) by Na(I)-

montmorillonite and Ca(II)-montmorillonite // Appl. Clay Sci. – 2015. - № 118. – P. 239–247.

61 Juang R.S., Wu F.C., Tseng R.L. Characterization and use of activated carbons prepared from bagasses for liquid-phase adsorption // Colloids Surf. A Physicochem. Eng. Asp. – 2002. - № 201. – P. 191–199.

62 Valix M., Cheung W.H., McKay G. Preparation of activated carbon using low temperature carbonisation and physical activation of high ash raw bagasse for acid dye adsorption // Chemosphere. – 2004. - № 56. – P. 493–501.

63 Velazquez-Jimenez L.H., Pavlick A., Rangel-Mendez J.R. Chemical characterization of raw and treated agave bagasse and its potential as adsorbent of metal cations from water // Ind. Crop. Prod. – 2013. - № 43. – P. 200–206.

64 Aygun A., Yenisoy-Karakas S., Duman I. Production of granular activated carbon from fruit stones and nutshells and evaluation of their physical, chemical and adsorption properties // Microporous Mesoporous Mater. – 2003. - № 66. – P. 189–195.

65 Имангалиева А.Н., Сейлханова Г.А., Акбаева Д.Н., Кәрібаева Ж. К., Сорбция ионов Cu (II), Ni (II) и Cd (II) модифицированными природными материалами // Изв. НАН РК. Сер. хим. – 2015. - № 5. – С. 154-160.

66 Имангалиева А.Н., Ишанова М.Н., Сейлханова Г.А., Композитные материалы на основе шрота расторопши для очистки водных растворов от ионов Pb^{2+} и Cd^{2+} // Вестник КазНУ. Сер. экол. – 2018. - № 3(56). - С. 68-76.

67 Бьеррум Я. Образование аминов металлов в водном растворе. - М.: Иностранная литература, 1961. – 274 с.

68 Kumar P.S., Ramalingam S., Kirupha S.D., Murugesan A., Vidhyadevi T., Sivanesan S. Adsorption behavior of nickel (II) onto cashew nut shell: equilibrium, thermodynamics, kinetics, mechanism and process design // Chem. Eng. J. – 2011. - №167. – P. 122–131.

69 Li X., Tang Y., Xuan Z., Liu Y., Luo F. Study on the preparation of orange peel cellulose adsorbents and biosorption of Cd^{2+} from aqueous solution // Sep. Purif. Technol. – 2007. - №55. - P. 69–75.

70 Thinakaran N., Panneerselvam P., Baskaralingam P., Elango D., Sivanesan S. Equilibrium and kinetic studies on the removal of acid red from aqueous solutions using activated carbons prepared from seed shells // J. Hazard. Mater. – 2008. - №158. – P. 142–150.

71 Tasaso P. Adsorption of copper using pomelo peel and depectinated pomelo peel // J. Clean Energy Technol. – 2014. - № 2. – P. 154–157.

72 Husein D.Z. Adsorption and removal of mercury ions from aqueous solution using raw and chemically modified Egyptian mandarin peel // Desalin. Water Treat. – 2013. - № 51. – P. 6761–6769.

73 Yadav D., Kapur M., Kumar P., Mondal M.K. Adsorptive removal of phosphate from aqueous solution using rice husk and fruit juice residue // Process. Saf. Environ. – 2015. - № 94. – P. 402–409.

74 Hossain M.A., Ngo H.H., Guo W.S., Setiadi T. Adsorption and desorption of copper (II) ions onto garden grass // Bioresour. Technol. – 2012. - №121. – P. 386–395.

75 Liu W., Liu Y., Tao Y., Yu Y., Jiang H., Lian H. Comparative study of adsorption of Pb(II) on native garlic peel and mercerized garlic peel // Environ. Sci. Pollut. Res. -2014. - № 21. – P. 2054–2063.

76 Zou W., Zhao L., Zhu L. Efficient uranium(VI) biosorption on grapefruit peel: Kinetic study and thermodynamic parameters // J. Radioanal. Nucl. Chem. - 2012. - № 292. – P. 1303–1315.

77 Aygun A., Yenisoy-Karakas S., Duman I. Production of granular activated carbon from fruit stones and nutshells and evaluation of their physical, chemical and adsorption properties // Microporous Mesoporous Mater. – 2003. - № 66. – P. 189–195.

78 Aydın H., Bulut Y., Yerlikaya C. Removal of copper (II) from aqueous solution by adsorption onto low-cost adsorbents // J. Environ. Manag. – 2008. - № 87. – P. 37–45.

79 Iqbal M., Saeed A., Kalim I. Characterization of adsorptive capacity and investigation of mechanism of Cu^{2+}, Ni^{2+} and Zn^{2+} adsorption on mango peel waste from constituted metal solution and genuine electroplating effluent // Sep. Sci. Technol. – 2009. - №44 - P. 3770–3791.

80 Huang K., Zhu H., Removal of Pb^{2+} from aqueous solution by adsorption on chemically modified muskmelon peel // Environ. Sci. Pollut. Res. – 2013. - №20. – P. 4424–4434.

81 Akmil-Basar C., Onal Y., Kilicer T., Eren D. Adsorptions of high concentration malachite green by two activated carbons having different porous structures // J. Hazard. Mater. – 2005. - №127. – P. 73–80.

82 Thinakaran N., Panneerselvam P., Baskaralingam P., Elango D., Sivanesan S. Equilibrium and kinetic studies on the removal of acid red 114 from aqueous solutions using activated carbons prepared from seed shells // J. Hazard. Mater. – 2008. - № 158. – P. 142–150.

83 Malik R., Ramteke D.S., Wate S.R. Adsorption of malachite green on groundnut shell waste based powdered activated carbon // Waste Manag. - 2007. - № 27. – P. 1129–1138.

84 Fiol N., Villaescusa I., Martínez M., Miralles N., Poch J., Serarols J. Sorption of Pb (II), Ni (II), Cu (II) and Cd (II) from aqueous solution by olive stone waste // Sep. Purif. Technol. – 2006. - № 50. – P. 132–140.

85 Moghadam M., Nasirizadeh N., Dashti Z., Babanezhad E. Removal of Fe(II) from aqueous solution using pomegranate peel carbon: equilibrium and kinetic studies // Int. J. Ind. Chem. – 2013. - №4. – P. 1–6.

86 Aman T., Kazi A.A., Sabri M.U., Bano Q. Potato peels as solid waste for the removal of heavy metal copper (II) from waste water/industrial effluent // Colloids Surf. B: Biointerfaces. – 2008. - № 63. – P. 116–121.

87 Ding Y., Jing D., Gong H., Zhou L., Yang X. Biosorption of aquatic cadmium (II) by unmodified rice straw // Bioresour. Technol. – 2012. - № 114. – P. 20–25.

88 Khoramzadeh E., Nasernejad B., Halladj R. Mercury biosorption from aqueous solutions by sugarcane bagasse // J. Taiwan Inst. Chem. Eng. – 2013. - № 44. – P. 266–269.

89 Pavan F.A., Lima E.C., Dias S.L.P., Mazzocato A.C. Methylene blue biosorption from aqueous solutions by yellow passion fruit waste // J. Hazard. Mater. – 2008. - № 150. – P. 703–712.

90 Feng N., Guo X., Liang S. Adsorption study of copper (II) by chemically modified orange peel // J. Hazard. Mater. – 2009. - № 164. – P. 1286–1292.

91 Liang S., Guo X., Feng N., Tian Q. Isotherms, kinetics and thermodynamic studies of adsorption of Cu^{2+} from aqueous solutions by Mg^{2+}/K^{+} type orange peel adsorbents // J. Hazard. Mater. – 2010ю - № 174. – P. 756–762.

92 Бурхан М.Ә., Имангалиева А.Н., Сейлханова Г.А. Композиционные материалы на основе растительного сырья для извлечения ионов тяжелых металлов // Международная научная конференция студентов и молодых ученых «Фарабиевские чтения». - Алматы, 9-10 апреля 2018. - С.184.

93 Liang S., Guo X., Tian Q. Adsorption of Pb^{2+} and Zn^{2+} from aqueous solutions by sulfured orange peel // Desalination. – 2011. - № 275. – P. 212–216.

94 Malik P.K. Use of activated carbons prepared from sawdust and rice-husk for adsorption of acid dyes: a case study of acid yellow 36 // Dyes Pigments. – 2003. - № 56. – P. 239–249.

95 Ding L., Zou B., Gao W., Liu Q., Wang Z., Guo Y., Wang X., Liu Y. Adsorption of rhodamine-B from aqueous solution using treated rice husk-based activated carbon // Colloids Surf. A. – 2014. - №446. – P. 1–7.

96 Tavlieva M.P., Genieva S.V., Georgieva V.G., Vlaev L.T. Kinetic study of brilliant green adsorption from aqueous solution onto white rice husk ash // J. Colloid Interface Sci. – 2013. - №409. – P. 112–122.

97 Bhatnagar A., Sillanpää M., Witek-Krowiak A. Agricultural waste peels as versatile biomass for water purification — a review // Chem. Eng. J. - 2015. - № 270. – P. 244–271.

98 Sreenivas K.M., Inarkar M.B., Gokhale S.V., Lele S.S. Re-utilization of ash gourd (Benincasa hispida) peel waste for chromium(VI) biosorption: equilibrium and column studies // J. Environ. Chem. Eng. – 2014. - № 2. – P. 455–462.

99 Basu M., Guha A.K., Ray L. Biosorptive removal of lead by lentil husk // J. Environ. Chem. Eng. - 2015. – Vol. 3, № 2. – P. 1088–1095.

100 Brown P. A., Gill S. A., Allen, S. J. Metal removal from wastewater using peat // Water Research. – 2000. - № 34. – P. 3907-3916.

101 Leiviskä T., Khalid M. K., Gogoi H., Tanskanen J. Enhancing peat metal sorption and settling characteristics // Ecotoxicology and environmental safety. - 2018. - № 148. – P. 346- 351.

102 Padma M.P. Ficus racemosa: An overview // Natural Products Radiance. – 2009. - № 8. – P. 84-90.

103 Anjaneyulu V., Babu I. S., Connolly J. D. Hydroxy mangiferonic acid. – Phytochemistry, 1994. – P. 1301-1303.

104 Singh S., Tripathi A., Srivastava S.K. Comparative biosorption competencies and seeds of Ficus Syzygium Mangifera for hexavalent chromium mitigation from polluted water // Journal of Environmental Biology. - 2018. - № 39. – P. 159-165.

105 Anwar J., Shafique U., Waheed Z., Salman M., Dar A., Anwar S. Removal of Pb(II) and Cd(II) from water by adsorption on peels of banana // Bioresour. Technol. – 2010. - № 101. – P. 1752–1755.

106 Wang C., Wang H., Gu G. Ultrasound-assisted xanthation of cellulose from lignocellulosic biomass optimized by response surface methodology for Pb (II) sorption // Carbohydrate Polymers. – 2018. - № 182. – P. 21–28.

107 Aranda-García E., Cristiani-Urbina E. Kinetic, Equilibrium, and Thermodynamic Analyses of Ni(II) Biosorption from Aqueous Solution by Acorn Shell of Quercus crassipes // Water Air Soil Pollut. – 2018. - № 229. – P. 119-136.

108 Holan Z.R., Volesky B., Prasetyo I. Biosorption of cadmium by biomass of marine algae // Biotechnol. Bioeng. – 1993. - № 41. – P. 819–825.

109 Raghavendra G. M., Jung J., Kim D., J. Seo Chitosan-mediated synthesis of flowery-CuO , and its antibacterial and catalytic properties // Carbohydr. Polym. - 2017. - № 172. - P. 78–84.

110 Gyliene O., Binkiene R., Baranauskas M., Mordas G., Plauškaite K., Ulevičius V. Influence of dissolved oxygen on Fe(II) and Fe(III) sorption onto chitosan // Colloids Surfaces A Physicochem. Eng. Asp. - 2014. – Vol. 461, № 1. - P. 151–157.

111 Jianlong W., Can C. Chitosan-based biosorbents: Modification and application for biosorption of heavy metals and radionuclides // Bioresour. Technol. - 2014. - № 160. - P. 136–140.

112 Liu B., Wang D., Yu G., Meng X. Adsorption of heavy metal ions, dyes and proteins by chitosan composites and derivatives – a review // J. Ocean Univ. China. - 2013. - № 12. - P. 500–508.

113 Popuri S. R., Vijaya Y., Boddu V. M., Abburi K. Adsorptive removal of copper and nickel ions from water using chitosan coated PVC beads // Bioresour. Technol. - 2009. - № 100. - P. 194–199.

114 Imangaliyeva A.N., Seilkhanova G.A., Ondasheva A. Zh., Telkhozhayeva M.S. Adsorption studies of Cu (II), Pb (II) and Cr (VI) by chitosan/unitiol composite // International journal of biology and chemistry. - 2018. – Vol. 12, №1 – P. 12-17.

115 Peng S., Meng H., Ouyang Y., Chang J. Nanoporous magnetic cellulose−chitosan composite microspheres: preparation, characterization, and application for Cu(II) adsorption // Ind. Eng. Chem. Res. – 2014. - № 53. – P. 2106–2113.

116 Siahkamaria M., Jamalia A., Sabzevari A. Removal of Lead (II) ions from aqueous solutions using biocompatible polymeric nano-adsorbents: A comparative study // Carbohydrate Polymers. – 2017. - № 157. – P. 1180–1189.

117 Rais A., Anam M. Facile one pot green synthesis of Chitosan-Iron oxide (CS-Fe_2O_3) nanocomposite // Journal of Cleaner Production. – 2018. - № 186. – P. 342-352.

118 Nasef M.M., Nallappan M., Ujang Z. Polymer-based chelating adsorbents for the selective removal of boron from water and wastewater: a review // React. Funct. Polym. – 2014. - № 85. – P. 54–68.

119 Gerente C., Andres Y., McKay G., Le Cloirec P. Removal of arsenic (V) onto chitosan: from sorption mechanism explanation to dynamic water treatment process // Chem. Eng. J. – 2010. – Vol. 158, № 3. – P. 593–598.

120 Aydin Y.A., Aksoy N.D. Adsorption of chromium on chitosan: optimization, kinetics and thermodynamics // Chem. Eng. J. – 2009. - № 151. – P. 188–194.

121 Herrero R., Lodeiro P., Rey-Castro C., Vilarino T., de Vicente M.E.S. Removal of inorganic mercury from aqueous solutions by biomass of the marine macroalga Cystoseira baccata // Water Res. – 2005. - № 39. – P. 3199–3210.

122 Vilar V.J.P., Botelho C.M.S., Boaventura R.A.R. Equilibrium and kinetic modelling of Cd (II) biosorption by algae Gelidium and agar extraction algalwaste // Water Res. – 2006. - № 40. – P. 291–302.

123 Gupta V.K., Rastogi A. Biosorption of hexavalent chromium by raw and acid treated green alga Oedogonium hatei from aqueous solutions // J. Hazard. Mater. – 2009. - № 163. - P. 396–402.

124 McLelland J.K., Rock C.A. Pretreating landfill leachate with peat to remove metals // Water Air Soil Pollut. - 1988. - № 37. – P. 203–215.

125 Sepehr M.N., Amrane A., Karimaian K.A., Zarrabi M., Ghaffari H.R. Potential of waste pumice and surface modified pumice for hexavalent chromium removal: characterization, equilibrium, thermodynamic and kinetic study // J. Taiwan Inst. Chem. Eng. – 2014. - № 45. – P. 635–647.

126 Chen J.P., Yang L. Chemical modification of Sargassumsp for prevention of organic leaching and enhancement of uptake during metal biosorption // Ind. Eng. Chem. Res. – 2005. - № 44. – P. 9931–9942.

127 Martins B.L., Cruz C.C.V., Luna A.S., Henriques C.A. Sorption and desorption of Pb^{2+} ions by dead Sargassum sp. Biomass // Biochem. Eng. J. – 2006. - № 27. – P. 310–314.

128 Sahiner N., Ozay H., Ozay O. New catalytic route : Hydrogels as templates and reactors for in situ Ni nanoparticle synthesis and usage in the reduction of 2- and 4-nitrophenols // Applied Catal A, Gen. – 2010. - № 385. – P. 201–207.

129 Gkizis P.L., Stratakis M., Lykakis I.N. Catalytic activation of hydrazine hydrate by gold nanoparticles: Chemoselective reduction of nitro compounds into amines // Catal Commun. – 2013. - № 36. – P. 48–51.

130 Lawrence S.A. Amines: Synthesis, Properties and Applications. - Cambridge. New York, 2004. – 371 p.

131 Sunil P. B., Sudhirprakash B.S. Hydrogenation of p-nitrophenol to metol using Raney nickel catalyst: Reaction kinetics // Appl Catal A Gen. – 2005. - № 293. – P. 162–170.

132 Wang F., Ren J., Cai Y. Palladium nanoparticles confined within ZSM-5 zeolite with enhanced stability for hydrogenation of p-nitrophenol to p-aminophenol // Chem. Eng. J. – 2016. - № 283. – P. 922–928.

133 He L., Wang L.C., Sun H. Efficient and selective room-temperature gold-catalyzed reduction of nitro compounds with CO and H_2O as the hydrogen source // Angew Chemie – Int. Ed. – 2009. - № 48. – P. 9538–9541.

134 Ramdar M., Kazemi F., Kaboudin B. A photocatalytic green system for chemoselective reduction of nitroarenes // Chem. Pap. – 2017. - № 71. – P. 1155–1163.

135 Zhou J., Yang Q. Facile synthesis of monodisperse noble-metal nanoparticles and high catalytic performance for organic reactions in both water and oil systems // Chem. - An Asian J. – 2012. - № 7. – P. 2045–2050.

136 Padervand M., Salari H., Darabi F.S. Kinetic and mechanistic study of p-nitrochlorobenzene photoreduction and Bacillus inactivation over aluminosilicate-based nanocomposites // Monatshefte fur Chemie. – 2013. - № 144. – P. 589–596.

137 Veerakumar P., Velayudham M., Lu K.L. Polyelectrolyte encapsulated gold nanoparticles as efficient active catalyst for reduction of nitro compounds by kinetic method // Appl. Catal. A Gen. – 2012. – Issue 11. - P. 439–440.

138 Rostami-Vartooni A., Alizadeh M., Bagherzadeh M. Green synthesis, characterization and catalytic activity of natural bentonite-supported copper nanoparticles for the solvent-free synthesis of 1-substituted 1H-1,2,3,4-tetrazoles and reduction of 4-nitrophenol // Beilstein J Nanotechnol. – 2015. - №6. – P. 2300–2309.

139 Li S., Guo S., Yang H. Enhancing catalytic performance of Au catalysts by noncovalent functionalized graphene using functional ionic liquids // J. Hazard Mater. – 2014. - № 270. – P. 11–17.

140 Schrinner M., Ballauff M., Talmon Y. Single Nanocrystals of Platinum Prepared by Partial Dissolution of Au-Pt Nanoalloys // Science. – 2009. - № 323. – P. 617–620.

141 Lee J., Park J.C., Song H. A. Nanoreactor framework of a $Au@SiO_2$ yolk/shell structure for catalytic reduction of p-nitrophenol // Adv Mater. – 2008. - № 20. – P. 1523–1528.

142 Zeng J., Zhang Q., Chen J. A comparison study of the catalytic properties of Au-based nanocages, nanoboxes, and nanoparticles // Nano Lett. – 2010. - № 10. – P. 30–35.

143 Li S., Guo S., Yang H., et al. Enhancing catalytic performance of Au catalysts by noncovalent functionalized graphene using functional ionic liquids // J. Hazard Mater. – 2014. - № 270. – P. 11–17.

144 Khan M.N., Bashir O., Khan T.A., et al. Catalytic Activity of Cobalt Nanoparticles for Dye and 4-Nitro Phenol Degradation: A Kinetic and Mechanistic Study. // Int. J. Chem. Kinet. – 2017. - № 49. – P. 438–454.

145 Giri S., Das R., van der Westhuyzen C. An efficient selective reduction of nitroarenes catalyzed by reusable silver-adsorbed waste nanocomposite // Appl. Catal. B Environ. – 2017. - № 209. – P. 669–678.

146 Lu S., Yu J., Cheng Y. Preparation of silver nanoparticles/polydopamine

functionalized polyacrylonitrile fiber paper and its catalytic activity for the reduction 4-nitrophenol // Appl. Surf. Sci. - 2017. - № 411. – P. 163–169.

147 Kaur B., Tumma M., Srivastava R. Transition-metal-exchanged nanocrystalline ZSM-5 and metal-oxide- incorporated SBA-15 catalyzed reduction of nitroaromatics // Ind. Eng. Chem. Res. – 2013. - № 52. – P. 11479–11487.

148 Subramanian T., Pitchumani K. Selective Reduction of Nitroarenes by using Zeolite-Supported Copper Nanoparticles with 2-Propanol as a Sustainable Reducing Agent // Chem. Cat. Chem. – 2012. - № 4. – P. 1917–1921.

149 Kumar A., Saxena A. Facile synthesis of size-tunable copper and copper oxide nanoparticles using reverse microemulsions // RSC Adv. – 2013. - № 3. – P. 5015–5021.

150 Dong Z., Le X., Dong C., et al. Applied Catalysis B : Environmental Ni@Pd core – shell nanoparticles modified fibrous silica nanospheres as highly efficient and recoverable catalyst for reduction of 4-nitrophenol and hydrodechlorination of 4-chlorophenol // Applied Catal B, Environ. – 2015. - № 162. – P. 372–380.

151 Rath P.C., Saikia D., Mishra M., et al. Exceptional catalytic performance of ultrafine Cu_2O nanoparticles confined in cubic mesoporous carbon for 4-nitrophenol reduction // Appl. Surf. Sci. – 2018. - № 427. – P. 1217–1226.

152 Su Y., Fan B., Wang L., et al. MnO_x supported on carbon nanotubes by different methods for the SCR of NO with NH_3 // Catal. Today. – 2013. - № 201. – P. 115–121.

153 Yoshida A., Mori Y., Ikeda T., et al. Enhancement of catalytic activity of Ir/TiO_2 by partially reduced titanium oxide in aerobic oxidation of alcohols // Catal. Today. – 2013. - № 203. – P. 153–157.

154 Cárdenas-Lizana F., Gómez-Quero S., Perret N. Gold catalysis at the gas-solid interface: Role of the support in determining activity and selectivity in the hydrogenation of m-dinitrobenzene // Catal. Sci. Technol. – 2011. - № 1. – P. 652–661.

155 Horáček J., Šťávová G., Kelbichová V., et al. Zeolite-Beta-supported platinum catalysts for hydrogenation/hydrodeoxygenation of pyrolysis oil model compounds // Catal. Today. - 2013. - № 204. – P. 38–45.

156 Islam H., Tamer S.S., Eman Z.H. Preparation, characterization and utilization of (Ni:Cu) bimetallic system loaded on zeolites // J. Alloys Compd. – 2010. - № 506. – P. 923–927.

157 Seilkhanova G.A., Imangaliyeva A.N., Akbayeva D.N., Kenzhalina Zh. Zh. Modified raw materials : synthesis, characterization and application for Cd^{2+} ions removal // Stud Univ Babes-Bolyai Chem. - 2017. – Vol. LXII. – P. 35–50.

158 Natkański P., Białas A., Kuśtrowski P. The synthesis of poly (acrylic acid) -bentonite and polyacrylamide-bentonite composites for adsorption applications // Chemik. – 2012. – Vol. 66, № 7. – P. 746–749.

159 Clegg F., Breen C., Khairuddin Synergistic and competitive aspects of the adsorption of poly(ethylene glycol) and poly(vinyl alcohol) onto Na-bentonite // J. Phys. Chem. B. – 2014. - №118. – P. 13268–13278.

160 Šimáková P., Gautier J., Procházka M., Aubert K. and Choupra I. Polyethylene-glycol-Stabilized Ag Nanoparticles for Surface-Enhanced Raman Scattering Spectroscopy: Ag Surface Acessibility Studied Using Metalation of Free-Base Porphyrins // J. Phys. Chem. – 2014. - №118. – P. 7690–7697.

161 Абдреимова Р.Р., Фаизова Ф.Х., Борангазиева А.К., Каримова А.А., Полимбетова Г.С. Кинетика накопления продуктов окисления желтого фосфора в спиртовых растворах соединений меди (II) и железа(III) // Изв. Нац. академ. наук сер. хим. – 2009. - №5.- С.14-18.

162 Ernstberger M. L., Hull L.W. // Chem. Abstr. – 1955. - Vol.49., №3. - P. 1774.

163 Дорфман Я.И., Абдреимова Р.Р. // Ж. общ. хим. – 1993. - Т.63. – С. 289.

164 Дорфман Я.И., Абдреимова Р.Р., Акбаева Д.Н. // Кин. и кат. – 1996.- Т. 36., №1. – С.103.

165 Абдреимова Р.Р. // Известия НАН РК. Сер. хим. – 2007. - №1. – С. 42-57.

166 Абдреимова Р.Р., Фаизова Ф.Х., Борангазиева А.К. Каримова А.А., Полимбетова Г.С. // Изв. НАН РК Сер. Хим. – 2010. - №3. – С.51.

167 Черкасов Р.А. Новые фосфорсодержащие лиганды в комплексах переходных металлов // Металлоорг. химия. - 1989. - Т. 2, № 1. - С. 13-25.

168 Liua X., Guo M., Zhang M., Wang X., Guo X., Chou K. Effects of PVP on the preparation and growth mechanism of monodispersed Ni nanoparticles // Rare Metals. – 2008. - Vol. 27. - Issue 6. - P. 642-647.

169 Okamoto Y., Kusano T., Takamuku S. //Bull. Chem.Soc. Jpn. – 1988. - Vol.61. - P. 3359 – 4027.

170 Акбаева Д.Н., Сейлханова Г.А., Бектигулова А.Н., Кенжалина Ж.Ж., Имангалиева А.Н., Копышев А.М., Полимбетова Г.С., Ибраимова У.Ж., Борангазиева А.К. Каталитическая система на основе полиакриловой кислоты и хлорида меди (II) в реакции окисления жёлтого фосфора // Изв. НАН РК. Сер. хим. и техн. – 2015. – № 4. – С. 12-17.

171 Ballard D.G.H. Organometallic Polymers // J. Polym. Sci.: Polym. Chem. Ed. - 1975. - Vol. 13, № 10. - P. 2191-2212.

172 Ермаков Ю.И., Захаров В.А., Кузнецов Б.Н. Закрепленные комплексы на оксидных носителях в катализе. - Новосибирск: Наука, 1980. – 248 с.

173 Benaglia M., Puglisi A., Cozzi F. Polymer supported organic catalysts // Chem. Rev. - 2003. - Vol.103. - P. 3401-3429.

174 Leznoff C. The use of insoluble polymer supports in organic chemical synthesis // Chem. Soc. Rev. - 1974. - № 3. - P.65-85.

175 Fine Chemicals through Heterogeneous Catalysis / Eds. Sheldon R. A., van Bekkum H. Weinheim: Wiley- VCH, 2001. – 437 p.

176 Fraile J.M., Mayoral J.A., Royo A.J., Salvador R.V., Altava Â., Luis S.V., Burguete M.I. Supported chiral amino alcohols and diols functionalized with aluminium and titanium as catalysts of Diels-Alder reaction // Tetrahedron. - 1996. - № 52. - P. 9853-9862.

177 Trost A. M., Warner R.W. Macrocyclization via an isomerization reaction at high concentrations promoted by palladium templates // J. Am. Chem. Soc. - 1982. - Vol. 104. - P. 6112-6118.

178 Yu H., Zheng X., Lin Z., Hu Q., Huang W., Pu L. Polymer-metal complexes as a catalyst for the growth of carbon nanostructures // J. Org. Chem. - 1999. - Vol. 34. - P. 8149-8156.

179 Fuente A.M., Pulgar G., Gonzalez F., Pesquera C., Blanco C. Activated carbon supported Pt catalysts; effect of support texture and metal precursor on activity of acetone hydrogenation // Appl. Catalysis. A: General. - 2001. - Vol. 208. - P. 35–46.

180 Li L., Zhu Z.H., Yan Z.F., Lu G.Q., Rintoul L. Catalytic ammonia decomposition over Ru/carbon catalysts: The importance of the structure of carbon support // Appl. Catalysis. A: General. - 2007. - Vol. 320. - P. 166–172.

181 Ауезханова А.С., Алтынбекова К.А., Ефремова С.В., Кадышева Ж., Жармагамбетова А.К. Полимер модифицированные медные катализаторы на углеродсодержащем носителе в реакциях разложения пероксида водорода и окисления циклогексана // Вестник КазНУ. Сер. хим. - 2011. - № 4. - С. 24-26.

182 Пописов И.М. Матричная полимеризация и другие матричные и псевдоматричные процессы как путь получения композиционных материалов // Высокомолек. соед. - 1997. - Т. 39, № 3. - С. 562-574.

183 Литманский А.А., Пописов И.Н Получение нанокомпозитов в процессах, контролируемых макромолекулярными псевдоматрицами // Высокомолек. соед. - 1997. - Т.39, № 2. - С. 323-326.

184 Литманович О.Е., Литманович А.А., Пописов И.М. Формирование полимер-металлических нанокомпозитов восстановлением двухвалентной меди из ее комплексов и полиэтиленимином // Высокомолек. соед. - 1997. - Т. 39, № 9. - С. 1506-1510.

185 Трахтенберг Л.И., Герасимов Г.Н., Потапов В.К., Ростовщикова Т.Н., Смирнов В.В, Зуфман В.Ю. Нанокомпозиционные металлполимерные пленки: сенсорные, каталитические и электрофизические свойства // Вестник МГУ. Сер. хим. – 2001. – Т. 42, № 5. – С. 325-331.

186 Жармагамбетова А.К., Доля Н.А., Ибраева Ж.Е., Каримова А.А., Дюсеналин Б.К., Кудайбергенов С.Е. Физико-химические и каталитические свойства полимер-протектированных и гель-иммобилизованных наночастиц палладия в реакции гидрирования 2-пропен-1-ола // Изв. НАН РК. Сер. хим. – 2010 – № 3. – С. 6-9.

187 Щербакова Я.И., Ефимов Н.Н., Михайлова А.В. Особенности комплексообразования переходных металлов с гидрогелями // Ж. неорг. хим. – 2013. – Т. 58, № 7. – С. 936-939.

188 Сидельковская Ф.П. Химия N-винилпироллидона и его полимеров. - М.: Наука, 1970. – 150 с.

189 Chanda M., O'Driscoll K.F., Rempel G.L. Polymer supported metal complexes as catalysts for oxidation of thiosalts by molecular oxygen IV.

Quaternised poly(4-vinyl pyridine) complexes with Cu ‒ as template // Journal of Molecular Catalysis. – 1981. - Vol. 12, № 2. - P. 197-211.

190 Gupta S.S., Bhattacharyya K.G. Treatment of water contaminated with Pb (II) and Cd (II) by adsorption on kaolinite, montmorrilonite and their acid activated forms // Indian Journal of Chemical Technology. – 2009. - № 16. - P. 457-470.

191 Imangaliyeva A.N., Seilkhanova G.A., Mastai Y. Catalytic characterization of the bentonite-PEG supported copper composite for the reduction of 4-nitrophenol // 4th International Russian-Kazakh Scientific and Practical conference “Chemical Technology of Functional Materials”. - Almaty, 2018. – P. 179-181.

192 Казицина Л.А., Куплетская Н.Б. Применение УФ-, ИК- и ЯМР-спектроскопии в органической химии. - Изд-во "Высшая школа" Москва, 1971. - 264 с.

193 Kuo S.W., Huang C.F., Wu C.H., Chang F.C. Thermal and spectroscopic properties of zinc perchlorate/poly(vinylpyrrolidone) blends and a comparison with related hydrogen bonding systems // Polymer. – 2004. – Vol. 45, № 19. – P. 6613–6621.

194 Акбаева Д.Н., Сейлханова Г.А., Бәкірова Б.С., Кенжалина Ж.Ж., Томкович М.В., Соколов В.В., Борангазиева А.К. Физико-химические характеристики комплекса на основе хлорида меди (II) и поливилпирролидона // Известия Сер. хим. – 2017. – Т. 4, №424. – С. 19-25.

195 Никифорова Т.Е., Козлов В.А., Исляйкин М.К. Кислотно-основные взаимодействия и комплексообразование при извлечении катионов меди(II) из водных растворов целлюлозным сорбентом в присутствии поливинилпирролидона // Ж. физ. хим. – 2012. – Т. 86, № 12. – С. 1974-1984.

196 Wang Z., Xu C., Gao G. Facile synthesis of well-dispersed Pd–graphene nanohybrids and their catalytic properties in 4-nitrophenol reduction // RSC Adv. – 2014. - №4. – P. 13644–13651.

197 Liu B., Yu S., Wang Q. Hollow mesoporous ceria nanoreactors with enhanced activity and stability for catalytic application // Chem. Commun. (Camb). – 2013. - № 49. – P. 3757–3759.

198 Акбаева Д.Н., Сейлханова Г.А., Имангалиева А.Н., Кенжалина Ж.Ж. Способ получения фосфорной кислоты // Патент на полезную модель № 1513, ЦФХМА - опубл. 30.06.2016; Бюл. - № 6б.

199 Акбаева Д.Н., Сейлханова Г.А., Имангалиева А.Н., Кенжалина Ж.Ж., Бәкірова Б.С., Бектигулова А.Н. // Способ получения ортофосфорной кислоты // Патент на полезную модель № 2283, ЦФХМА - опубл. 31.07.2017; Бюл. - № 14.

200 Нифантьев Э.Е., Васянина Л.К. Спектроскопия ЯМР ^{31}Р. – М.: Изд. МГПИ, 1986. – 150 с.

201 Арбузов А.Е. Избранные труды по химии фосфорорганических соединений. – М.: Химия, 1977. – 356 с.

202 Нифантьев Э.Е Химия фосфорорганических соединений. – М.: Изд. МГУ, 1971. – 352 с.

203 Дорфман Я.А., Абдреимова Р.Р. Окислительное алкоксилирование тетрафосфора // Ж. общ. химии. - 1993. – Т. 63, № 2. - С. 289-303.

204 Seilkhanova G.A., Imangaliyeva A.N., Mastai Y., Rakhym A.B. Bentonite Polymer Composite for Water Purification // Bulletin of Materials Science. – 2019. - Vol. 42:60, Issue 2. - P. 1-8.